4-18-2018 2:00 PM

Functional Anatomy of Palmar Musculature

Colin W. Moore, *The University of Western Ontario*

Supervisor: Rice, Charles L., *The University of Western Ontario*

A thesis submitted in partial fulfillment of the requirements for the Doctor of Philosophy degree in Kinesiology
© Colin W. Moore 2018

Abstract

The palmaris longus (PL) and palmaris brevis (PB) are upper limb muscles considered atavistic remnants of those found in animal species. Despite their use in surgical grafting and tendon transfer procedures, the functional role of the PL and PB have not been investigated comprehensively *in vivo*. Using a multi-modal experimental approach consisting of indwelling fine wire electromyography (EMG), ultrasonography and immunohistochemical muscle staining techniques, the function of the PL and PB in the hand was evaluated both in *in vivo* and *in situ*.

The purpose of Study 1 was to determine whether the PL provides synergistic contributions to thenar contractions by recording PL muscle activity using indwelling EMG during thumb movements; and to quantify changes in PL muscle architecture using ultrasonography. This study supports morphological observations indicating the PL acts as an extrinsic hand muscle in enhancing thenar muscle actions.

The purpose of Study 2 was to compare the proportion of type I and type II muscle fibers in the abductor pollicis brevis (APB) based on its morphological relationship with the PL tendon for indirect insight into the functional synergy, contractile capacity and digastric arrangement amongst contiguous APB and PL musculature. The results indicate that APB fascicles arranged in a digastric relationship with the PL have greater type II fiber type proportions, which support observations of greater thenar abduction strength attributed to PL musculature.

The purpose of Study 3 was to investigate PB EMG activity during dynamic grasping tasks, and to quantify its changes in muscle morphology using ultrasound imaging. The results indicate that the PB is voluntarily activated during prehensile movements of the hand with significant changes in muscle architecture, which supports its proposed protective role as a muscular barrier to neurovasculature within the ulnar canal.

The purpose of Study 4 was to histologically examine the PB by determining the proportion of type I and type II muscle fibers using immunohistochemistry. The results indicate that the PB is composed primarily of type I muscle fibers (>70%), which may allow the PB to contract for prolonged durations during repetitive intermittent grasping tasks based on its fiber type profile.

Keywords

Co-Authorship Statement

This thesis contains material from published manuscripts (Chapters 2, 4, 5). On all manuscripts, Colin W. Moore is the first author and Dr. Charles L. Rice is co-author. In Chapter 2, Jacob Fanous was co-author. In Chapter 5, Tyler S. Beveridge was co-author. All experimental data were collected, analyzed and interpreted by Colin W. Moore.

Acknowledgments

To my doctoral supervisor, mentor, and friend, Dr. Charles Rice, thank you for your guidance and for supporting my research studies in the realm of functional anatomy. I am very fortunate to have been a member of the neuromuscular lab and for the many travel opportunities to share my research. I have had an incredible doctoral experience and learned some interesting lab techniques while studying some unique muscles (anconeus, palmaris longus and brevis). Importantly, my four years have been memorable and enjoyable, and I'm going to miss all the good times we've had inside and outside the lab.

A special thank you to my PhD advisory committee: Dr. Brian Allman, Dr. Greg Marsh, and Dr. Tim Wilson for your valuable insights, and guidance towards my projects and research interests, including those related to muscle histology, functional imaging, and anatomy education. I am grateful to have been involved in collaborative research projects with Tyler Beveridge, and Dr. Brian Allman through the Department of Anatomy & Cell Biology, and for their willingness to provide support and expertise in learning immunohistochemical techniques. Also, I am grateful to have been involved in collaborative research projects in anatomy education with Dr. Tim Wilson, and for his support in pursuing the role of variant anatomy in anatomical education.

To my current neuromuscular lab mates – Kevin, Eric, Dave, Kalter, and Jacob, thank you all for your support, enthusiasm, valuable insights, and good-natured humor that made the lab a fun place to work and study. Despite the strong likelihood for multiple needle insertions into your hands and the potential to become human pincushions, you all were still eager and willing to participate – thank you for your patience. To Dr. Matti Allan, thank you for your guidance, insights, and collaborative efforts as I began my PhD journey in the lab.

So I follow the tides
On currents far and wide
Chalking up the stories and the miles
Yes, I follow the tides
Big blue rides
And that's the reason I will never lose my smile

- Jimmy Buffett
  "Tides"

Table of Contents

List of Tables

List of Figures

List of Appendices

Chapter 1

1 General Introduction

1.1 Functional Anatomy: A Brief Historical Overview

A comprehensive study pertaining to muscle structure and function would be incomplete without recognition of Andreas Vesalius, the 16th Century anatomist, denoted by scholars as the "father" of modern human anatomy and author of the historical text, *De Humani Corporis Fabrica (On the Fabric of Man)*. The anatomical observations made by Vesalius were greatly improved over his predecessor, Galen, whose anatomical observations were based primarily on animal dissections and not of human corpses. A new field, electrophysiology, emerged from Galvani's observations of twitch contractions in frog legs upon electrical stimulation (Galvani, 1791). The French medical doctor, Guillaume Duchenne, made further contributions into muscle function by investigating movements produced by faradic stimulation of individual muscles (Duchenne, 1959). Through historical anatomical and physiological investigations, the method of electromyography became a modern day tool for anatomists, kinesiologists, neurologists and orthopedic surgeons in studying muscle function (Basmajian, 1974). Basmajian (1980) wrote, "structure and function are inseparable, and each supports the other. Only by appreciating the functions of muscle tissue, individual muscles and muscle groups can we appreciate the complexities of structure". Today, individual muscle function can be revealed through a variety of modern techniques including functional imaging, histological muscle properties, and electromyographical recordings. From a functional and evolutionary perspective, two human upper limb muscles, the palmaris longus and palmaris brevis, are considered remnants of those more developed in animal species (Jones, 1920). Although Vesalius may have first recorded the absence of the palmaris longus in man in 1543 (Brinkman and Hage, 2016), he overlooked the palmaris brevis altogether in his classical dissections (Tubbs et al., 2007). Although their morphological appearance has been comprehensively studied, the functional anatomy of the palmaris longus and palmaris brevis in the human hand has yet to be explored.

1.2   Palmaris Longus

1.2.1   Anatomy

The PL is among four superficial forearm muscles of the common flexor mass originating from the medial epicondyle of the humerus (Moore et al., 2014). The PL is a fusiform muscle consisting of a characteristically long thin tendon that terminates into the palmar aponeurosis in the hand (Gilroy, 2013; Moore et al., 2014). Known for its variant morphology, the PL has been observed in several forms consisting of reversed (Backhouse and Churchill-Davidson, 1975), or duplicated PL muscle bellies (Pai et al., 2008), and may terminate in aberrant tendon insertions (Stecco et al., 2009). Moreover, the PL is absent in approximately 14% of the population worldwide (Moore et al., 2014); however, the incidence of PL agenesis may vary remarkably by geographical region as observed in Turkish (63.9%) (Ceyhan and Mavt, 1997) and Korean populations (0.6%) (Ahn et al., 2000). Although bilateral PL agenesis is common, unilateral presence of PL musculature can be limited to either the left or right limb (Eric et al., 2011; Reimann et al., 1944). Furthermore, PL absence may be related to hand dominance with PL absence observed more frequently in the non-dominant hand (Eric et al., 2011). Investigation of familial PL inheritance patterns in a Brazilian population indicated that PL presence is an autosomal dominant trait; however, the exact genetic mechanism of inheritance remains unclear as the study demonstrated variable expressivity in parents with bilateral PL presence generating children with unilateral PL absence (Morais et al., 2013). From a phylogenetic perspective, the PL may be undergoing an evolutionary recession in humans (Montague, 1947).

1.2.2   Function

Classically, the PL is described as a weak wrist flexor and tensor of the palmar aponeurosis. The tension applied to the palmaris aponeurosis may anchor the palmar skin and fascia to protect against horizontal shear forces when grasping various implements (Standring and Gray, 2008). Although the PL is routinely harvested as an autologous tendon graft in several surgeries such as facial reconstruction (Jeng et al., 2004), ulnar

collateral ligament reconstruction ("Tommy John Surgery")(Cain and Mathis, 2016), and palmar opponensplasty (Camitz, 1929; Rymer and Thomas, 2016), several functional and surgical studies have indicated that PL function may extend beyond roles such as a weak wrist flexor and tensor of the palmar aponeurosis. Although no differences in grip strength were observed between individuals with and without PL musculature (Sebastin et al., 2005), the PL may contribute significant strength to the thenar eminence based on its morphological relationship with the abductor pollicis brevis (APB). Gangata et al. (2010) compared thumb abduction strength between contralateral limbs in individuals with unilateral PL musculature. After accounting for differences in hand dominance, significantly greater thenar abduction strength was observed in the hand possessing the PL muscle (Gangata et al., 2010). Cadaveric morphological studies indicate that the PL terminal tendon serves as an origin to fascicles of the APB (Fahrer, 1973a, 1977; Simard and Roberge, 1988), which may provide the physical means for the transmission of force from the PL to the thenar eminence. Although the morphological relationship between the PL and APB has been described, there is a paucity of functional evidence of the PL in thenar function *in vivo*.

To date, the functional evidence supporting the PL in thenar contractions *in vivo* is limited to textbook descriptions (Kaplan, 1984), and brief conference proceedings (Fahrer, 1973b) that describe the PL as a synergist in thenar opposition and abduction movements. Furthermore, previous descriptions of electromyographic recordings of the PL during thenar abduction were recorded non-selectively over the skin surface and were likely confounded by signals of adjacent forearm musculature of the common flexor mass (Fahrer, 1973b). Therefore, the current understanding remains unclear whether the PL provides contributions to thenar movements.

1.3   Palmaris Brevis

1.3.1   Anatomy

Kaplan (1984) described the PB as the most mysterious muscle from a functional and developmental perspective. Located anterior to the hypothenar eminence, the PB originates from the palmar aponeurosis and inserts into the palmar skin and fascia of the ulnar aspect of the palm (Przystasz, 1977). Upon contraction, the PB produces visible dimpling along the ulnar aspect of the palm by drawing the skin radially. The supporting dorsal fascia of the PB contributes to the anterior wall of the piso-hamate tunnel, which contains both the ulnar artery and nerves (Shrewsbury et al., 1972). The PB is considered a phylogenetic remnant of the *panniculus carnosus*; an extensive sheet of skeletal muscle found in lower animal species (Bergman et al., 1985; Patil, 2013). The PB varies in morphological appearance and has been classified based on its development and course of muscle fibers (Przystasz, 1977). In a study of 104 upper limbs, the PB morphological variants were observed in almost equal frequencies with developed and regressive forms in 53 (52%) and 48 (48%) of cases, respectively. The developed forms of the PB can consist of one or more solid muscular plates, or muscle bundles, with the muscle fibers arranged either transversely or in a fan-shaped orientation (Przystasz, 1977). The regressive forms contain fewer muscle fibers that are interspersed in adipose tissue with a chaotic fiber arrangement (Przystasz, 1977). Absence of the PB was considered rare with only three extremities (2.9%) in which the PB could not be identified (Przystasz, 1977). Interestingly, no representative muscle fibers have been identified in the plantar fascia of the foot that could be considered homologous to the PB muscle (Jones, 1920). Despite comprehensive PB morphological investigations (Patil, 2013; Przystasz, 1977), there is lack of consensus in the literature regarding the functional role of the PB in the hand.

1.3.2   Function

From anatomical textbooks, the PB is purported to improve palmar grip by deepening the hollow of the palm thereby accentuating the hypothenar eminence (Moore et al., 2014; Standring and Gray, 2008); however, this has been questioned by some based

on comparative anatomy observations, in which, the PB persists in animal species incapable of palmar grasping (Shrewsbury et al., 1972). An alternative function proposed describes the PB in the protection of the neurovasculature of the piso-hamate tunnel during palmar compression and repetitive grasping (Przystasz, 1977; Shrewsbury et al., 1972); however, PB muscle architecture has not been investigated during dynamic conditions to confirm whether the PB is capable of significant changes in muscle architecture to provide a presumed protective barrier. Furthermore, the PB has been described as being under involuntary control (Eswaradass et al., 2014; Serratrice et al., 1995), which may suggest a smooth muscle composition consistent with other *panniculus carnosus* muscle derivatives such as the dartos muscle and corrigutar cutis ani (Bergman et al., 1985; Patil, 2013). Although several functional roles of the PB have been proposed, these functions have been inferred from static cadaveric observations and have not been evaluated experimentally under dynamic contraction conditions *in vivo*.

1.4　　Skeletal Muscle Histology

A skeletal muscle is composed of muscle fascicles, or bundles, containing multinucleated muscle fibers (Ross and Pawlina, 2011). Each muscle fiber may consist of up to 2000 myofibrils, which contain overlapping thick (myosin) and thin (actin) myofilaments that give skeletal muscle its characteristic striated appearance under light microscopy (Ross and Pawlina, 2011) (Figure 1.1). The actin and myosin are proteins bound between adjacent Z-lines within sarcomeres; the anatomical contractile units of myofibrils. Specifically, the myosin molecule is composed of two myosin heavy chains (MHC) and four myosin light chains. Each globular head of the myosin molecule contains an actin binding site and adenosine triphosphate (ATP) binding site responsible for cross-bridge formation and ATP hydrolysis, respectively (Ross and Pawlina, 2011). The myosin ATPase catalytic enzyme and MHC isoforms can provide a means for distinguishing muscle fiber identity. The basis for muscle fiber classification involves

identification of a specific enzyme or structural protein indicative of its contractile and metabolic function; however, not all methods are considered steadfast techniques.
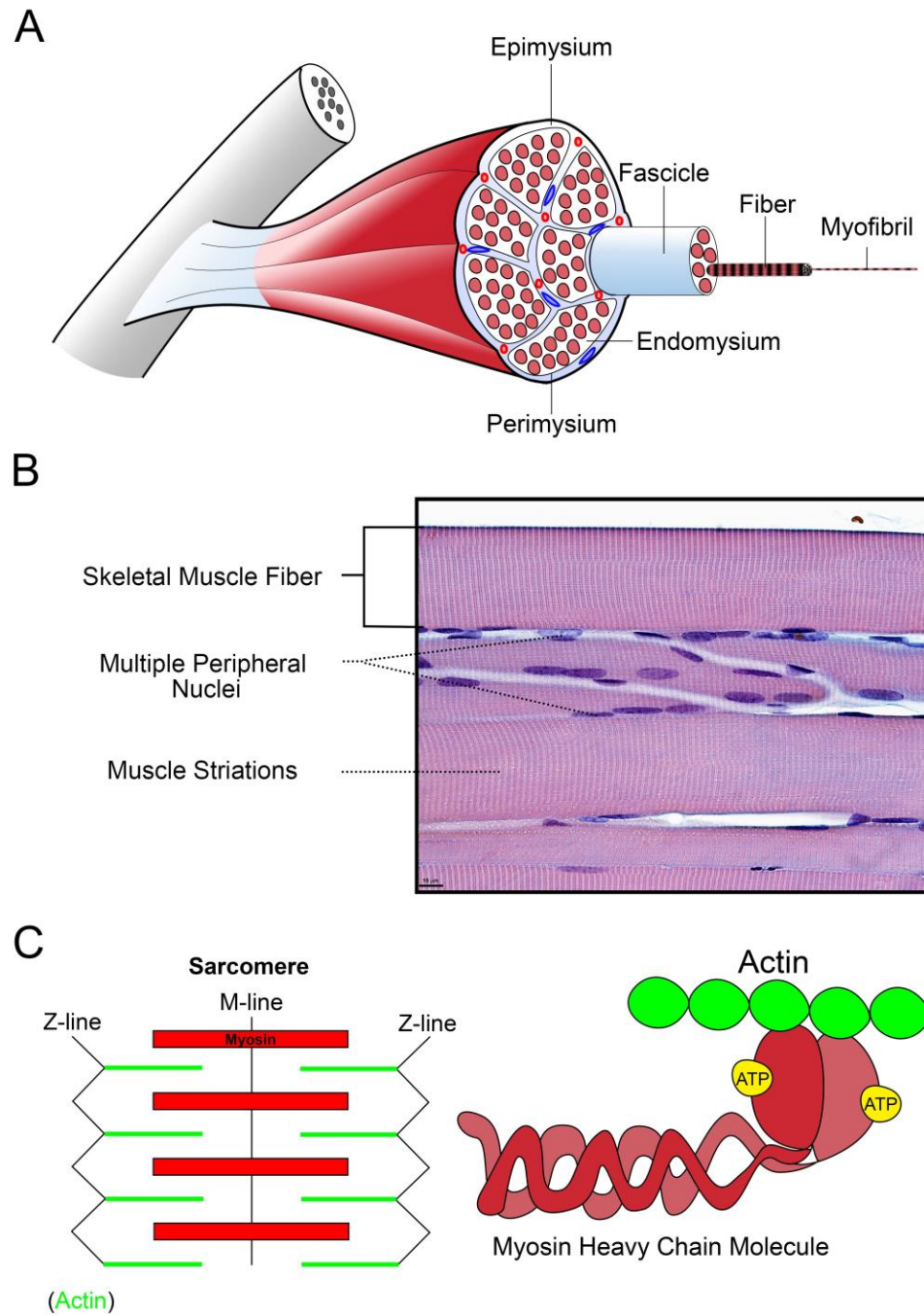
Figure 1.1 Anatomical Organization of Skeletal Muscle

(A) Gross structure and organization of skeletal muscle; (B) Histological appearance of skeletal muscle tissue; (C) Sarcomere structure and constituent myofilaments proteins: actin and myosin. Histological image inset from Hill (2018)

1.5   Muscle Function Determination Methods

1.5.1   Muscle Fiber Type Classification

Human skeletal muscles are composed of a heterogeneous fiber type composition resulting in a mosaic pattern of muscle fibers with differential physiological, metabolic, and biochemical properties. The fiber type heterogeneity within a skeletal muscle allows the tissue to adapt to a variety of functional demands. Several fiber type classification systems have been developed using histochemical (myosin ATPase), biochemical (oxidative enzymes), and immunohistochemical (MHC isoforms) staining techniques (Bottinelli and Reggiani, 2000) that provide insight into metabolic and contractile function of muscle fibers. Knowledge of the constituent fiber population of a given skeletal muscle can provide further insight into its functional specialization, especially if a predominant fiber type is evident.

1.5.1.1   Myosin ATPase Fiber Type Classification

Histochemical staining utilizes by-products from chemical reactions occurring within the tissues as the means for fiber identification. In actin and myosin cross-bridge formation, ATP hydrolysis occurs on the ATP binding site on the myosin globular head (Figure 1.1), in which, myosin ATPase acts as catalyst according to the following reaction (MacIntosh et al., 2006):

Mysosin ATPase

$$ATP + H_2O \rightarrow ADP + P_i + H^+$$

By reacting inorganic phosphate (P_i) with calcium through a series of steps to form calcium phosphate, a dark precipitate forms when further reacted with cobalt sulfide highlighting the metabolic activity of the muscle fiber. Importantly, by pre-incubating the muscle tissue in acidic or basic environments, the myosin ATPase activity can be inhibited in fast (IIa, IIx), and slow (I) fibers, respectively, thereby allowing for identification of different fiber types based on staining intensity (Brooke and Kaiser, 1970). Using this technique, three original fiber types have been identified as type I, IIA,

IIB, and several other intermediate types; however, the classification system may be problematic as the staining intensities may be grouped differently depending on the researcher and procedures (Scott et al., 2001). Furthermore, myosin ATPase hydrolysis rates of fast fibers are two to three times greater than slow fibers; however, the myosin ATPase staining does not reflect the relative ATPase hydrolysis rates, but only their staining intensities (Scott et al., 2001).

1.5.1.2   Biochemical Enzymatic Classification

Biochemical techniques staining for oxidative mitochondrial enzymes, or glycolytic enzymes has led to classification of fibers based on their metabolic properties: slow-twitch (SO), fast-twitch oxidative (FOG), fast-twitch glycolytic (FG) (Scott et al., 2001). Although type I fibers identified through myosin ATPase staining correlate with fibers relying on oxidative metabolism (slow-twitch oxidative), type IIA and IIB fiber classifications cannot be used interchangeably with FOG or FG fibers as they do not always correlate strongly with their metabolism (Scott et al., 2001) (Table 1.1). Unsuccessful fiber type classification using metabolic enzymes is largely due to the variability in aerobic/anaerobic enzyme activities, irrespective of the myosin ATPase fiber identity (Bottinelli and Reggiani, 2000).

Table 1.1 Comparison of Muscle Fiber Type Classification Systems

Table adapted from Scott et al. 2001

1.5.1.3   Immunohistochemical Identification of Myosin Heavy Chain Isoforms

The functional and contractile properties of human muscles depend on the specific myosin isoforms found within their constituent muscle fibers. Using myosin-specific antibodies, major human myosin isoforms have been identified, MHC I, MHC IIa, MHC IIx, which correspond to the myosin ATPase-based fibers (I, IIA, IIB) likely due to the globular myosin head acting as a molecular motor and the site of ATP hydrolysis (Scott et al., 2001) (Table 1).   From single muscle fiber studies, the complement of MHC isoforms is a major determinant of several functional fiber properties including shortening velocity, isometric tension, power, and ATP consumption (Schiaffino and Reggiani, 2011). Generally, all mammalian muscle fibers demonstrate an orderly increase in peak power (isometric tension x shortening velocity) from slow to fast myosin isoforms (MHC I < MHC IIa < MHC IIx) (Schiaffino and Reggiani, 2011). Furthermore, the ATP consumed per unit time and per unit tension is less in slow compared to fast MHC isoforms, which makes slow fibers more energetically suitable for maintaining tension for muscles of postural activity such as the soleus (>80% type I) (Johnson et al., 1973; Schiaffino and Reggiani, 2011).

1.5.1.3.1   Myosin Heavy Chain Co-expression

Muscle fibers expressing a single MHC isoform are considered pure fibers, whereas those fibers co-expressing multiple MHC isoforms within its sarcoplasm are considered hybrid fibers (Pette and Staron, 2001). Hybrid fibers demonstrate co-expression of combinations of MHC isoforms (ex: I/IIa, IIa/IIx) and are often observed in aged muscle (Scott et al., 2001). In normal healthy aging, a progressive loss of muscle mass leads to a reduction in muscle function and reduces the functional capacity of elderly individuals in the performance of activities of daily living. Age-related muscle atrophy results from concomitant loss of type I and type II motor units with potential for preferential type II motor unit loss (Scott et al., 2001). The mechanism associated with MHC co-expression is reinnervation of "abandoned" muscle fibers by adjacent healthy

neurons, which may also lead to fiber type grouping (Hepple and Rice, 2016). In the vastus lateralis muscle tissue from aged people (>85y), fibers co-expressing type I/IIa and IIa/IIx MHC isoforms consisted of 29% and 22% of the fiber population, respectively (Andersen et al., 1999). Although muscle fibers co-expressing two isoforms have intermediate force-velocity properties compared to their pure counterparts (Bottinelli et al., 1996), the functional contributions of fibers with multiple MHC isoforms to whole-muscle function remains unclear.

1.5.1.3.2   The Motor Unit

The former section described muscle fibers as independent structures; however, the functional unit of the neuromuscular system and the basis for electromyography is the motor unit: an alpha motor neuron and all the muscle fibers it innervates (MacIntosh et al., 2006). Importantly, the muscle fibers of a single motor unit are identical in fiber type and within the given muscle volume the fibers of single units are intermingled with other units, which contribute to the mosaic pattern observed upon fiber type staining (MacIntosh et al., 2006). From single motor unit studies, three types of motor units have been identified based on their contraction time, twitch force and histochemical fiber type appearance: S (slow contracting), FR (Fast, Fatigue Resistant), FF (Fast, Fatigable) (MacIntosh et al., 2006). The proportion of slow to fast motor units within a skeletal muscle will contribute to its overall muscle function based on their contractile and histochemical characteristics (Table 1.2).

Table 1.2 Motor Unit Classification

Properties	Motor Unit Types		
	Slow (S)	Fast (FR)	Fast (FF)
Fiber Identity	SO / I	FOG / IIA	FG / IIX
Twitch Speed	Slow	Fast	Fast
Twitch Force	Small	Intermediate	Large
Fatigability	Low	Low	High
Red Color	Dark	Dark	Pale
Myoglobin	High	High	Low
Capillary Density	Rich	Rich	Poor
Mitochondria	Many	Many	Few
Glycogen	Low	High	High
Oxidative Enzymes	High	Medium-high	Low

FR: Fast fatigue resistant, FF: Fast fatigable, SO: Slow oxidative, FOG: Fast oxidative/glycolytic, FG: Fast glycolytic. Table adapted from MacIntosh et al. (2006)

1.5.2　Fine Wire Electromyography

Electromyography (EMG) is a valuable technique for studying muscle activity and human movement (Kamen and Gabriel, 2010). Recording and comparing the summation of action potentials obtained from motor units during specific movements can be useful in determining muscle function. Gross muscle activity can be recorded using surface electrodes or more focused and stable motor unit recordings can be obtained using indwelling fine wire recording techniques. Although surface EMG is frequently used in research exploring human muscular actions, the EMG signals recorded at the skin surface are summated action potentials likely generated by several motor units of adjacent and deep musculature in addition to the muscle of interest (cross-talk phenomenon) (Mogk and Keir, 2003). Furthermore, a muscle may move significantly relative to the recording electrodes fixed on the skin surface, which may further confound surface EMG recordings. A minimally invasive technique that can overcome these issues is the use of indwelling EMG electrodes.

Fine wire electrodes involve inserting hook-tipped wires (gauge: 50-100μm) into an individual muscle through a hypodermic needle (Basmajian and Stecko, 1962). Indwelling fine wire electrodes overcome many of the limitations associated with surface EMG including cross-talk contamination and recording specificity during dynamic contractions (Kamen and Gabriel, 2010). Indwelling fine wire EMG has been useful in determining the functional anatomy of muscles composed of several compartments (van Oudenaarde and Oostendorp, 1995) and several distinct muscular heads (Basmajian et al., 1972) such as the abductor pollicis longus and the quadriceps muscle. Although there are many advantages to this technique, the indwelling fine wires may cause some participant discomfort upon placement. Overall, indwelling fine wire recordings allow for study of individual muscles, which cannot be achieved confidently or reliably using surface EMG recordings.

1.5.3   Ultrasound Imaging

The gross architectural arrangement of muscle fibers can further contribute to the understanding of muscle function. Although magnetic resonance imaging is considered the gold standard for muscle architecture measurements, ultrasound imaging is considered a valid technique for parameters such as muscle length, width, thickness, and cross-sectional area (Whittaker and Stokes, 2011). Conventional brightness mode (B-mode) ultrasound imaging involves generating a gray-scale image based on tissue reflection of ultrasound waves. The image generated is dependent upon location, amplitude, and reflection time of the ultrasound waves relative to the probe (Whittaker and Stokes, 2011). Ultrasound images are sensitive to the collagen content of tissues as regions with dense collagen reflect ultrasound waves more readily than regions of sparse collagen content, and appear bright (hyperechoic) or dark (hypoechoic), respectfully (Whittaker and Stokes, 2011). Because muscles are highly compartmentalized with distinct connective tissue boundaries (epimysium, perimysium, endomysium) (Figure 1.1), the epimysium layer appears hyperechoic, whereas the muscle tissue proper appears hypoechoic due to the presence of tissue fluids (Ross and Pawlina, 2011; Whittaker and Stokes, 2011) (Figure 1.2).

Ultrasound imaging is advantageous for its ability to visualize dynamic movements of skeletal muscle in both relaxed and contracted states. Although ultrasound is useful in detecting dynamic changes in muscle, the image is a two-dimensional representation of a three-dimensional structure, and therefore, requires a fundamental knowledge of cross-sectional gross anatomy and appreciation of how adjacent musculature might influence morphological changes in the muscle of interest. For example, reductions in rectus femoris muscle width and cross-sectional area were observed in maximal knee extension possibly due to competing forces from the vastus medialis, lateralis and intermedius (Delaney et al., 2010). Despite these challenges, ultrasound imaging is a valuable method in assessing muscle function by quantifying the change in muscle architecture during functional contraction tasks.
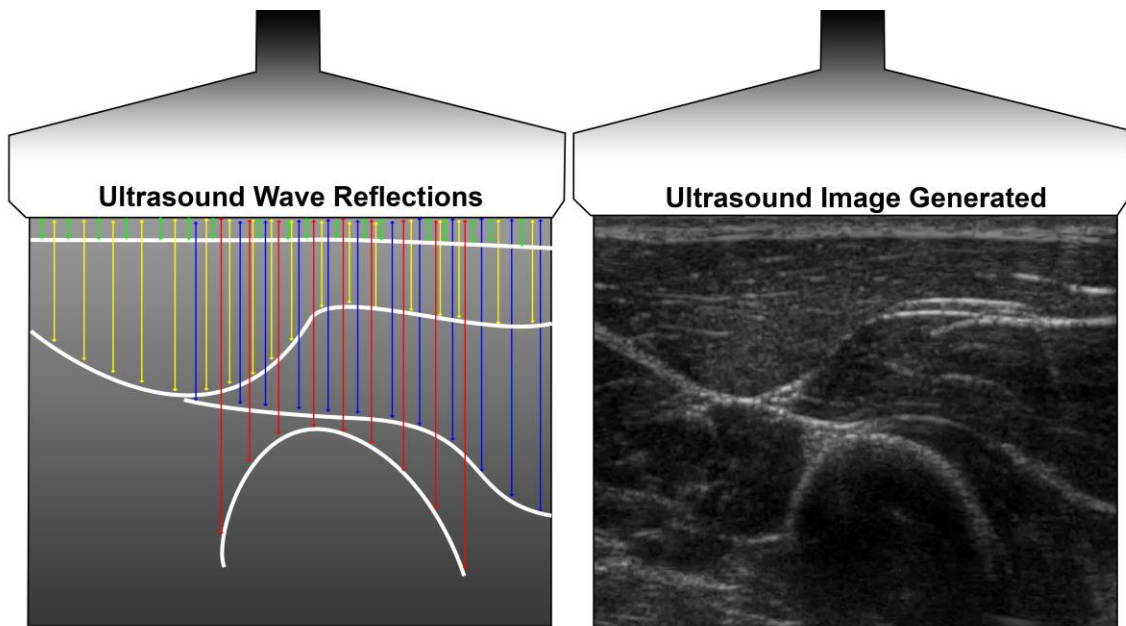
Figure 1.2 Reflection of Sound Waves in Ultrasound Image Generation

Left panel: Ultrasound waves are directed from the linear array probe and appear bright when reflected from regions of densely packed collagen (ex: epimysium, bone); *Right panel*: An exemplar ultrasound image demonstrating bright (hyperechoic) and dark (hypoechoic) reflections from human tissues.

1.6   Purpose

Using several experimental techniques briefly reviewed above, the overall purpose of this dissertation was to determine the functional role of the PL and PB in the hand. Previous investigations of these muscles are limited to cadaveric observations and have not been studied comprehensively during dynamic movements *in vivo*. In Chapter 2 the purpose was to determine whether the PL contributes to thenar contractions by recording its relative muscle activity and changes in muscle architecture during specific thumb movements. Thus, this study was fundamental in determining whether the palmaris longus functions as a synergist in thenar contractions. In Chapter 3 the purpose was to investigate the muscle fiber type composition of the APB with respect to its contiguous morphological relationship with the palmaris longus. Thus, the results of this study provide further insight into the PL and APB acting as a digastric unit with distinct fiber type characteristics when contiguously arranged. In Chapter 4, the purpose was to investigate the functional role of the PB by recording its muscle activity during specific grasping movements and quantifying changes in muscle architecture in response to voluntary contractions of the fifth digit. Thus, the results provide further insight into postulates suggesting the PB functions as a muscular barrier to ulnar neurovasculature. In Chapter 5, the PB muscle fiber type composition was investigated to determine the proportions of type I and type II muscles fibers. Thus, the results provide further indirect insight into the contractile capacity of the PB and its potential protective function during intermittent grasping movements. Overall, this dissertation provides functional insight into the role of the PL and PB in the human hand, *in vivo*. By using several experimental modalities *in vivo* and *in situ*, the proposed role of the PL and PB as an extrinsic thenar muscle and protective barrier can be evaluated, respectfully. These studies contribute to the literature by improving our functional understanding of hand musculature.

1.7   References

Ahn DS, Yoon ES, Koo SH, Park SH. 2000. A prospective study of the anatomic variations of the median nerve in the carpal tunnel in Asians. Ann Plast Surg 44:282-287.

Andersen JL, Terzis G, Kryger A. 1999. Increase in the degree of coexpression of myosin heavy chain isoforms in skeletal muscle fibers of the very old. Muscle Nerve 22:449-454.

Backhouse K, Churchill-Davidson D. 1975. Anomalous palmaris longus muscle producing carpal tunnel-like compression. Hand 7:22-24.

Basmajian JV. 1974. Muscles alive: their functions revealed by electromyography, 3rd ed. Baltimore: Williams & Wilkins.

Basmajian JV. 1980. Electromyography--dynamic gross anatomy: a review. Am J Anat 159:245-260.

Basmajian JV, Harden TP, Regenos EM. 1972. Integrated actions of the four heads of quadriceps femoris: an electromyographic study. Anat Rec 172:15-20.

Basmajian JV, Stecko G. 1962. A new bipolar electrode for electromyography. J Appl Physiol 17:849-849.

Bergman RA, Thompson SA, Afifi AK, Saadeh FA. 1985. Anatomy Atlases: Illustrated encyclopedia of human anatomic variation: Opus I: Muscular system: Alphabetical listing of muscles: P: Panniculus Carnosus. In.

Bottinelli R, Canepari M, Pellegrino MA, Reggiani C. 1996. Force-velocity properties of human skeletal muscle fibres: myosin heavy chain isoform and temperature dependence. J Physiol 495 (Pt 2):573-586.

Bottinelli R, Reggiani C. 2000. Human skeletal muscle fibres: molecular and functional diversity. Prog Biophys Mol Biol 73:195-262.

Brinkman RJ, Hage JJ. 2016. The first description of the absence of the palmaris longus muscle. J Plast Surg Hand Surg 50:56-58.

Brooke MH, Kaiser KK. 1970. Three "myosin adenosine triphosphatase" systems: the nature of their pH lability and sulfhydryl dependence. J Histochem Cytochem 18:670-672.

Cain EL, Mathis TP. 2016. Ulnar collateral ligament reconstruction: current philosophy in 2016. Am J Orthop (Belle Mead NJ) 45:E534-E540.

Camitz H. 1929. Surgical treatment of paralysis of opponens muscle of thumbs. Acta Chir Scand 65:77-81.

Ceyhan O, Mavt A. 1997. Distribution of agenesis of palmaris longus muscle in 12 to 18 years old age groups. Indian J Med Sci 51:156-160.

Delaney S, Worsley P, Warner M, Taylor M, Stokes M. 2010. Assessing contractile ability of the quadriceps muscle using ultrasound imaging. Muscle Nerve 42:530-538.

Duchenne G-B. 1959. Physiology of motion demonstrated by means of electrical stimulation and clinical observation and applied to the study of paralysis and deformities: WB Saunders.

Eric M, Koprivcic I, Vucinic N, Radic R, Krivokuca D, Leksan I, Selthofer R. 2011. Prevalence of the palmaris longus in relation to the hand dominance. Surg Radiol Anat 33:481-484.

Eswaradass PV, Kalidoss R, Ramasamy B, Gnanashanmugham G. 2014. Familial palmaris brevis spasm syndrome. Ann Indian Acad Neurol 17:141-142.

Fahrer M. 1973a. Lumbricals of Thumb. J Anat 114:157.

Fahrer M. 1973b. Proceedings: the role of the palmaris longus muscle in the abduction of the thumb. J Anat 116:476.

Fahrer M. 1977. On the form and function of the abductor pollicis brevis muscle. Aust N Z J Surg 47:243-247.

Galvani L. 1791. D viribus electricitatis in motu musculari: Commentarius. Bologna: Tip Istituto delle Scienze, 1791; 58 p: 4 tavv ft; in 4; DCC f 70.

Gangata H, Ndou R, Louw G. 2010. The contribution of the palmaris longus muscle to the strength of thumb abduction. Clin Anat 23:431-436.

Gilroy A. 2013. Anatomy An Essential Textbook. New York: Thieme Medical Publishers.

Hepple RT, Rice CL. 2016. Innervation and neuromuscular control in ageing skeletal muscle. J Physiol 594:1965-1978.

Hill MA. 2018. Embryology Skeletal muscle histology 007.jpg. In.

Jeng SF, Kuo YR, Wei FC, Su CY, Chien CY. 2004. Total lower lip reconstruction with a composite radial forearm-palmaris longus tendon flap: a clinical series. Plast Reconstr Surg 113:19-23.

Johnson MA, Polgar J, Weightman D, Appleton D. 1973. Data on the distribution of fibre types in thirty-six human muscles. An autopsy study. J Neurol Sci 18:111-129.

Jones FW. 1920. The Principles of Anatomy as Seen in the Hand. London: J. &. A. Churchill.

Kamen G, Gabriel D. 2010. Essentials of electromyography: Human kinetics.

Kaplan EB. 1984. Kaplan's functional and surgical anatomy of the hand. Philadelphia: Lippincott Williams & Wilkins.

MacIntosh BR, Gardiner PF, McComas AJ. 2006. Skeletal muscle: form and function: Human Kinetics.

Mogk JP, Keir PJ. 2003. Crosstalk in surface electromyography of the proximal forearm during gripping tasks. J Electromyogr Kinesiol 13:63-71.

Montague MF. 1947. The missing forearm muscle; a case of non-familial bilateral absence of the palmaris longus muscle in man. J Hered 38:7-9.

Moore KL, Dalley AF, Agur AMR. 2014. Clinically Oriented Anatomy, 7th ed. Philadelphia Lippincott Williams & Wilkins.

Morais M, Santos W, Malysz T. 2013. Agenesis of Palmaris longus muscle: is this a phenotype of variable expressivity. J Morphol Sci 30:249-253.

Pai MM, Prabhu LV, Nayak SR, Madhyastha S, Vadgaonkar R, Krishnamurthy A, Kumar A. 2008. The palmaris longus muscle: its anatomic variations and functional morphology. Rom J Morphol Embryol 49:215-217.

Patil S. 2013. Clinico-anatomical Considerations Of Palmaris Brevis Muscle. International Journal of Advanced Research 1:341-344.

Pette D, Staron RS. 2001. Transitions of muscle fiber phenotypic profiles. Histochem Cell Biol 115:359-372.

Przystasz T. 1977. Morphology of the palmaris brevis muscle in man. Folia Morphol (Warsz) 36:77-82.

Reimann AF, Daseler EH, Anson BJ, Beaton LE. 1944. The palmaris longus muscle and tendon a study of 1600 extremities. Anat Rec 89:495-505.

Ross MH, Pawlina W. 2011. Histology: a text and atlas : with correlated cell and molecular biology, 6th ed. Philadelphia: Wolters Kluwer/Lippincott Williams & Wilkins Health.

Rymer B, Thomas PB. 2016. The Camitz transfer and its modifications: a review. J Hand Surg Eur Vol 41:632-637.

Schiaffino S, Reggiani C. 2011. Fiber types in mammalian skeletal muscles. Physiol Rev 91:1447-1531.

Scott W, Stevens J, Binder-Macleod SA. 2001. Human skeletal muscle fiber type classifications. Phys Ther 81:1810-1816.

Sebastin SJ, Lim AY, Bee WH, Wong TC, Methil BV. 2005. Does the absence of the palmaris longus affect grip and pinch strength? J Hand Surg Br 30:406-408.

Serratrice G, Azulay JP, Serratrice J, Pouget J. 1995. Palmaris brevis spasm syndrome. J Neurol Neurosurg Psychiatry 59:182-184.

Shrewsbury MM, Johnson RK, Ousterhout DK. 1972. The palmaris brevis--a reconsideration of its anatomy and possible function. J Bone Joint Surg Am 54:344-348.

Simard T, Roberge J. 1988. Human abductor pollicis brevis muscle "divisions" and the nerve hila. Anat Rec 222:426-436.

Standring S, Gray H. 2008. Gray's anatomy: the anatomical basis of clinical practice, 40th, anniversary ed. Edinburgh: Churchill Livingstone/Elsevier.

Stecco C, Lancerotto L, Porzionato A, Macchi V, Tiengo C, Parenti A, Sanudo JR, De Caro R. 2009. The palmaris longus muscle and its relations with the antebrachial fascia and the palmar aponeurosis. Clin Anat 22:221-229.

Tubbs RS, Louis RG, Jr., Loukas M, Gupta AA, Shoja MM, Oakes J. 2007. The first description of the palmaris brevis muscle. J Hand Surg Eur Vol 32:382-383.

van Oudenaarde E, Oostendorp RAB. 1995. Functional-Relationship between the Abductor Pollicis Longus and Abductor Pollicis Brevis Muscles - an Emg Analysis. J Anat 186:509-515.

Whittaker JL, Stokes M. 2011. Ultrasound imaging and muscle function. J Orthop Sports Phys Ther 41:572-580.

Chapter 2

2 Investigating the Palmaris Longus as a Thenar Synergist[1]

2.1 Introduction

The palmaris longus (PL) is a slender fusiform muscle situated in the proximal forearm between the flexor carpi radialis (FCR) laterally and the flexor carpi ulnaris medially. Considered one of the most variable muscles in the human body, the PL is absent in approximately 13% of forearms with bilateral agenesis (8%) occurring more frequently than unilateral agenesis compared to left (4%) and right (5%) forearms alone (Reimann et al. 1944). In certain mammalian species (Orangutans) that use their forelimbs for weight bearing and ambulation, the PL is well developed which may explain its regression in the forearms of humans (Stecco et al. 2009). Anatomical textbooks typically characterize the PL as a weak wrist flexor and tensor of the palmar aponeurosis (Gilroy, 2013; Moore et al. 2014); however, the PL may also act as a functional anchor to the palmar skin and fascia in resisting horizontal shear forces (Standring, 2008). Although generally considered a muscle of insignificance in humans, the PL may provide further functional contributions *in vivo* beyond wrist flexion as a thenar synergist in conjunction with the abductor pollicis brevis.

For hand surgeons, restoring thumb opposition by surgical tendon transfer is challenging because this action requires a complex combination of thumb abduction, flexion, and pronation of the metacarpophalangeal (MCP) joint (Park et al. 2010). Camitz (1929) developed a surgical technique to restore thumb opposition that mobilizes the PL

---

[1] A version of this chapter has been published. Used with permission from John Wiley and Sons Inc.

Moore CW, Fanous J, Rice CL. 2017. Revisiting the Functional Anatomy of the Palmaris Longus as a Thenar Synergist. Clin Anat. (IN-PRESS)

tendon with a continuous extension of palmar fascia for insertion on radial side of the MCP joint. Through surgical PL tendon transfer approaches, restoration of functional palmar movements can be achieved allowing patients to perform activities of daily living such as writing and the ability to pick up fine objects (Foucher et al. 1991; Gilbert et al. 1999). Kaplan (1984) considered the PL as a synergist in thumb opposition and described its insertion into the abductor pollicis brevis as a consistent feature, which may explain its effectiveness in restoring functional thumb movements through surgical tendon transfer (Foucher et al. 1991; Rymer and Thomas, 2016).

Despite the proposal for the universal acceptance of thenar abduction as a normative function of the PL (Gangata et al. 2010), little direct functional evidence in support of the PL in thumb abduction can be found in the literature beyond brief descriptions from conference proceedings (Fahrer, 1973) and cadaveric descriptions (Fahrer and Tubiana, 1976). By establishing that a functional synergy exists between the PL and thenar musculature, mechanistic insight into the clinical efficacy of the PL in surgical tendon transfer can be gained, and may provide evidence for alternative surgical transfer approaches utilizing the PL in conjunction with discrete fascicles of the abductor pollicis brevis as proposed by Fahrer and Tubiana (1976). Thus, the purpose of this study was to systematically investigate PL muscle activity in healthy participants *in vivo* during specific thumb movements using indwelling fine wire electromyographic (EMG) recording techniques. Furthermore, dynamic changes in PL muscle architecture during thumb movements were visualized using ultrasound imaging to support the EMG findings. It was hypothesized that the greatest relative PL muscle activity and changes in muscle architecture would be observed during thumb abduction based on previous morphological evidence and isometric strength assessments reported in the literature.

2.2   Materials and Methods

2.2.1   Participants

Ten healthy Caucasian males (ages: 26 ± 5 years) were recruited to participate in the EMG investigation. The local research ethics board approved the study procedures and informed written consent was obtained from each participant prior to testing. The PL and flexor carpi radialis (FCR) were investigated in the dominant limb (right forearm: 8) in all participants except in two participants in which the non-dominant limb (left forearm: 2) was investigated due to PL absence, and the other had a previous history of surgical intervention at the wrist. Schaeffer's test was used to determine the presence of the palmaris longus tendon at the wrist, in which participants were instructed to oppose the thumb to the fifth digit in each hand (Schaeffer, 1909). A positive test indicated the presence of the PL tendon. The experimental protocol required participants to attend two separate testing sessions: (1) PL and FCR EMG session followed by (2) a PL ultrasound session.

Two cadaveric upper limbs were dissected and photographed to visualize some of the morphological relationships found between the PL tendon and the APB at the wrist. All cadaveric specimens used in this study were obtained through the local institution's body donation program with permission from the Committee for Cadaveric Use in Research (REF#: 21092016).

2.2.2   EMG Experimental Setup

In each participant, the PL was identified using ultrasound imaging and the location of the muscle belly was marked on the skin to facilitate insertion of indwelling fine wires (See *ultrasound imaging*). Because the PL may play a minor role in elbow stabilization, an additional muscle of the common flexor origin, the FCR, was also investigated concurrently for relative EMG contributions to the wrist and thumb actions. The position of the FCR also was determined using ultrasound imaging and its location was marked on the skin. For the EMG recordings, the skin was prepared by applying a

70% ethanol solution prior to insertion of hooked-tip bipolar indwelling fine wires (California Fine Wire Company, Grover Beach, CA; 100 μm). Use of indwelling fine wire electrodes was necessary to provide direct evidence of PL activation beyond previous descriptions of PL EMG recordings from the skin surface in which signals from adjacent forearm musculature (FCR, flexor carpi ulnaris, flexor digitorum superficialis) can confound EMG recordings (Fahrer, 1973). After autoclave sterilization procedures, the wire insulation was removed by brief exposure to a flame creating a recording surface on the wire tips of approximately five mm. The indwelling fine wires were inserted into the PL and FCR muscles via a sterilized hypodermic needle (25 G x 5/8 Becton Dickinson EclipseTM Needle, Franklin Lakes, NJ) (Basmajian and Stecko, 1962), which was withdrawn leaving the hooked wires embedded temporarily in the muscle for the duration of the EMG experimentation session. Surface EMG was recorded from the thumb musculature by placing two Ag–AgCl cloth electrodes (H59P monitoring electrodes, Kendall, Mansfield, MA, USA) on the thenar eminence.

2.2.3   EMG Normalization

Participants were seated at a Cybex Humac Norm Dynamometer (CSMi Medical Solutions, Stoughton, MA) with their forearm fully supinated and supported by a padded bar while grasping a torque manipulandum (Figure 2.1). Wrist flexion torque was recorded from the dynamometer and sampled at 500 Hz with a 12-bit analog-to-digital converter (Power 1401, Cambridge Electronic Design, Cambridge, UK) using Spike2 software (v. 7.0, Cambridge Electronic Design). Three maximal isometric voluntary contractions (MVCs) of wrist flexion were performed and the PL and FCR EMG recordings from the largest MVC were used to normalize EMG recorded during the specific thumb movements (Figure 2.1). The MVC bouts were separated by three minutes of rest to minimize fatigue. Verbal encouragement and a visual display of the torque tracings were displayed on a computer monitor for each participant.
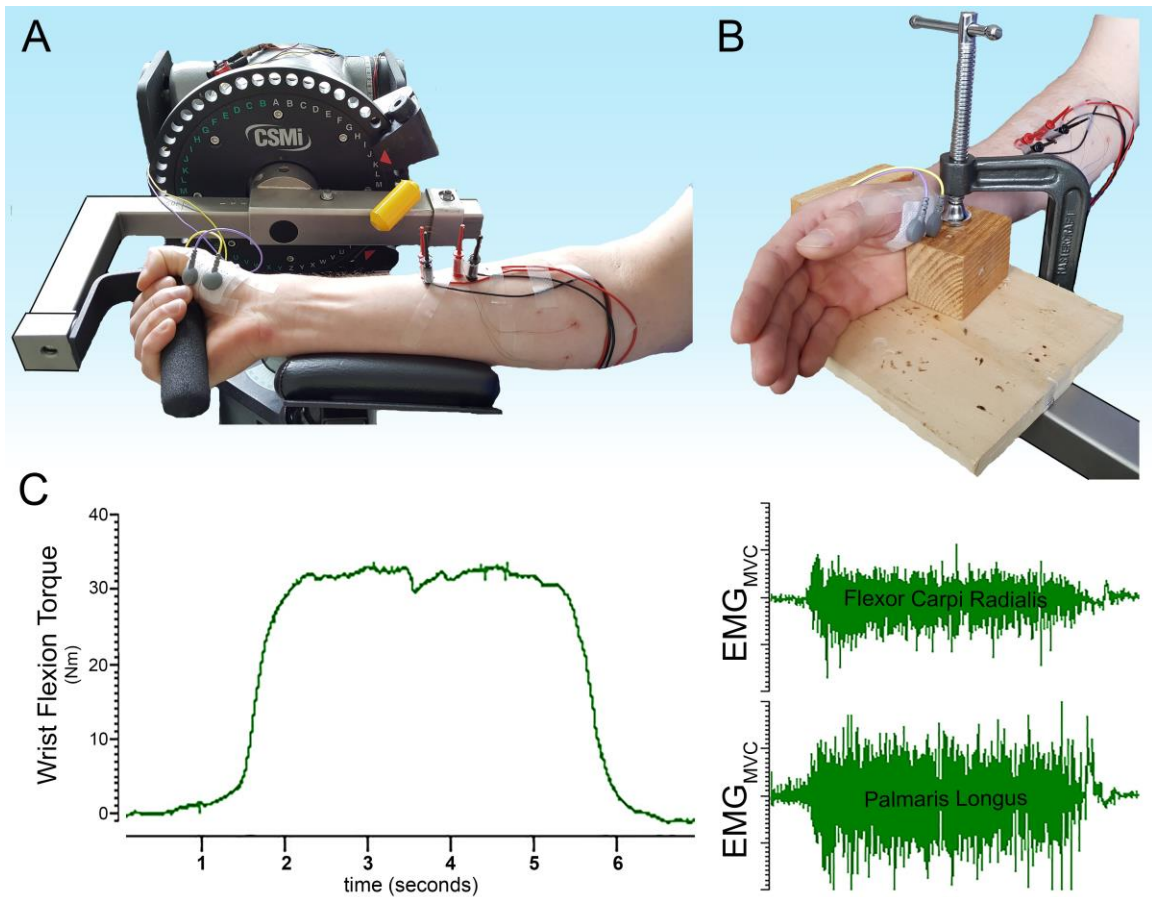
Figure 2.1: Electromyography Experimental Setup and Recordings

(A) Indwelling electromyography (EMG) experimental setup to record palmaris longus (PL) and flexor carpi radialis (FCR) muscle activity during maximal wrist flexion contractions. (B) Custom-made apparatus used to secure the wrist in a neutral position to record PL and FCR activity during thenar movements alone (C) Exemplar PL and FCR EMG recordings during the maximal wrist flexion contraction recorded over a 6-second time interval.

2.2.4   Experimental Setup for Thenar Movement Tasks

To examine the potential role of the PL as a synergist in thumb movement, the wrist was secured in a neutral position to prevent wrist flexion using a custom-made apparatus (Figure 2.2). A wooden block secured the wrist in a neutral position, but still allowed for free movements of the thumb. Participants were instructed to make the following thumb movements while secured in the apparatus: abduction, flexion, opposition, extension, adduction, and circumduction (Figure 2.2). Participants were instructed to make maximal isometric contractions when completing each thumb movement, except for circumduction, which was a non-resisted task consisting of circular thumb movements. Importantly, each resisted task was standardized amongst all participants, in which, the thumb movements were performed against a fixed rigid metal plate (abduction, adduction, extension), cylinder (flexion) or between the thumb and fifth digit (opposition) (Figure 2.2).

Muscle activity was recorded from the PL and FCR during each thumb movement. The root mean square (RMS) amplitude was averaged over a one second time interval for each thumb action. The relative activations of the PL and FCR during the thumb movements were determined by dividing the respective RMS amplitudes during each individual thumb movement by the maximal RMS amplitude recorded from the PL and FCR during maximal wrist flexion over an identical time epoch of one second. A minimum rest period of two minutes was provided between thumb movement tasks to prevent muscle fatigue.
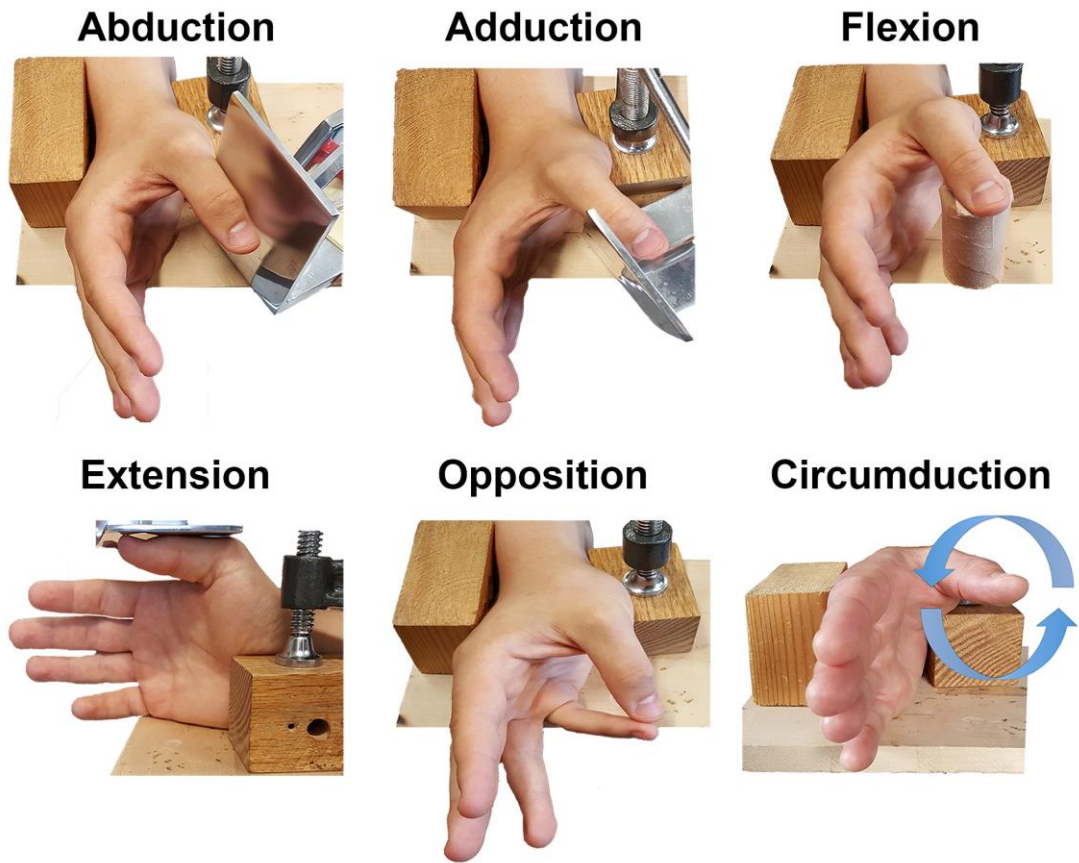
Figure 2.2 Standardized Hand Positions for Thenar Contractions Tasks

Standardized thenar contraction tasks in which palmaris longus and flexor carpi radialis electromyographic recordings were monitored. Note: all movements were maximal contractions except circumduction, which was a non-resisted task.

2.2.5   Ultrasound Imaging

A Vivid-7 ultrasound system (GE Healthcare, Mississauga, ON, Canada; linear array probe: GE model M12L, 4.9 mm, 5–13 MHz) was used to visualize morphological changes in PL muscle thickness (M_T) from rest to contraction when performing thumb abduction and adduction. All muscle measurements were made using the following scan parameters: depth = 4.0 cm, frequency = 11.4 MHz, frames per second = 13.7, power = 0 dB. Ultrasound images at rest and contraction were made at the midpoint of the PL muscle belly, which was determined by measuring half the distance between the PL myotendinous junction (determined by ultrasound) and the medial epicondyle of the humerus (Figure 2.2). A large piece of cloth tape was placed transversely on the skin at the midpoint of the PL muscle to facilitate consistent placement of the ultrasound probe. A liberal application of ultrasound gel (Aquasonic 100 Ultrasound transmission gel, Parker Laboratories) was applied to the skin surface to facilitate optimal imaging quality. Upon securing the wrist in the custom-made apparatus described above, the participants were instructed to perform a series of maximal isometric thumb abduction and adduction movements against a rigid metal plate (Figure 2.3). Participants were instructed to gradually abduct and adduct their thumbs to prevent abrupt forearm movements that could affect placement of the ultrasound probe. The PL was imaged three times at rest and contraction during abduction and adduction, respectively.

Ultrasound images were exported and analyzed using OsiriX imaging software (version 8.0.2, Geneva, Switzerland). The PL muscle borders were determined using the hyper-echoic reflections produced by the epimysium surrounding the muscle (Figure 2.4) (Pillen, 2010). PL M_T was determined at rest and contraction by measuring the distance between the superficial and deep muscle borders using the length tool in OsiriX. The three PL M_T measurements from the thumb abduction and adduction tasks were averaged to obtain a mean M_T score for rest and contraction.
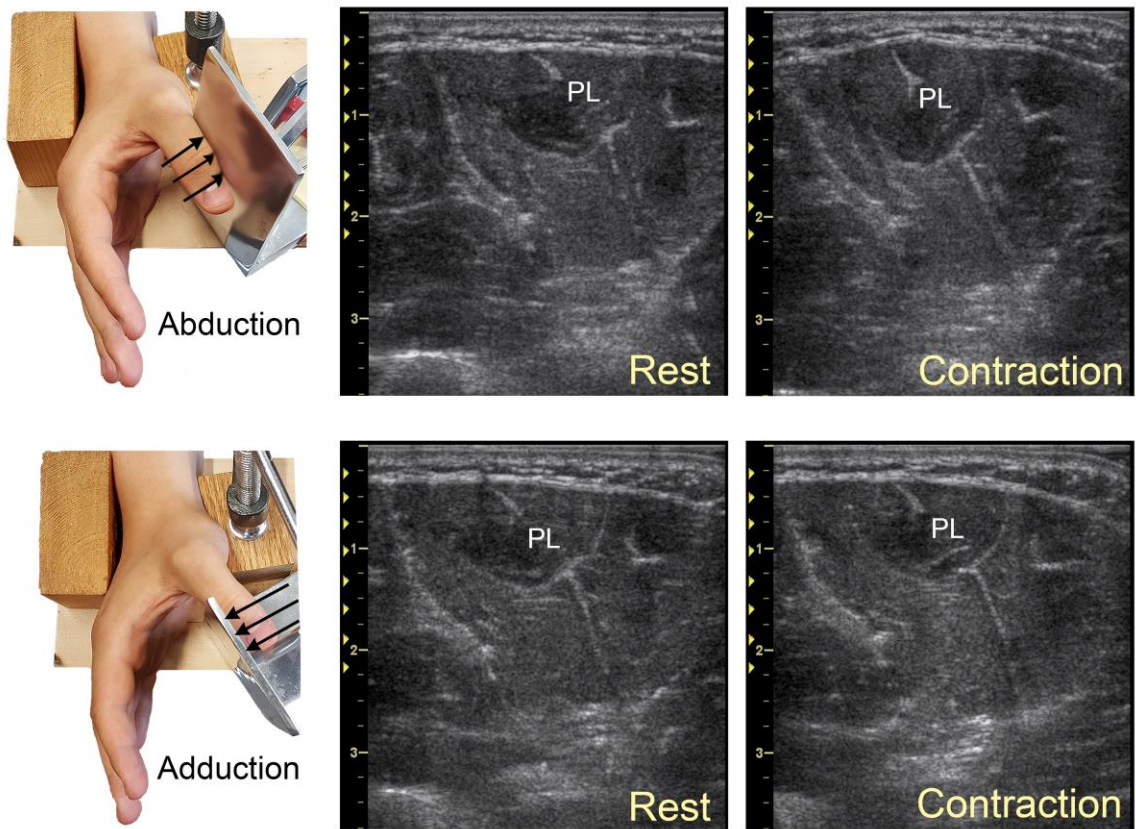
Figure 2.3 Ultrasound Appearance of the Palmaris Longus During Thenar Contractions
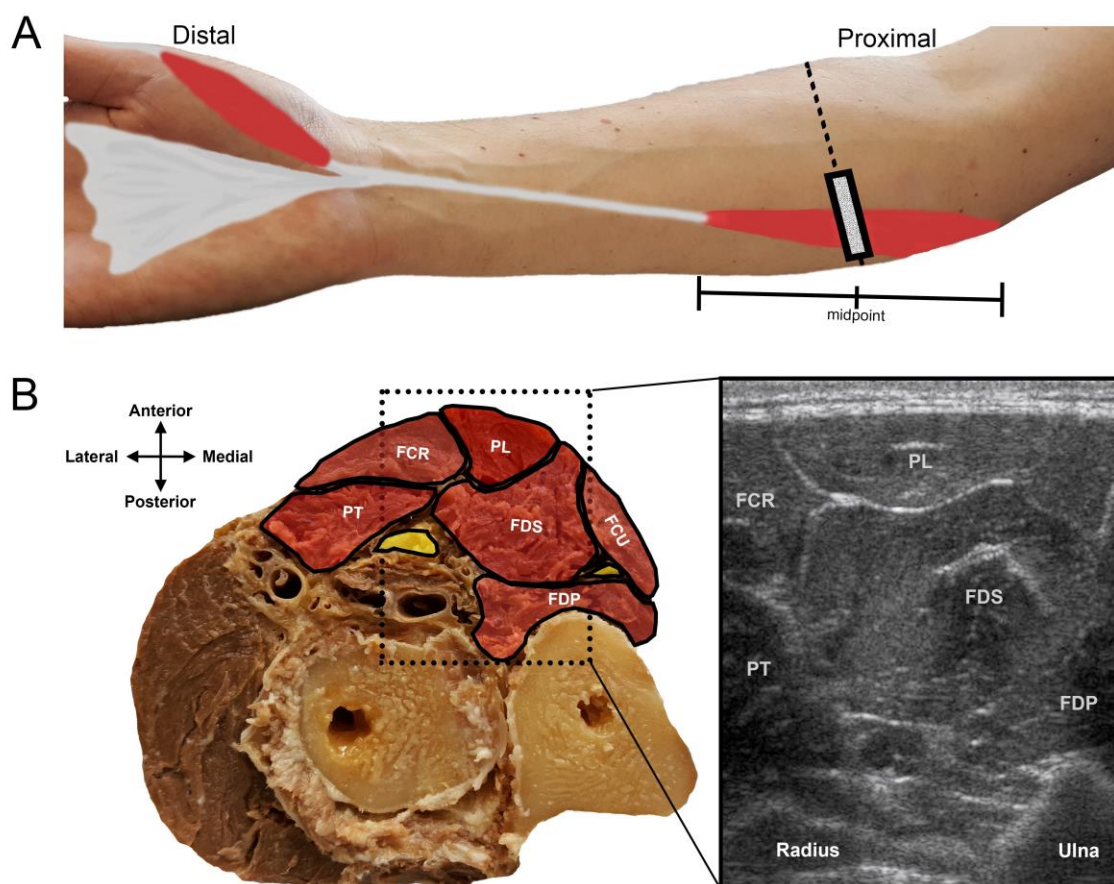
Figure 2.4 Surface Anatomy of the Palmaris Longus for Ultrasound Imaging

(A) Illustration depicting the proposed digastric arrangement of the palmaris longus (PL) and the abductor pollicis brevis. The mid-belly of the PL was determined using ultrasound imaging with the ultrasound probe placed in a transverse orientation (B) Ultrasound appearance of the PL and other forearm musculature in comparison to a cadaveric cross-section in a similar region. FCR: flexor carpi radialis, FDP: flexor digitorum profundus, FCU: flexor carpi ulnaris, FDS: flexor digitorum superficialis, PT: pronator teres. Note: the rectangle in panel A represents the ultrasound probe. Illustration was adapted from descriptions provided by Fahrer and Tubiana (1976).

2.2.6 Ultrasound Reliability

For intra-rater reliability, an experienced ultrasound operator scanned each participant's forearm three times at rest and during maximal thumb abduction. The first and third scans were used to assess intra-rater reliability. For inter-rater reliability, the M_T measures were repeated in all subjects independently by a second ultrasound operator on a different day and averaged to obtain a mean M_T score for each condition (rest, contraction). A mean M_T score was calculated from all three measurements made by the first ultrasound operator and compared with the mean M_T score of the second operator. Intra-class correlation coefficients (ICCs) were calculated for intra-rater and inter-rater reliability and reported with 95% confidence interval (CI).

2.2.7 Statistical Analysis

Data were analyzed using SPSS statistical software (version 24, SPSS Inc., Chicago, IL). A two-way repeated measures analysis of variance (ANOVA) was conducted to examine the effect of the muscle group (PL, FCR) and thumb position (abduction, flexion, opposition, extension, adduction) on the percentage of muscle activity (%EMG_{MVC}). Pairwise comparisons were performed of a significant main effect using a Bonferroni correction.

A paired-samples t test was used to determine differences in M_T from rest to contraction in both thumb abduction and adduction, respectively. A Bonferroni correction was used to account for multiple comparisons resulting in statistical significance set at $P = 0.0125$. Statistical comparisons between PL M_T measurements in its resting states prior to abduction and adduction were determined. Similarly, statistical comparisons between PL muscle thickness measurements in its contracted state post-abduction and adduction were also determined. All data are presented as Mean ± standard deviation.

2.3 Results

Schaeffer's test indicated the presence of bilateral PL muscles in nine of the ten participants. In the participant with unilateral PL musculature, investigation of the PL in

the non-dominant limb (left forearm) was necessary due to negative Schaeffer's test indicating absence of the PL muscle in the dominant limb (right forearm).

2.3.1   Electromyography

A two-way repeated measures ANOVA was conducted that examined the effect of forearm muscle (PL, FCR) and thumb position (abduction, flexion, opposition, adduction, extension) on PL muscle activity (% EMG_{MVC}). Mauchly's test of sphericity indicated that the within subject effects had met the assumption of sphericity. There was a statistically significant main effect of muscle ($F(1,9) = 29.576$, $P = 0.0004$) and thumb position ($F(4,36)=22.683$, $P < 0.001$) on muscle activity. However, a statistically significant interaction was detected between the effects of the forearm muscle (PL, FCR) and thumb position (abduction, flexion, opposition, adduction, extension) on the muscle activity ($F(4,36) = 4.923$, $P = 0.003$). A post-hoc power analysis (G*Power, version 3.1.9.2) revealed the significant interaction effect was of large size ($f = 0.74$) with an achieved power of 0.88 given the sample size ($n = 10$). The largest mean PL muscle activity was recorded during thumb abduction (% PL $EMG_{MVC} = 46 \pm 20\%$) followed by opposition (% PL $EMG_{MVC} = 37 \pm 14\%$), flexion (% PL $EMG_{MVC} = 35 \pm 13\%$), extension (% PL $EMG_{MVC} = 19 \pm 13\%$), and adduction (% PL $EMG_{MVC} = 7 \pm 4\%$) movements. Similarly, the largest FCR mean muscle activity was recorded during thumb abduction (% FCR $EMG_{MVC} = 26 \pm 16\%$), followed by flexion (% FCR $EMG_{MVC} = 14 \pm 9\%$), opposition (% FCR $EMG_{MVC} = 11 \pm 9\%$), adduction (% FCR $EMG_{MVC} = 7 \pm 4\%$) and extension (% FCR $EMG_{MVC} = 6 \pm 5\%$). Analysis of simple main effects revealed that the relative % PL EMG_{MVC} was significantly greater than the relative % FCR EMG_{MVC} during all thumb movement tasks ($P < 0.05$) except during thumb adduction ($P = 0.96$) (Figure 2.5). For the PL, simple main effects analysis revealed that the muscle activity recorded during thumb abduction was not statistically significant between the thumb flexion ($P = 0.54$), and opposition contractions ($P = 1.0$) but was significantly different from adduction ($P = 0.002$) and extension contraction tasks ($P = 0.002$) (Figure 2.5). When compared to thumb adduction, simple main effects revealed significantly greater PL muscle activity during thumb abduction ($P = 0.002$),

flexion ($P = 0.001$), and opposition ($P = 0.001$) (Figure 2.5). Synchronous EMG bursts were detected in 90% (9/10) of participants upon unopposed circumduction of the thumb (Figure 2.6)
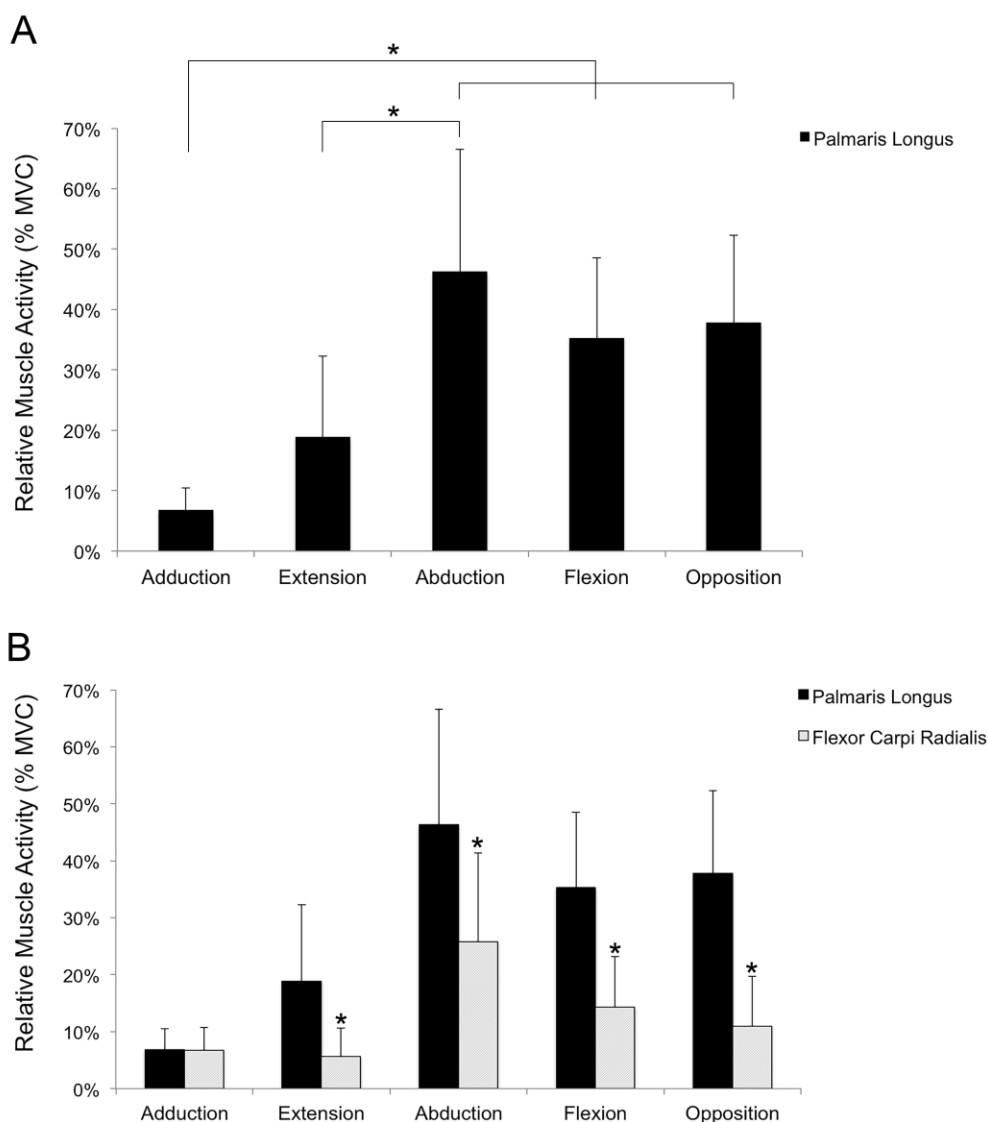
Figure 2.5 Relative Muscle Activity Recorded During Thenar Contractions

A) Relative muscle activity recorded from the palmaris longus (PL) during maximal thenar movement contractions. Note: the relative PL muscle activity recorded during abduction, flexion and opposition contractions were not statistically significant from each other ($P > 0.05$). (B) Comparison of the relative muscle activity of the PL and flexor carpi radialis during the standardized maximal thenar movement contractions. MVC: maximal voluntary wrist flexion contraction. *Denotes statistically significant ($P < 0.05$). All data presented as Mean ± standard deviation.
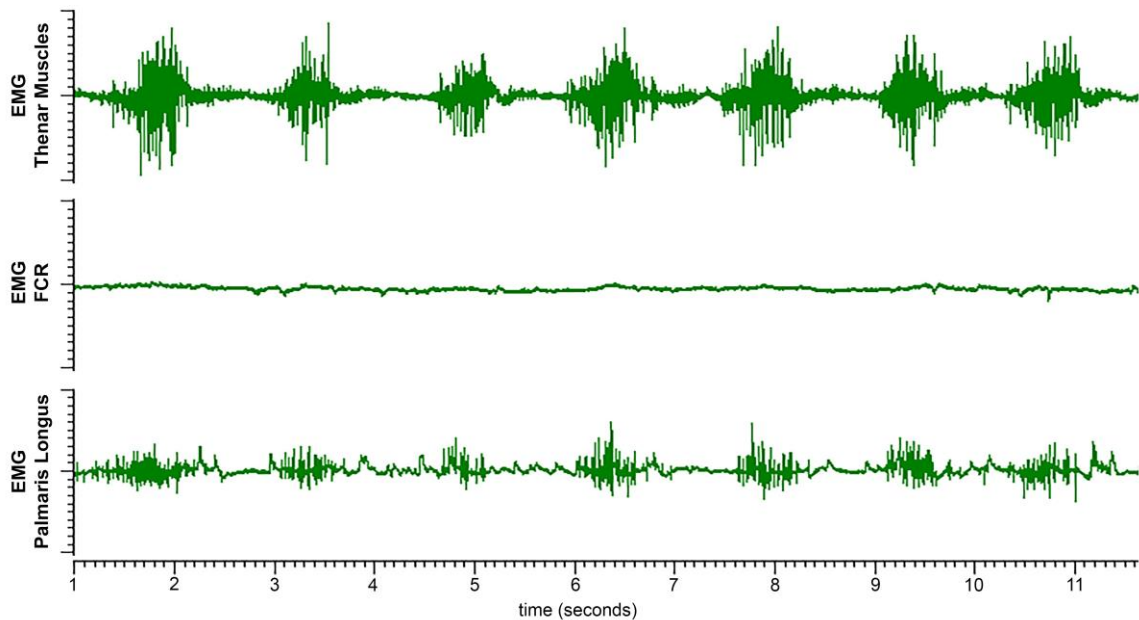
Figure 2.6 Synchronous EMG bursts among Thenar and Palmaris Longus Musculature

Exemplar unprocessed electromyogram depicting synchronous intermittent contractions of the thenar muscles with the palmaris longus (PL) during unopposed circumduction. Note the quiescence of the flexor carpi radialis (FCR) muscle throughout the contractions. Thenar muscle activity was recorded using surface electrodes, while the muscle activity of the PL and FCR were recorded using indwelling fine wire electrodes.

2.3.2   Ultrasound Imaging

During thumb abduction, PL M_T significantly increased by $21 \pm 12\%$ ($P < 0.001$). PL M_T significantly decreased upon thumb adduction by $-4 \pm 4\%$ ($P = 0.001$). No significant differences were found between PL M_T measurements at rest prior to abduction and adduction ($P = 0.50$). The PL M_T was significantly greater due to abduction contraction when compared to the PL M_T during the adduction contraction ($P < 0.001$). Furthermore, high intra- (ICC ≥ 0.92) and inter-rater reliabilities (ICC ≥ 0.85) were found for the ultrasound measurements made by the two operators. See Tables 2.1 and 2.2 for a summary of the M_T and ultrasound reliability measurements, respectively.

Table 2.1 Palmaris Longus Muscle Thickness During Maximal Thenar Contractions

Thumb Action	Muscle Thickness (cm)		*P*-value
	Rest	**Contraction**	
Abduction	0.92 ± 0.1 $(0.60 - 1.12)$	$1.09 \pm 0.1^*$ $(0.84 - 1.27)$	$P < 0.001$
Adduction	0.90 ± 0.1 $(0.63 - 1.10)$	$0.86 \pm 0.1^{*\dagger}$ $(0.60 - 1.02)$	$P = 0.01$

*Denotes statistically significant from resting condition ($P<0.0125$); †denotes statistically significant from contraction during abduction ($P<0.0125$); All data presented as Mean ± Standard Deviation (Range)

Table 2.2 Intra- and Inter-Rater Reliability of Palmaris Longus Muscle Thickness Ultrasound Measurements

Intra-rater Reliability		
Thumb Action	**Rest ICC (95% CI)**	**Contraction ICC (95% CI)**
Abduction	0.96 (0.73 – 0.98)	0.95 (0.81 – 0.99)
Adduction	0.94 (0.76 – 0.99)	0.92 (0.67 – 0.98)
Inter-rater Reliability		
Thumb Action	**Rest ICC (95% CI)**	**Contraction ICC (95% CI)**
Abduction	0.85 (0.13 – 0.97)	0.91 (0.67 – 0.98)
Adduction	0.87 (0.21 – 0.97)	0.89 (0.58 – 0.97)

ICC: intraclass correlation coefficient; CI: confidence interval

2.4   Discussion

This study investigated the role of the PL as a synergist in thumb movement by recording PL muscle activity during maximal thenar muscle contractions throughout the movement planes of the first digit. The results indicate that the PL acts as a synergist in thumb abduction, flexion, and opposition based on the relative PL muscle activity (% PL EMG_{MVC}) recorded during these tasks. Furthermore, using ultrasound imaging a significant increase in PL M_T was observed during maximal thumb abduction. Collectively, these results provide direct support of literature proposing the PL acts as part of the extrinsic-intrinsic system of thenar musculature in conjunction with the abductor pollicis longus and brevis (Fahrer, 1977; Fahrer and Tubiana, 1976; Gangata et al. 2010; Kaplan, 1984).

2.4.1   Morphological Evidence of the PL in Thumb Abduction

The synergistic contribution of the PL to thumb abduction has been attributed to the spatial relationship between the PL tendon and the abductor pollicis brevis (Fahrer, 1977; Fahrer and Tubiana, 1976; Kaplan, 1984). Although continuous with the palmar aponeurosis, the PL also terminates as a lateral tendon that serves as the origin for a portion of the abductor pollicis brevis, which has been referred to colloquially as the "lumbrical of the thumb" due to its insertion into the extensor expansion (Fahrer, 1977; Fahrer and Tubiana, 1976). However, other morphological variations may occur including a connection between the PL and abductor pollicis brevis in the absence of bifurcating PL tendon (Figure 2.7). In a morphological study of 44 dissected hands, the abductor pollicis brevis was connected to the lateral PL tendon directly (23 hands, 52%), or through a fibrous arcade in association with the abductor pollicis longus (21 hands, 48%) (Fahrer, 1977). Although we could not directly investigate the tendon morphology in our participants, the PL muscle activity recorded during the thumb contractions indicates synergistic activity between the PL and the abductor pollicis brevis with the PL tendon providing a physical connection between the two muscles.
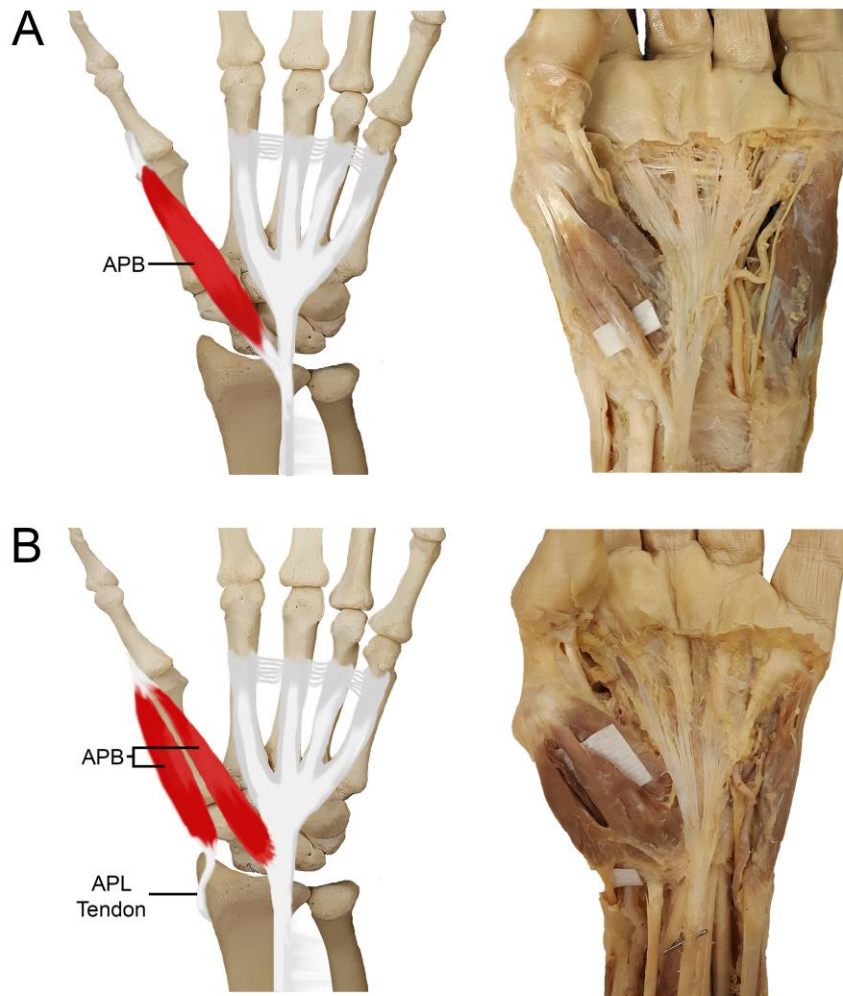
Figure 2.7 Anatomical Variations of the Palmaris Longus (PL) Tendon in Relationship to the Abductor Pollicis Brevis (APB)

(A) APB originating from a bifurcating PL terminal tendon. (B) APB originating from the PL tendon and proximal palmar aponeurosis. Note an additional APB muscle belly originating from the abductor pollicis longus (APL) tendon in panel B.

During the thenar contractions, a similar percentage of PL muscle activation was observed across abduction, flexion, and opposition movements (%PL EMG$_{MVC}$: 46%, 35%, 37%), respectively (Fig. 2.5). Because thenar musculature acts in unison as a functional unit, it is expected that any thumb movement directed ventrally from the palm will produce muscle contraction in the abductor pollicis brevis, which could explain PL muscle co-contraction across these movements. The abductor pollicis brevis provides functional contributions to the extension of the interphalangeal joint (Fahrer, 1977), which may explain the PL muscle activity recorded (19%) during thumb extension movements through a potential digastric relationship. Although the PL may play a minimal role in elbow stabilization based on its humeral origin, the relative muscle activity recorded from another muscle of the common flexor mass, the FCR, was significantly less compared to the PL throughout all contractions (Fig. 2.5), indicating that the PL may provide functional contributions beyond the role of mere elbow stabilization. The PL seems to function primarily as a wrist flexor as the mean muscle activity remained submaximal throughout the thenar contractions relative to the activity recorded during maximal isometric wrist flexion. Thus, in its presence, the PL should be perceived as a muscle of functional importance in the thumb based on the premise that it contributes a viable contribution of force transmission into the thenar eminence.

Further evidence of the PL as a thenar synergist is apparent in the intermittent bursts of PL muscle activity recorded during unopposed circumduction. A contraction synchrony was observed between the muscles of the thenar eminence and the PL, while the FCR remained relatively quiescent (Fig. 2.6). This synchrony was observed in all participants except one, which could be explained by the presence of variant PL muscle anatomy in this individual. Several PL morphological variants have been identified in the literature such as those with aberrant PL insertions at the wrist, which may include tendon bifurcation and trifurcation (Sunil et al. 2015), or termination into the antebrachial fascia alone (Stecco et al. 2009). Other reported cases include a reverse PL in which the muscle belly is located in the distal forearm and can cause symptoms of carpal tunnel syndrome due to median nerve compression (Backhouse and Churchill-Davidson, 1975).

Furthermore, the distal PL tendon can serve as an origin for other variant musculature such as the flexor digiti minimi brevis in some cases (Moore and Rice, 2017a). Therefore, because of potential variable and complex anatomy, presence of the PL muscle may not always provide significant contributions to either thenar movements or to wrist flexion depending on its insertion pattern.

2.4.2   Functional Implications

Thumb abduction is necessary to perform several activities of daily living including keyboard typing, grasping objects such as coffee cups, opening scissors, and playing a variety of musical instruments (Gangata et al. 2010). Removal of the PL may not overtly compromise function in most individuals, but it may affect the learned motor control patterns of some movements receiving contributions from the PL based on its potential synergistic activation with the thumb. From cadaveric measurements, it is known that the PL is approximately twice the muscle volume (9.0 cm^3) of the abductor pollicis brevis (4.9 cm^3)(Cooney et al. 1984), which may explain reports of significant thenar abduction strength contributions attributed to the presence of the PL (Gangata et al. 2010). If the PL functions in a digastric manner (Fahrer and Tubiana, 1976; Kaplan, 1984), a significant loss of thumb abduction strength would be detected upon removal. However, this would likely depend on the PL morphological form present and to what degree the PL contributes to fine motor control of the thumb.

Due to their importance in activities of daily living, pinch and grip strength are clinical measures often used to assess hand function after invasive hand surgery (Gellman et al. 1989). A comparative study in a healthy Asian population reported no functional decrements in pinch and grip strength among individuals with and without hereditary PL agenesis (Sebastin et al. 2005). To achieve the pinch position, the thumb must adduct to the second digit to ensure pulp-to-pulp contact. Similarly, hand-grip dynamometers typically assess strength of the forearm flexors and require the thumb to primarily adduct when grasping the device. Our results indicated minimal PL muscle activity (7%) and a decrease (-4%) in PL M_T during thumb adduction, which supports the lack of apparent

differences reported in pinch and grip measures when comparing individuals with and without PL agenesis. Our results indicated a significant decrease in PL M_T, which was likely observed due to the tension of surrounding forearm musculature pulling on the PL muscle. Thus, the functional contributions of the PL are limited to select thumb movements directed ventrally from the palm.

2.4.3   Surgical Evidence of Palmaris Longus Synergy

In thenar paralysis, restoration of function can be achieved by several surgical approaches involving PL tendon transfer to the insertion site of the abductor pollicis brevis to restore thumb abduction function (Camitz Opponensplasty) (Camitz, 1929; Rymer and Thomas, 2016). A modified approach to Camitz opponensplasty in treatment of severe carpal tunnel syndrome mobilizes the PL tendon through the radial or ulnar portion of the incised flexor retinaculum for use as a pulley for better approximation of pure opposition movements (Foucher et al. 1991; Kato et al. 2014; Littler and Li, 1967; Macdougal, 1995; Park et al. 2010; Terrono et al. 1993). Although the site of the PL insertion is transferred from the wrist to the interphalangeal joint of the first digit, patients require no specific rehabilitation perhaps due to an established neuromuscular facilitation, or synergy, already existing between the PL and abductor pollicis brevis (Kato et al. 2014). Therefore, in other surgical interventions in which the ipsilateral PL is routinely harvested, such as ulnar collateral ligament reconstruction (Cain and Mathis, 2016), the role of the PL in palmar function should be considered based on its potential synergy with thenar musculature. Removing the PL for tendon grafts or other restorative surgeries may affect learned muscle activation patterns, especially in palms of individuals in which routine stereotyped movements are necessary such as in some elite or professional-level sports.

Ultrasound imaging is a useful noninvasive tool to record and quantify static and dynamic changes in muscle geometry (Hodges et al. 2003). Quantitative ultrasound measures in muscles undergoing isometric contractions have been investigated in several limb muscles including the biceps brachii (Hodges et al. 2003), tibialis anterior (Hodges

et al. 2003), semitendinosus (Karagiannidis et al. 2017), and the palmaris brevis (Moore and Rice, 2017b). Although we observed a small change in absolute PL M_T (1.7 mm), this change represented a 21% increase in mean PL M_T, indicative of three-dimensional changes in PL muscle geometry (i.e.: fascicle shortening, tendon excursion, muscle thickness) in response to thenar abduction. Similar absolute changes in M_T have been observed in other isometric limb muscle contractions (tibialis anterior: 3.6 mm)(Hodges et al. 2003); however, the extent of an absolute change in M_T likely depends on the fusiform or pennate structure of the muscle investigated (Hodges et al. 2003). In a cadaveric feasibility study, Fahrer and Tubiana (1976) proposed an alternative surgical mobilization of the PL tendon by maintaining its connections to the abductor pollicis brevis in order to restore functional thumb movements in thenar paralysis. By applying strong traction to the mobilized cadaveric PL tendon, several functional movements at the MCP joint were observed including abduction, pronation, and interphalangeal joint extension (Fahrer and Tubiana, 1976). Knowledge of the change in PL M_T in response to thumb abduction by making pre- and post-surgical tendon transfer measures may be useful clinically in evaluating the effectiveness of alternative opponensplasty surgical procedures, as suggested in the aforementioned cadaveric feasibility study. Furthermore, ultrasound imaging may be useful in the preoperative planning of locating the PL muscle and tendon, which may not be prominent at the wrist depending on its morphology and pattern of insertion.

2.5   Conclusion

Although harvested in several restorative surgeries, the PL may provide significant synergistic contributions to functional thenar movements based on recordings of PL intramuscular activity and changes in muscle architecture, respectively. Understanding the functional synergistic relationship between the abductor pollicis brevis and PL may allow for continued development of alternative opponensplasty approaches utilizing the PL and abductor pollicis brevis muscles together as a functional digastric unit. Furthermore, knowledge of the established synergy *in vivo* may prove useful in

functional rehabilitation strategies from various hand injuries by appreciating that the PL may provide significant contributions to thenar motor control.

2.6   References

Backhouse K, Churchill-Davidson D. 1975. Anomalous palmaris longus muscle producing carpal tunnel-like compression. Hand 7:22-24.

Basmajian JV, Stecko G. 1962. A new bipolar electrode for electromyography. J Appl Physiol 17:849-849.

Cain EL, Mathis TP. 2016. Ulnar collateral ligament reconstruction: current philosophy in 2016. Am J Orthop (Belle Mead NJ) 45:E534-E540.

Camitz H. 1929. Surgical treatment of paralysis of opponens muscle of thumbs. Acta Chir Scand 65:77-81.

Cooney WP, Linscheid RL, An KN. 1984. Opposition of the thumb: an anatomic and biomechanical study of tendon transfers. J Hand Surg Am 9:777-786.

Fahrer M. 1973. Proceedings: the role of the palmaris longus muscle in the abduction of the thumb. J Anat 116:476.

Fahrer M. 1977. On the form and function of the abductor pollicis brevis muscle. Aust N Z J Surg 47:243-247.

Fahrer M, Tubiana R. 1976. Palmaris longus, anteductor of the thumb. Hand 8:287-289.

Foucher G, Malizos C, Sammut D, Braun FM, Michon J. 1991. Primary palmaris longus transfer as an opponensplasty in carpal tunnel release. A series of 73 cases. J Hand Surg Br 16:56-60.

Gangata H, Ndou R, Louw G. 2010. The contribution of the palmaris longus muscle to the strength of thumb abduction. Clin Anat 23:431-436.

Gellman H, Kan D, Gee V, Kuschner SH, Botte MJ. 1989. Analysis of pinch and grip strength after carpal tunnel release. J Hand Surg Am 14:863-864.

Gilbert A, Masquelet AC, Tubiana R. 1999. An atlas of surgical techniques of the hand and wrist. London: Taylor & Francis.

Gilroy A. 2013. Anatomy An Essential Textbook. New York: Thieme Medical Publishers.

Hodges PW, Pengel LH, Herbert RD, Gandevia SC. 2003. Measurement of muscle contraction with ultrasound imaging. Muscle Nerve 27:682-692.

Kaplan EB. 1984. Kaplan's functional and surgical anatomy of the hand. Philadelphia: Lippincott Williams & Wilkins.

Karagiannidis E, Kellis E, Galanis N, Vasilios B. 2017. Semitendinosus muscle architecture during maximum isometric contractions in individuals with anterior cruciate ligament reconstruction and controls. Muscles Ligaments Tendons J 7:147-151.

Kato N, Yoshizawa T, Sakai H. 2014. Simultaneous modified Camitz opponensplasty using a pulley at the radial side of the flexor retinaculum in severe carpal tunnel syndrome. J Hand Surg-Eur Vol 39:632-636.

Littler JW, Li CS. 1967. Primary restoration of thumb opposition with median nerve decompression. Plast Reconstr Surg 39:74-75.

Macdougal BA. 1995. Palmaris longus opponensplasty. Plast Reconstr Surg 96:982-984.

Moore CW, Rice CL. 2017a. Rare muscular variations identified in a single cadaveric upper limb: a four-headed biceps brachii and muscular elevator of the latissimus dorsi tendon. Anat Sci Int. 93: 311-116

Moore CW, Rice CL. 2017b. Structural and functional anatomy of the palmaris brevis: grasping for answers. J Anat 231:939-946.

Moore KL, Dalley AF, Agur AMR. 2014. Clinically Oriented Anatomy, 7th ed. Philadelphia: Lippincott Williams & Wilkins.

Park IJ, Kim HM, Lee SU, Lee JY, Jeong C. 2010. Opponensplasty using palmaris longus tendon and flexor retinaculum pulley in patients with severe carpal tunnel syndrome. Arch Orthop Trauma Surg 130:829-834.

Pillen S. 2010. Skeletal muscle ultrasound. European J Transl Myol 20:145-156.

Reimann AF, Daseler EH, Anson BJ, Beaton LE. 1944. The palmaris longus muscle and tendon a study of 1600 extremities. Anat Rec 89:495-505.

Rymer B, Thomas PB. 2016. The Camitz transfer and its modifications: a review. J Hand Surg Eur Vol 41:632-637.

Schaeffer JP. 1909. On the variations of the palmaris longus muscle. Anat Rec 3:275-278.

Sebastin SJ, Lim AY, Bee WH, Wong TC, Methil BV. 2005. Does the absence of the palmaris longus affect grip and pinch strength? J Hand Surg Br 30:406-408.

Standring S. 2008. Gray's Anatomy: The Anatomical Basis of Clinical Practice, 40th ed. Edinbrugh: Churchill Livingstone.

Stecco C, Lancerotto L, Porzionato A, Macchi V, Tiengo C, Parenti A, Sanudo JR, De Caro R. 2009. The palmaris longus muscle and its relations with the antebrachial fascia and the palmar aponeurosis. Clin Anat 22:221-229.

Sunil V, Rajanna S, Gitanjali, Kadaba J. 2015. Variation in the insertion of the palmaris longus tendon. Singapore Med J 56:e7-9.

Terrono AL, Rose JH, Mulroy J, Millender LH. 1993. Camitz palmaris longus abductorplasty for severe thenar atrophy secondary to carpal-tunnel syndrome. J Hand Surg-Am 18a:204-206.

Chapter 3

3 Fiber type Composition of the Palmaris Longus and "Lumbrical"-like Fascicles of the Abductor Pollicis Brevis: Implications for Thenar Function[2]

3.1 Introduction

The palmaris longus (PL) is known for its variant morphology and is absent in approximately 14% of forearms in the population (Moore et al., 2014). Although considered a weak wrist flexor and tensor of the palmar aponeurosis (Gilroy, 2013, Moore et al., 2014), the PL may provide significant thenar abduction strength contributions based on its morphological relationship with the thenar musculature (Gangata et al., 2010). Although the abductor pollicis brevis (APB) has been generally depicted as a thin, bipartite muscle of the proximolateral thenar eminence (Standring and Gray, 2008, Napier, 1952), Simard and Roberge (1988) described it as consisting of three muscular heads with several discrete fascicular sub-divisions representing a substantial proportion of the thenar muscle mass. Of the three APB muscular heads, the superficial head consisted of a discrete fusiform fascicle continuous with the PL (Simard and Roberge, 1988). These discrete fascicles are considered homologous to lumbricals (Fahrer and Tubiana, 1976) or interossei (Le Double, 1897) based on their insertion into the dorsal aponeurotic expansion and presumed functional role in the extension of the interphalangeal joint of the 1st digit. Discrete APB fascicles may originate from several PL tendon locations including a bifurcated PL tendon, a region proximal to the palmar aponeurosis, or from an accessory abductor pollicis longus tendon (Fahrer and Tubiana, 1976, Fahrer, 1977, Moore et al., 2017b, Kaplan, 1984). The morphological connection between the APB muscle and PL tendon suggests that the PL and APB muscles may act as a functional digastric unit contributing synergistically to thenar muscle contractions.

---

[2] A version of this chapter has been submitted to the Journal of Anatomy

The omohyoid, occipito-frontalis, and the digastric muscle proper are examples of muscles engaged in functional synergistic relationships. The nomenclature of the digastric muscle reflects its morphological arrangement indicating the presence of two discrete muscle bellies separated by an intermediate tendon. The functional relationship between the digastric muscle bellies has been investigated histologically by determining the fiber type identity of its constituent muscles fibers. Despite a disparate cranial innervation, a predominance of type II muscle fibers exist among both anterior (type I: 37%, type II: 63%) and posterior bellies (type I: 36%, type II: 64%) of the digastric muscle indicating a functional relationship irrespective of innervation and site of embryological development (Monemi et al., 1999). Because type II muscle fibers have greater shortening velocity and fatigability compared to type I muscle fibers, the predominant type II muscle fiber type consistency amongst digastric bellies reflect its gross function in performing powerful movements necessary for jaw function (Monemi et al., 1999, Pette and Staron, 2000). Similarly, the medial and lateral heads of the quadratus plantae demonstrate fiber type homogeneity indicative of a shared function despite their variable absence in 20% of the population (Schroeder et al., 2014). The quadratus plantae fiber type homogeneity persists among its heads despite differences in their phylogenetic origins with the lateral head common with mammals and the medial head found only in humans (Sooriakumaran and Sivananthan, 2005, Schroeder et al., 2014). The PL and APB are arranged in similar morphological arrangement as the digastric muscle through the PL terminal tendon (Fahrer, 1977, Moore et al., 2017b). Although the APB fiber type composition has been shown to consist of a predominant proportion of type I muscle fibers (>60%) (Johnson et al., 1973), the APB fiber type composition has not been investigated with respect to its contiguous morphological arrangement with the PL muscle.

In severe carpal tunnel syndrome, median nerve compression can impair the functional actions of the APB including thenar abduction, metacarpophalangeal (MCP) joint rotation, and true pulp-to-pulp contact of the digits (Napier, 1952). Restoring functional hand movements in patients with thenar paralysis can be achieved using an

autologous tendon transfer of the PL to the 1st digit (Rymer and Thomas, 2016, Camitz, 1929). Opponensplasty success has been attributed to an intrinsic synergy of the PL with the APB such that no specific muscular retraining is needed upon tendon transfer (Kato et al., 2014). This synergy has been demonstrated in young participants *in vivo*, in which, synchronous electromyographic (EMG) activity was recorded between the PL and thenar musculature during abduction, flexion, opposition, and circumduction movements (Moore et al., 2017b); however, this synergistic relationship may not be adequately established in all individuals due to morphological differences. If differences in APB fiber type proportions are evident between individuals with robust and rudimentary connections with the PL tendon, a lack of fiber type homogeneity between individuals may reveal those APB muscles engaged in a synergistic relationship with the PL muscle. Knowledge of the morphological connection between the APB and the PL tendon may be indicative of the quality of synergy established *in vivo*, which could be useful in predicting the success of the PL in opponensplasty tendon transfer.

Therefore, the purpose of this study was to investigate whether differences in the proportions of type I and type II muscle fibers exist among the APB fascicles originating from the PL tendon. When arranged in a digastric manner with the PL, the APB may be capable of producing more forceful contractions due to greater type II muscle fiber proportions, which may contribute to the significant thenar abduction strength attributed to the presence of PL musculature (Gangata et al., 2010). We hypothesized that the APB fascicles with discrete continuity with the PL will have significantly greater type II fiber type proportions compared to the APB musculature with rudimentary connections, or non-exclusive origins, with PL musculature. Knowledge of the APB fiber type composition with respect to its morphological relationship with the PL may be useful to further characterize the complexity of thenar contractile function and assist surgeons in functional restoration of thumb prehension and dexterous hand movements.

3.2   Materials and Methods

3.2.1   Cadaveric Specimens

Twenty-four contiguous PL and APB muscles were harvested from the forearms (left: 12, right: 12) and hands (left: 12, right: 12) of twelve embalmed cadavers [Mean age: 74 ± 10 years (range: 55-87y); 6 males, 6 females], respectively. The PL was present bilaterally in all cadavers. Cadaveric specimens were obtained from the local institution's body donation program and approved for research use by the Committee for Cadaver Use in Research (REF# 21092016). The cadavers received through the body donation program are embalmed within 24 hours postmortem. To ensure muscle fiber type proportions were not influenced by other comorbidities, the cadaveric specimens were excluded if neuromuscular diseases, rheumatoid, or osteoarthritis were indicated in the cause of death report, or by visual evidence of hand deformation.

3.2.2   Morphological Classification of the Abductor Pollicis Brevis and Palmaris Longus

The forearms and hands of each cadaveric specimen were dissected and photographed by a single investigator to investigate the PL tendon morphology and its continuity with the abductor pollicis brevis muscle as described by Fahrer and Tubiana (1976). The 24 hands were stratified into two groups based on morphology of the APB and its relationship with the PL tendon. The APB muscles were classified into two groups based on the following morphological criteria: (1) APB muscle with discrete PL tendon connections (APB_D), or (2) APB muscle with non-discrete, or rudimentary, PL tendon connections (APB_{ND}).

3.2.3   Immunohistochemistry

Whole PL muscle tissue sections were harvested from its midpoint, which was determined by measuring half the distance between the medial epicondyle and PL myotendinous junction. In each hand, the superficial muscular fascicles of the APB muscles were identified and harvested by measuring half the distance between the

scaphoid and the proximal phalanx of the thumb. At the PL and APB midpoints, 0.5 cm width muscle sections were excised for immunohistochemical analysis. The PL and APB were stained using previously established immunohistochemical staining procedures as per Moore et al. (2017a). The specimens were immediately immersed in a 10% formalin solution for a minimum of 24 hours upon harvesting. All tissues were serially sectioned at a thickness of 5 μm using a Microtome (Microm HM-325). The tissue slides were heated to 37 °C for a minimum of 24 hours prior to immunohistochemical procedures. Antigen retrieval was performed in citrate buffer (pH 6.0) in a de-cloaking chamber. Slides were blocked in 10% horse serum, and subsequently, incubated with mouse monoclonal antibodies specific to either myosin heavy chain (MHC) type I (Sigma-Aldrich NOQ7.5.4D) or MHC type II (Sigma-Aldrich MY-32) at a dilution of 1: 3200 for one hour at room temperature as established by previous experimentation (Moore et al., 2017a). The antibodies NOQ7.5.4D and MY-32 label type I (slow-twitch) fibers and all type II (i.e. type IIa and IIx) (fast-twitch) fibers, respectively. The secondary antibody, ImmPRESS Anti-Mouse Ig Peroxidase Polymer Detection Kit (Vector Laboratories, Cat. No. MP-7402), was applied prior to labeling with DAB (DAB Peroxidase Substrate Kit, 3,3′–diaminobenzidine, Vector Laboratories, Cat. No. SK-4100). Specimen-matched negative control sections underwent identical procedures, except for the application of the primary antibody. Hematoxylin counterstain was used in all tissue sections.

3.2.4   Statistical Analysis

Handling of data and calculations were performed using Excel Software (Version 13.5.8, 2011, Microsoft Corporation). Statistical analysis was performed using SPSS statistical software (Version 25, SPSS Inc., Chicago, IL, USA). A two-way analysis of variance (ANOVA) was used to determine the effect of morphology (APB_{ND}, APB_D), and fiber type (type I, type II, or hybrid) on muscle fiber percentage. A three-way ANOVA was used to determine the effect of morphology (APB_{ND}, APB_D), muscle (APB, PL), and fiber type (type I, type II, or hybrid) on muscle fiber percentage. Follow-up post-hoc comparisons of significant main effects were performed with a Bonferroni correction applied. All descriptive statistics are presented as mean ± SD.

3.3   Results

3.3.1   Morphological Classification

The superficial fascicle of the APB originated from a bifurcated PL tendon in 9/24 hands (37%), or directly from the PL tendon in the remaining 15/24 hands (63%). The APB fascicles from 11 hands (46%) were classified as discrete based on their distinct continuity with the PL tendon. Conversely, the APB fascicles from 13 hands (54%) were classified as non-discrete due to rudimentary or minimal connections with the PL tendon (Figure 3.1).

APB Fascicles: Discrete PL Connections

APB Fascicles: Non-Discrete / Rudimentary PL Connections
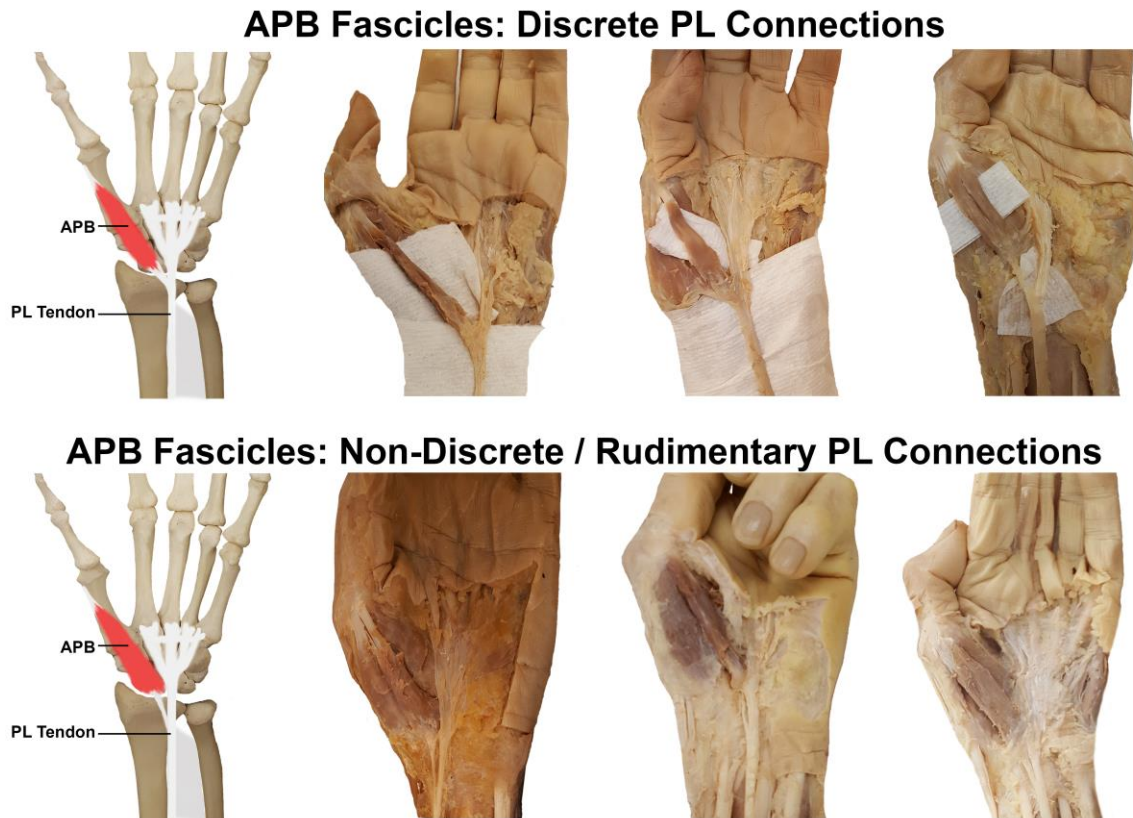
Figure 3.1 The "Lumbrical"-like Fascicular Divisions of the Abductor Pollicis Brevis (APB).

Upper Row: APB fascicular divisions with discrete origins from the palmaris longus tendon (PL); *Lower row*: APB fascicular divisions with non-discrete/rudimentary origins from the palmaris longus tendon. The discrete APB fascicular divisions were relatively mobile and originated primarily from the PL tendon. Conversely, the non-discrete APB fascicular divisions were affixed primarily to the carpal bones and had only rudimentary connections with the PL tendon through thin fascial extensions.

3.3.2   Muscle Fiber Quantification

A total of 55,267 PL (left forearms: 28,412; right forearms: 26,855) and 52,042 APB (left hands: 26,537; right hands: 25,505) muscle fibers were examined throughout the serial histological sections. Of the fibers quantified in the PL, 25,019 were type I (left forearms: 13,285; right forearms: 11, 634), 27,212 were type II (left forearms: 13,584; right forearms: 13,628), and 3036 were hybrid muscle fibers (left forearms: 1443; right forearms: 1593). Of the fibers quantified in the APB, 32,162 were type I (left hands: 16,981; right hands: 15,181), 13,627 were type II (left hands: 5900; right hands: 7727), and 6253 hybrid muscle fibers (left hands: 3656, right hands: 2597).

A two-way ANOVA was used to examine the effect of morphology (APB_D, APB_{ND}) and fiber type (type I, type II, hybrid) on the proportion of APB muscle fibers quantified. There was a statistically significant interaction effect between morphology, and fiber type on the proportion of muscle fibers examined ($F_{2, 66} = 34.396$, $p < 0.001$). The proportion of type I fibers were significantly less in APB fascicles with discrete continuity with the PL (APB_D: 44 ± 16%) compared to those APB of non-discrete continuity (APB_{ND}: 75 ± 10%)($p < 0.001$). Conversely, the proportion of type II fibers were significantly greater in APB fascicles with discrete continuity with the PL (APB_D: 41 ± 19%)($p < 0.001$) compared to those APB fascicles with non-discrete connections with the PL (APB_{ND}: 15 ± 8%). No statistical difference was detected in the proportion of hybrid fibers between the APB_{ND} (10 ± 6%) and APB_D (15 ± 10%)($p = 0.228$) fascicles. The results of the statistical analysis are displayed graphically in Figure 3.2.
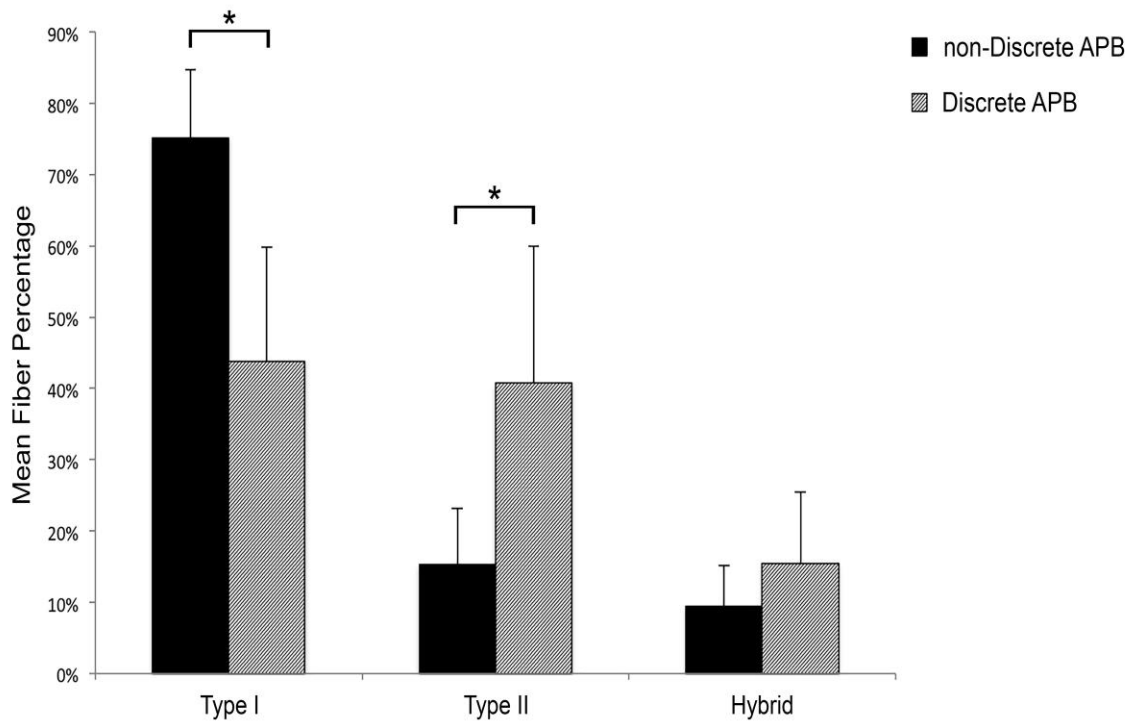
Figure 3.2 Fiber Type Composition of the "Lumbrical"-like Fascicles of the Abductor Pollicis Brevis (APB).

Note the differences in APB fiber type composition between fascicles with discrete and non-discrete/rudimentary connections with the palmaris longus. All values are mean ± SD; * denotes, $p < 0.05$

A three-way ANOVA was used to examine the effect of morphology (APB_D, APB_{ND}), muscle (PL, APB), and fiber type (type I, type II, hybrid) on the proportion of muscle fibers quantified. There was a statistically significant interaction effect between morphology, muscle, and fiber type on the proportion of muscle fibers examined ($F_{2, 132}$ = 11.957, p< 0.001). For PL and APB_D muscles discretely connected by the PL tendon, simple interaction effect analysis revealed a statistically significant difference in fiber type composition amongst type II (APB_D: 41 ± 19%, PL: 55 ± 12%, p = 0.003) and hybrid (APB_D: 15 ± 10%, PL: 4 ± 3%, p = 0.013) fibers; however, a similar fiber type percentage was observed amongst type I fibers (APB_D: 44 ± 16%, PL: 41 ± 11%, p = 0.573). For PL and APB muscles arranged in a rudimentary or non-discrete manner with the PL tendon, simple interaction effects analysis revealed a statistically significant difference in fiber type composition amongst type I (APB_{ND}: 75 ± 10%, PL: 49 ± 10%, p <0.001) and type II (APB_{ND}: 15 ± 8%, PL: 45 ± 9%, p <0.001) fibers; however, a similar fiber type percentage was observed amongst hybrid fibers (APB_{ND}: 10 ± 6%, PL: 6 ± 4%, p = 0.470). The results of the statistical analysis are displayed graphically in Figure 3.3.
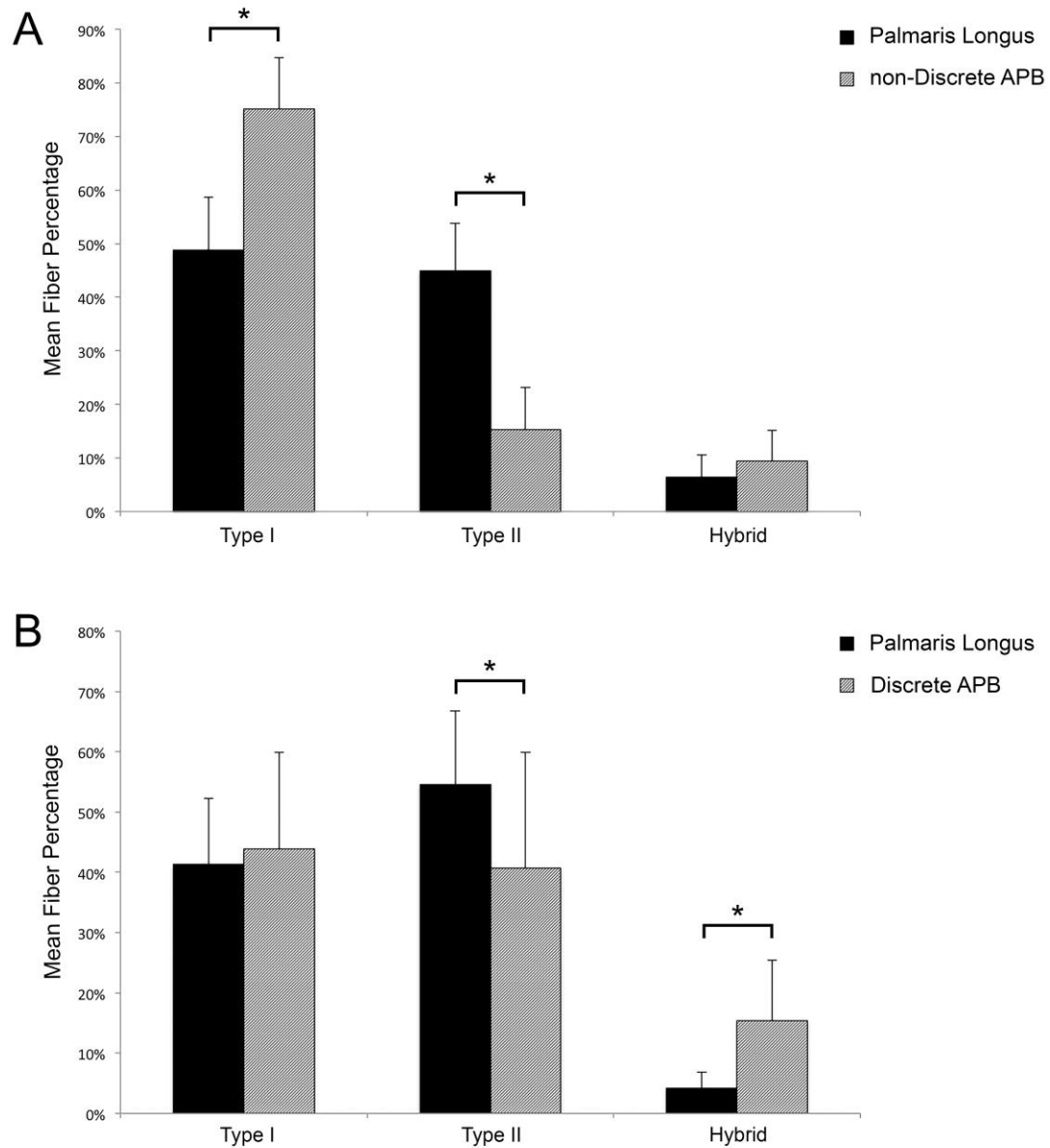
Figure 3.3 Comparison of Fiber Type Composition between Contiguous Abductor Pollicis Brevis (APB) and Palmaris Longus (PL) Musculature

(A) Fiber type composition of the PL and APB connected by a non-discrete, or rudimentary, PL tendon insertion; (B) Fiber type composition of the palmaris longus and APB in cadaveric specimens in which the PL tendon is arranged in a digastric relationship. All values are mean ± SD; * denotes, $p < 0.05$

3.4   Discussion

The PL is regarded as a muscle whose clinical importance as an autologous tendon graft may supersede its functional purpose *in vivo*; however, recent PL functional investigations have demonstrated that its utility may extend beyond weak wrist flexion to provide significant strength contributions to thenar musculature based on a functional synergy with the APB (Moore et al., 2017b, Gangata et al., 2010). In the present study, the APB and PL muscles from 24 cadaveric limbs were examined histologically to determine if their morphological arrangement influenced the APB fiber type proportions. Importantly, by determining the constituent APB fiber type proportions based on its morphological arrangement with the PL, a better understanding of the complexity of thenar contraction may be gained, and this knowledge may assist surgeons in surgical restoration of opposition movements in cases of severe thenar paralysis. Using immunohistochemical techniques, a differential proportion of type I and II muscle fibers were found amongst APB musculature with contiguous discrete (APB$_D$), and rudimentary, non-discrete (APB$_{ND}$), morphological connections with the PL tendon. This may provide further evidence of the quality of the digastric relationship and functional synergy established *in vivo*.

3.4.1   "Lumbricals" of the Thumb

Textbooks typically describe the APB as originating from the scaphoid tubercles, trapezium, and the flexor retinaculum prior to its insertion into the base of proximal phalanx of the 1st digit (Gilroy, 2013, Moore et al., 2014); however, morphological studies describe the APB as consisting of three muscular groups with discrete superficial fascicles also inserting into the dorsal aponeurotic expansion of the 1st digit (Simard and Roberge, 1988). In 44 dissected upper limbs with PL musculature, Fahrer (1977) observed several "lumbrical"-like APB fascicles arising from the tendons of extrinsic musculature including the PL and abductor pollicis longus tendons. A discrete APB fascicle originated from the PL tendon in 23 (52%) hands, and the remaining APB

fascicles originated from a fibrous arch between the PL and abductor pollicis longus tendons (48%, 21/44) (Fahrer, 1977). In the absence of the PL, a radial APB muscle belly originated consistently from the abductor pollicis longus tendon (Fahrer, 1977). In the present study, the APB fascicles originated from either a distinct lateral PL terminal tendon (37%), or directly from the PL tendon proximal to the palmar aponeurosis (63%); however, only in 11/24 hands did the PL serve as an exclusive origin to a relatively mobile APB fascicle (Figure 3.1). In the remaining hands (n=13), the APB was primarily affixed to its carpal origins with the PL providing only a rudimentary, or non-discrete, connection (Figure 3.1). Compared to Fahrer (1977), the fibrous arch between the PL and abductor pollicis longus was not observed in our sample, but was illustrated in a previous investigation (Moore et al., 2017b).

Lumbricals are known for their unique worm-like appearance (Latin, *lumbricus*: earthworm) and function in both digital flexion and extension of the MCP and interphalangeal joints, respectively (Moore et al., 2014). The fiber type composition of the lumbrical acting upon the index finger is a relatively heterogeneous composition of type I (43%) and II (57%) muscle fibers (Hwang et al., 2013) (Table 3.1), which was consistent with the fiber type composition of the "lumbrical"-like APB_D fascicles in continuity with the PL (type I: 44%, type II: 56%[†]) (Figure 2). Conversely, we observed a predominance of type I (75%) muscle fibers in the APB_{ND} fascicles, which is consistent with type I APB (63%) fiber proportions harvested from tissues of young cadavers (range: 22-30y) (Johnson et al., 1973). Interestingly, the lumbricals share a similar heterogeneous fiber type composition with the flexor digitorum profundus (Table 3.1), which acts as the origin to the true lumbricals of the second to fifth digits. Although they may not be true lumbricals, the APB_D fascicles share a morphological and functional homology with proper lumbricals based on their tendinous origins from extrinsic

---

[†] includes hybrid fibers: type II (41%) + hybrid (15%)

musculature, assistance in MCP joint flexion and interphalangeal joint extension, and a consistency in phenotypic muscle fiber type profile.

3.4.2   Thenar Muscles as a Series of Digastric Complexes

3.4.2.1   Palmaris Longus & Abductor Pollicis Brevis

The thenar eminence has been described as a system of extrinsic-intrinsic musculature consisting of the APB, opponens pollicis, flexor pollicis longus and brevis, PL, and abductor pollicis longus (Fahrer and Tubiana, 1976). When considered as a functional unit, the PL and APB_D share similar morphological features with the digastric muscle including the presence of two muscular heads interconnected by an intermediate tendon (Figure 3.4). The anterior and posterior bellies of the digastric muscle from aged cadavers (mean: 73y) both consist of a predominance of type II (anterior: 63%, posterior: 64%) muscle fibers, despite independent cranial innervation patterns (Monemi et al., 1999) (Table 3.1). The APB_D type I muscle fiber proportions (44%) were similar to those observed in the PL (41%); however, significantly fewer type II muscle fibers were observed in the APB_D fascicles (44%) compared to the PL muscle (55%) (Figure 3.3). In healthy human aging, a loss of type I and II motor units, and decrease in muscle fiber diameter contribute to muscle atrophy and weakness associated with old age (Berger and Doherty, 2010). Preservation of muscle function may occur through collateral reinnervation processes in which denervated type II muscle fibers are reinnervated by adjacent slower type I motor units producing hybrid muscle fibers co-expressing both slow and fast MHC isoforms (Andersen et al., 1999, Hepple and Rice, 2016). Although the APB_D fibers had significantly less type II muscle fibers, a significantly greater proportion of hybrid fibers (15%) were observed in the APB_D fascicles compared to the PL (4%) (Figure 3.3), which may be indicative of age-related type II motor unit loss and collateral reinnervation processes. Although hybrid fibers co-express multiple MHC isoforms, their contractile properties may function "fast-like" compared to pure type I fiber types (Pette and Staron, 2001, Bottinelli et al., 1996). If the percentage of APB_D

hybrid fibers (I/IIa) are pooled with type II fibers, the contiguous APB_D and PL muscles share similar type I (APB_D: 44%, PL: 41%) and type II (APB_D: 56%, PL: 59%) fiber type proportions; a feature consistent with the digastric muscle. Compared to the predominant type I muscle fiber proportions typical of thenar musculature (Table 3.1), the heterogeneous APB_D fiber composition may represent a functional advantage allowing for more forceful thenar abduction contractions for activities of daily living, fine thenar motor control and hand dexterity.

Table 3.1 Fiber Type Composition of Select Musculature of the Head, Neck and Upper Limb

Muscle	Fiber Type		Reference:
	% Type I	% Type II	
Palmaris Brevis	72%	28%[†]	Moore et al. (2017b)
Adductor Pollicis	80%	20%	Round et al. (1984)
Abductor Pollicis Brevis	63%	37%	Johnson et al. (1973)
Lumbrical (Index finger)	43%	57%	Hwang et al. (2013)
Flexor Digitorum Profundus	47%	53%	Johnson et al. (1973)
Digastric Muscle (Anterior)	37%	63%	Monemi et al. (1999)
Digastric Muscle (Posterior)	36%	64%	

†includes hybrid fibers
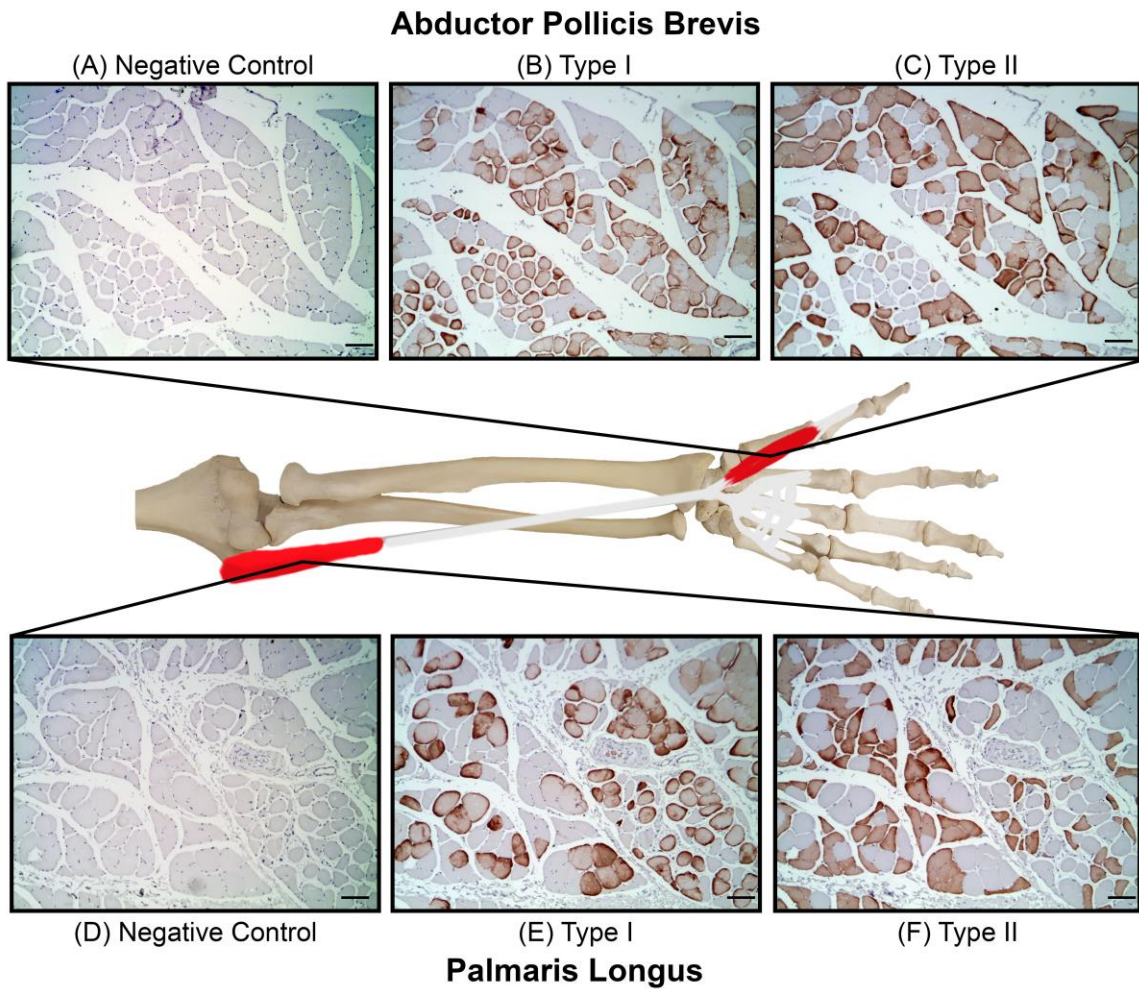
Figure 3.4 Histological Appearance of the Abductor Pollicis Brevis and Palmaris Longus Muscles Stained for Type I and Type II Myosin Heavy Chain Isoforms.

Both muscles consist of a heterogeneous proportion of Type I and II muscle fibers. Note: the histological sections were harvested from a cadaveric specimen with the PL tendon serving as a discrete origin to the abductor pollicis brevis. Scale bar: 100μm

The functional relationship between the PL and thenar musculature has been investigated *in vivo* in young participants using indwelling fine wire electromyography and ultrasound imaging techniques (Moore et al., 2017b). In response to maximal thenar abduction contractions, an increase in PL muscle thickness (21%) and PL muscle activity (46%) was recorded indicating the PL functions as an extrinsic thenar muscle *in vivo* (Moore et al., 2017b). Comparing those with congenital PL absence, Gangata et al. (2010) observed significant thenar abduction strength in those with PL musculature and attributed the PL tendon as the means for transmitting additional force to the thenar eminence. In the APB_D fascicles, the greater proportion of type II muscle fibers could further contribute to the contraction strength along with the additional force contributions from the PL muscle mass.

In severe carpal tunnel syndrome, open carpal tunnel release in conjunction with PL opponensplasty allows for restoration of functional, dexterous hand movements to perform activities of daily living during recovery of thenar muscle atrophy (Durban et al., 2017, Rymer and Thomas, 2016, Kato et al., 2014, Park et al., 2010, Macdougal, 1995, Terrono et al., 1993, Foucher et al., 1991, Camitz, 1929). In a study of 21 patients, moderate to abundant muscle contractions were observed in the PL post-tendon transfer using ultrasound imaging during opposition (90%, 19/21) and abduction (81%, 17/21) movements; however, PL muscle contraction was minimal or absent in the remaining patients (Durban et al., 2017). The surgical outcome of PL opponensplasty is likely multifactorial and may depend on individual factors such as PL muscle and tendon morphology, and the extent of the synergistic relationship established *in vivo* between the PL and APB prior to tendon transfer. In our sample of hands, rudimentary, or non-discrete, connections of the PL with the APB_{ND} were observed in 54% of cases, and were accompanied by a predominant proportion of type I muscle fibers (75%). In a portion of these cases, the synergistic relationship between the PL and APB_{ND} fascicles may be minimal due to rudimentary PL tendon extensions to the thenar eminence (Figure 3.1). In a previous functional investigation, the absence of synchronous synergistic EMG activity between the PL and APB was attributed to variant PL tendon morphology at the wrist

(Moore et al., 2017b). The variant anatomy of the PL tendon may influence the functional recovery and opponensplasty success, if an adequate synergy fails to develop *in vivo*. Furthermore, Fahrer and Tubiana (1976) proposed surgical mobilization of the thenar "lumbricals" in conjunction with the PL terminal tendon as a complex to restore functional thenar abduction movements in patients with thenar paralysis; however, an established synergy, viable PL tendon, and adequate PL muscle mass may be required to achieve adequate force transmission to restore functional thenar movement capacity.

3.4.2.2   Abductor Pollicis Longus & Abductor Pollicis Brevis

Beyond the evidence demonstrating continuity of the PL with the APB, other known connections among extrinsic and intrinsic thumb musculature are found between the APB and abductor pollicis longus (van Oudenaarde and Oostendorp, 1995). The abductor pollicis longus located on the posterior forearm is divided into superficial and deep divisions (van Oudenaarde and Oostendorp, 1995). While the superficial division of the abductor pollicis longus inserts primarily on the first metacarpal, the deep division may have several insertions into the trapezium, joint capsule and capsular ligaments (van Oudenaarde and Oostendorp, 1995). Most notably, the deep division of the abductor pollicis longus consistently inserts into a radial muscle belly of the APB through an accessory tendon (range: 64-84% of cases) (Fahrer, 1977, Baba, 1954, Moore et al., 2017b, van Oudenaarde and Oostendorp, 1995). Although Le Double (1897) considered the connection between the APB and abductor pollicis longus as a malformation, surgical observations in stenosing tenosynovitis at the wrist (De Quervain's disease) indicate that variation in the abductor pollicis longus tendon is the rule rather than exception with ≥ 2 accessory tendons to the APB occurring in 76% of reported cases (Bahm et al., 1995). Failure to adequately release all abductor pollicis longus accessory tendons from the first dorsal compartment may result in incomplete tendon decompression leading to persistent wrist pain after surgical treatment (Patel et al., 2013). Along with receiving radial arterial branches, the radial APB muscle belly may receive radial innervation from the superficial

branch as observed in four cases of a small sample of dissected hands (n=10) (Fahrer, 1977), indicating that the APB may receive dual motor innervation from both the median and radial nerves in some individuals. However, it was not confirmed whether the superficial branches of the radial nerve consisted of motor neurons (Fahrer, 1977). Therefore, the several APB muscle bellies originating from the tendons of extrinsic forearm musculature suggests that fine thenar motor movements may function through a series of digastric muscular complexes *in vivo*.

3.5   Conclusion

The disparate fiber type proportions in the APB_D compared to APB_{ND} fascicles provide further support of the PL and APB in providing significant strength contributions to the thenar eminence based on a digastric relationship *in vivo*. The presence of a rudimentary PL morphological tendon relationship with APB musculature may prolong the motor learning and functional retraining of thenar movements from PL opponensplasty surgery, if a sufficient functional synergy fails to develop *in vivo*.

3.6   References

Andersen JL, Terzis G, Kryger A. 1999. Increase in the degree of coexpression of myosin heavy chain isoforms in skeletal muscle fibers of the very old. Muscle Nerve 22:449-454.

Baba MA. 1954. The accessory tendon of the abductor pollicis longus muscle. Anat Rec 119:541-547.

Bahm J, Szabo Z, Foucher G. 1995. The anatomy of de Quervain's disease. A study of operative findings. Int Orthop 19:209-211.

Berger MJ, Doherty TJ. 2010. Sarcopenia: prevalence, mechanisms, and functional consequences. Interdisciplinary topics in gerontology 37:94-114.

Bottinelli R, Canepari M, Pellegrino MA, Reggiani C. 1996. Force-velocity properties of human skeletal muscle fibres: myosin heavy chain isoform and temperature dependence. J Physiol 495 (Pt 2):573-586.

Camitz H. 1929. Surgical treatment of paralysis of opponens muscle of thumbs. Acta Chir Scand 65:77-81.

Durban CM, Antolin B, Sau CY, Li SW, Ip WY. 2017. Thumb Function and Electromyography Result after Modified Camitz Tendon Transfer. J Hand Surg Asian Pac Vol 22:275-280.

Fahrer M. 1977. On the form and function of the abductor pollicis brevis muscle. Aust N Z J Surg 47:243-247.

Fahrer M, Tubiana R. 1976. Palmaris longus, anteductor of the thumb. Hand 8:287-289.

Foucher G, Malizos C, Sammut D, Braun FM, Michon J. 1991. Primary palmaris longus transfer as an opponensplasty in carpal tunnel release. A series of 73 cases. J Hand Surg Br 16:56-60.

Gangata H, Ndou R, Louw G. 2010. The contribution of the palmaris longus muscle to the strength of thumb abduction. Clin Anat 23:431-436.

Gilroy A. 2013. Anatomy An Essential Textbook. New York: Thieme Medical Publishers.

Hepple RT, Rice CL. 2016. Innervation and neuromuscular control in ageing skeletal muscle. J Physiol 594:1965-1978.

Hwang K, Huan F, Kim DJ. 2013. Muscle fibre types of the lumbrical, interossei, flexor, and extensor muscles moving the index finger. J Plast Surg Hand Surg 47:268-272.

Johnson MA, Polgar J, Weightman D, Appleton D. 1973. Data on the distribution of fibre types in thirty-six human muscles. An autopsy study. J Neurol Sci 18:111-129.

Kaplan EB. 1984. Kaplan's functional and surgical anatomy of the hand. Philadelphia: Lippincott Williams & Wilkins.

Kato N, Yoshizawa T, Sakai H. 2014. Simultaneous modified Camitz opponensplasty using a pulley at the radial side of the flexor retinaculum in severe carpal tunnel syndrome. J Hand Surg-Eur Vol 39:632-636.

Le Double AF. 1897. Traité des variations du système musculaire de l'homme et de leur signification au point de vue de l'anthropologie zoologique. Paris: Schleicher frères.

Macdougal BA. 1995. Palmaris longus opponensplasty. Plast Reconstr Surg 96:982-984.

Monemi M, Thornell L, Eriksson P. 1999. Diverse changes in fibre type composition of the human lateral pterygoid and digastric muscles during aging. J Neurol Sci 171:38-48.

Moore CW, Beveridge TS, Rice CL (2017a) Fiber type composition of the palmaris brevis muscle: implications for palmar function. *J Anat,* **231,** 626-633.

Moore CW, Fanous J, Rice CL (2017b) Revisiting the Functional Anatomy of the Palmaris Longus as a Thenar Synergist. *Clin Anat*.

Moore KL, Dalley AF, Agur AMR. 2014. Clinically Oriented Anatomy, 7th ed. Philadelphia Lippincott Williams & Wilkins.

Napier JR. 1952. The attachments and function of the abductor pollicis brevis. J Anat 86:335-341.

Park IJ, Kim HM, Lee SU, Lee JY, Jeong C. 2010. Opponensplasty using palmaris longus tendon and flexor retinaculum pulley in patients with severe carpal tunnel syndrome. Arch Orthop Trauma Surg 130:829-834.

Patel KR, Tadisina KK, Gonzalez MH. 2013. De Quervain's Disease. Eplasty 13:ic52.

Pette D, Staron RS. 2000. Myosin isoforms, muscle fiber types, and transitions. Microsc Res Tech 50:500-509.

Pette D, Staron RS. 2001. Transitions of muscle fiber phenotypic profiles. Histochem Cell Biol 115:359-372.

Round JM, Jones DA, Chapman SJ, Edwards RH, Ward PS, Fodden DL. 1984. The anatomy and fibre type composition of the human adductor pollicis in relation to its contractile properties. J Neurol Sci 66:263-272.

Rymer B, Thomas PB. 2016. The Camitz transfer and its modifications: a review. J Hand Surg Eur Vol 41:632-637.

Schroeder KL, Rosser BW, Kim SY. 2014. Fiber type composition of the human quadratus plantae muscle: a comparison of the lateral and medial heads. J Foot Ankle Res 7:54.

Simard T, Roberge J. 1988. Human abductor pollicis brevis muscle "divisions" and the nerve hila. Anat Rec 222:426-436.

Sooriakumaran P, Sivananthan S. 2005. Why does man have a quadratus plantae? A review of its comparative anatomy. Croat Med J 46.

Standring S, Gray H. 2008. Gray's anatomy: the anatomical basis of clinical practice, 40th, anniversary ed. Edinburgh: Churchill Livingstone/Elsevier.

Terrono AL, Rose JH, Mulroy J, Millender LH. 1993. Camitz palmaris longus abductorplasty for severe thenar atrophy secondary to carpal-tunnel syndrome. J Hand Surg-Am 18a:204-206.

van Oudenaarde E, Oostendorp RAB. 1995. Functional-Relationship between the Abductor Pollicis Longus and Abductor Pollicis Brevis Muscles - an Emg Analysis. J Anat 186:509-515.

Chapter 4

4 Functional Anatomy of the Palmaris Brevis: Grasping for Answers[3]

4.1 Introduction

The palmaris brevis (PB) is a small muscle of variant morphology originating from the palmar aponeurosis to insert in the skin and fascia of the medial palm (Przystasz, 1977). The PB is uniquely innervated by the only motor component of the superficial branch of the ulnar nerve. Clinically, the innervation of the PB facilitates diagnosis of the site of ulnar nerve lesion at the wrist based on whether function to the PB is affected or remains intact (PB sign; Pleet & Massey, 1978). Interestingly, Andreas Vesalius overlooked the PB in his classical dissections of the human body perhaps due to its subcutaneous location (Tubbs et al. 2007). Unlike the relatively frequent absence of the palmaris longus (PL; ~14%; Moore et al. 2014), the PB is rarely absent (~ 3%) in humans (Przystasz, 1977). The PL is well developed in mammalian species that use the forelimb for weight-bearing and ambulation, and may explain its regression in humans (Stecco et al. 2009); however, the PB may still provide a functional role based on its position in the palm.

Several researchers have postulated various functions of the PB, ranging from deepening the palm to aiding in palmar grip; protecting the neurovasculature of the ulnar canal (Shrewsbury et al. 1972; Przystasz, 1977); and preventing the displacement of the hypothenar fat pad during grasping (Kirk, 1924). Cadaveric studies have investigated the gross anatomy of the PB, including descriptions of its muscle width, length of attachments at points of origin and insertion (Shrewsbury et al. 1972; Chiou-Tan et al.

---

[3] A version of this chapter has been published. Used with permission from John Wiley and Sons Inc.

Moore CW, Rice CL. 2017. Structural and functional anatomy of the palmaris brevis: grasping for answers. J Anat 231:939-946.

1998), and its variant morphology (Przystasz, 1977; Nayak & Krishnamurthy, 2007), yet morphological measures *in vivo* of PB muscle length (M_L) and thickness (M_T) during rest and contraction at the ulnar canal have not been assessed. Investigating PB muscle architecture during dynamic contractions using ultrasound imaging provides insight as to whether the PB acts as a protective muscular barrier or simply tenses with no significant change in M_L or M_T.

Surveying several texts and clinical electromyographic (EMG) investigations of the PB reveals a disparity in the hand movement necessary to evoke its muscle activity. Specific movements of the fifth digit (abduction, flexion, opposition; Serratrice et al. 1995; Chiou-Tan et al. 1998; Standring, 2008; Perotto et al. 2011) or applying mechanical pressure superficial to the pisiform bone (Serratrice et al. 1995; Liguori et al. 2003; Perotto et al. 2011) have been described as actions that evoke PB contraction. Furthermore, some PB descriptions from clinical case reports state that the PB is not under voluntary control (Serratrice et al. 1995; Iyer, 1998; Eswaradass et al. 2014), which may suggest a smooth muscle composition, under a conditioned (Montagu, 1952) or reflexive control (Boynton-Lee, 1888), like those found in other panniculus carnosus derivatives such as the dartos or corrugator cutis ani muscles (Patil, 2013). Although PB EMG has been investigated in clinical examinations, a systematic investigation of PB EMG activity during simple movements of the fifth digit and functional grasping tasks has yet to be explored. Furthermore, a histological investigation of the PB has yet to confirm the presence of smooth or striated muscle fibers, which could provide insight regarding PB activation through voluntary or involuntary means. Thus, the purpose of this study was to investigate the EMG activity of the PB as well as muscle architecture changes during specific hand movements to provide further insight into PB function in the palm. The structure of the PB was also examined histologically for the presence of skeletal muscle fibers.

4.2   Materials and Methods

4.2.1   Participants

Twelve healthy participants (11 men and one woman; age: 27 ± 4 years; height: 182 ± 7 cm; weight: 86 ± 11 kg) volunteered to participate in this study. PB EMG recordings could not be obtained from one participant and he was removed from the EMG portion of the study. The local research ethics board approved the study procedures, and informed written consent was obtained from each participant prior to testing. The study protocol required participants to attend two separate experimental sessions: (1) PB EMG session followed by (2) a PB ultrasound investigation. Session one required only visualization of the PB using ultrasound imaging, whereas the quantitative ultrasound measurements were collected in session two. The ultrasound investigation was performed in both the left and right hands, whereas the EMG investigation was restricted to the dominant hand (left handed: 1, right handed: 11) to minimize the discomfort associated with indwelling EMG insertion into the glabrous skin of the hand. Furthermore, PB muscle morphology is typically more developed in the right hand (Przystasz, 1977), which could potentially yield better EMG recordings than in the left hand.

4.2.2   Electromyography Experimental Setup

The medial palmar skin was swabbed with 70% ethanol prior to the EMG procedures. Custom-made indwelling fine wire, hooked-tipped electrode pairs (50 μm; California Fine Wire Company, Grover Beach, California, USA) were inserted into the PB via a small-diameter hypodermic needle (27G × 1/2; Becton Dickinson PrecisionGlideTM Needle, REF 305109; Basmajian & Stecko, 1962) using an approach angle parallel to the palm. Approximately 5 mm of insulation was removed from the fine wires, thereby exposing an adequate recording surface to create a global indwelling EMG interference pattern. Chiou-Tan et al. (1998) identified the PB from the abductor digiti minimi based on single motor unit rise times using a clinical needle examination. Because we could not determine MU rise times due to the use of global EMG recordings,

ultrasound imaging was used to visualize the location of the PB relative to the skin prior to needle insertion. A common ground electrode was placed on the skin at the metacarpophalangeal (MCP) joint of the thumb. Indwelling electrodes are advantageous over surface electrodes for PB recordings, because cross-talk from the hypothenar muscles may interfere with the EMG signal recorded at the skin surface. Furthermore, the indwelling fine wires allow participants to grasp objects while performing functional movements, which cannot be achieved when using clinical concentric needle electrodes.

The global EMG recorded from the indwelling fine wires was pre-amplified (1000×; NeuroLog System NL844 Pre-amplifier), band-pass filtered (10 Hz–10 kHz; 60 Hz notch filter) and sampled at 2500 Hz before being converted to a digital signal using a 16-bit analog-to-digital converter (Micro 1401 mkII board; Cambridge Electronic Design, CED). All EMG data analyses were performed offline using Spike2 software (v.7.0; CED, Cambridge, UK).

4.2.3   Prehensile and non-Prehensile Tasks

Participants were instructed to perform a series of movements of the fifth digit and grasping tasks while PB EMG activity was recorded from the indwelling fine wires. The non-prehensile tasks involved specific movements of the fifth digit: abduction, flexion at MCP joint only, and opposition to the thumb (Figure. 4.1). Abduction and flexion of the fifth digit were performed against a rigid surface to provide resistance to the movement. The functional tasks required participants to make two prehensile movements: grasping the shaft of a carpenter's hammer and tennis ball using a power grip and spherical grip, respectively (Napier, 1956; Figure 4.1). Participants were instructed to make maximal contractions during all movements, and each task was held isometrically for a minimum of three seconds.
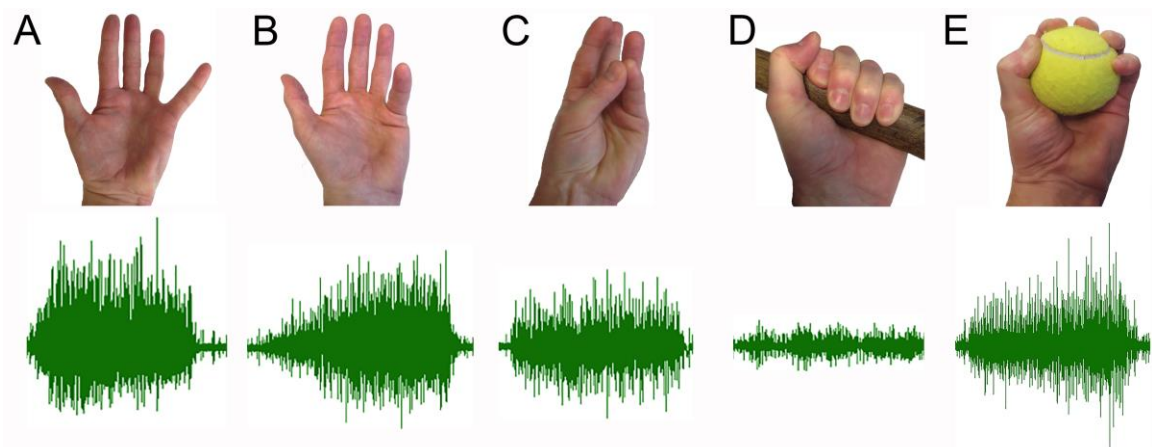
Figure 4.1 Unprocessed Electromyogram Recorded from the Palmaris Brevis during Maximal Effort Movements of the Fifth Digit and Grasping Tasks.

(A) Abduction of the fifth digit; (B) Fifth digit flexion (metacarpophalangeal joint only); (C) Opposition; (D) Power grip; (E) Spherical grip.

4.2.4   Electromyography Normalization

From the unprocessed EMG signal, the average root mean square (EMG_{RMS}) was calculated over a constant time interval of three seconds for all non-prehensile and prehensile tasks. To compare relative EMG_{RMS} recorded in each task among participants, the PB EMG_{RMS} recorded during each task was normalized to 100% of the three seconds PB EMG_{RMS} evoked during maximal abduction of the fifth digit. Normalization of EMG signals to maximal peak levels is a reliable and valid method to compare relative values of EMG activity among participants (Halaki & Ginn, 2012).

4.2.5   Ultrasound Imaging

Visualization of the PB prior to hypodermic needle insertion and dynamic morphological changes in PB architecture, M_L and M_T, were imaged using a Vivid-7 ultrasound system (GE Healthcare, Mississauga, ON, Canada; linear array probe: GE model M12L, 4.9 mm, 5–13 MHz). A single investigator with experience in musculoskeletal ultrasound acquired PB images from the palms using the following ultrasound settings: probe frequency $= 11.4$ MHz, frame rate: 19.0, power $= -2$ dB, dynamic range $= 9$, depth $= 4.0$ cm. To ensure adequate standoff distance for imaging superficial palmar structures, a liberal application of ultrasound gel (Aquasonic 100 Ultrasound transmission gel, Parker Laboratories) was applied and the ultrasound probe frequency was increased to its optimal setting (11.4 MHz). Multiple focus points were set on the ultrasound image within a two centimeter depth from the surface as the PB was typically located within this depth (Figure 4.4). Each hand was supported and fully supinated during the imaging. The ultrasound probe was rotated until the PB muscle fibers could be viewed in-plane and were visible from origin to insertion in the longitudinal plane. Static ultrasound images of the PB at rest were acquired from each participant at the point of maximal PB M_T. PB images during maximal contraction were acquired at the same position of maximal PB M_T. PB muscle contraction was imaged longitudinally during maximal abduction of the fifth digit (Figure 4.4). To prevent the

ultrasound probe from moving, participants were instructed to gradually abduct the fifth digit until maximum abduction was achieved.

Ultrasound images were exported from the ultrasound unit and analyzed using OsiriX imaging software (version. 8.0.2, Geneva, Switzerland). PB muscle borders were determined by visual inspection using the echogenicity of both epimysium surrounding the muscle, and the perimysium producing linear reflections surrounding and within the muscle along the longitudinal axis (Figures 4.2 and 4.4; Pillen, 2010). M_T and M_L measurements were performed using the length tool in OsiriX. Measurement lines were drawn perpendicular to the superficial and deep borders, and along the long axis of the muscle to determine M_T and M_L measures, respectively.
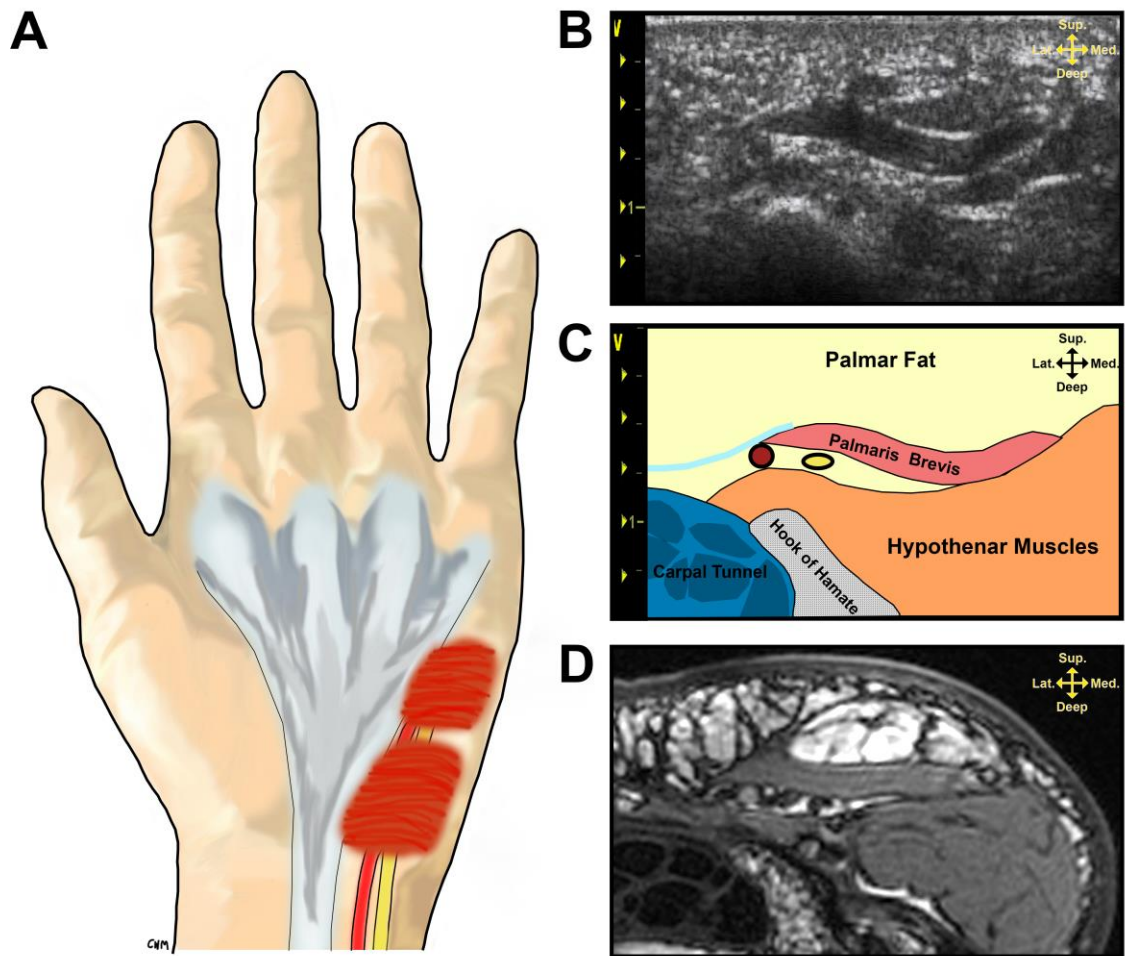
Figure 4.2 Palmaris Brevis (PB) Gross Morphology and its Ultrasound Appearance at the Level of the Hook of the Hamate.

(A) Illustration demonstrating the spatial relationship of the PB to the ulnar artery and nerve. (B) Ultrasound appearance of the PB at rest. (C) Schematic depiction of palmar structures located in the ultrasound image from (B). (D) Axial T2-weighted magnetic resonance image of the PB at similar location to the ultrasound in (B). Note the following structures in (C): palmar aponeurosis (turquoise), ulnar artery (red), ulnar nerve (yellow)

4.2.6   Histological Analysis

Palmaris brevis specimens were harvested from the hands of four (three fresh frozen, one formalin-embalmed) cadavers [four left hands, four right hands; mean age at death: 78 years (range: 44–88 years)]. Cadaveric specimens were obtained with permission from the body bequeathal program at the University of Western Ontario, London, ON, Canada, and approved for research use by the Committee for Cadaver Use in Research (REF#: 21092016). Tissue samples were immediately immersed in a 10% formalin solution for a minimum of 24 hours prior to paraffin embedding. Specimens were sectioned 5 μm thick using a Microm HM-325 Microtome. Tissues were mounted on slides and warmed at 60 °C for 30 min. Longitudinal- and transverse-orientated PB tissue samples were stained with hematoxylin-eosin and hematoxylin only, respectively. Histology slides were imaged using a Zeiss AxioCam MRc microscope camera.

4.2.7   Statistical Analysis

Data were analyzed using spss statistical software (Version 24, SPSS, Chicago, IL, USA). A Shapiro–Wilk test determined that the normalized EMG during the spherical grip task was not normally distributed. Therefore, a non-parametric test (Friedman) was used to determine whether a significant main effect was present in the % PB $EMG_{RMS/ABD}$ recorded during the hand positions. Pairwise comparisons were performed as a *post hoc* analysis (Wilcoxon signed-ranks test) of a significant main effect during the five hand movements (fifth digit: abduction, flexion, opposition; and power and spherical grips). For the ultrasound measures, a Shapiro–Wilk test determined that the variable, M_T (right hand, contracted state), was not normally distributed. Therefore, a non-parametric *t*-test (Wilcoxon signed-rank test) was used to determine whether a statistically significant change occurred in mean PB M_L and M_T, at rest and during contraction of both the left and right hands. Effect sizes (*r*) from Wilcoxon signed-rank tests were calculated manually using Microsoft Excel software (version 14.5.8). The effect sizes are categorized as small (r = 0.1), medium (r = 0.3), and large (r = 0.5). A Bonferroni

correction was applied to both the EMG and ultrasound data to account for multiple statistical comparisons. All data are presented as means ± SD.

4.3   Results

4.3.1   Electromyography

Of the two contraction types used in clinical examination, the PB EMG$_{RMS}$ evoked during abduction of the fifth digit was selected as a method of normalization as this contraction task evoked the greatest PB muscle activity in seven of the 11 (~60%) participants (Figure 4.3). In the remainder of subjects, flexion of the fifth digit evoked the greatest PB EMG activity and was only 5% less compared with the % PB EMG evoked during fifth digit abduction. An analysis of main effects revealed a significant difference in the % PB EMG recorded during prehensile and non-prehensile hand movements [$\chi 2$ (4) = 23.799, $P = 0.0001$]. *Post hoc* analysis with Wilcoxon signed-rank tests was conducted with a Bonferroni correction applied, resulting in a significance level set at $P = 0.005$.

There were no significant differences in the mean PB muscle activity between abduction and flexion of the fifth digit ($P = 0.44$, $r = 0.16$). The PB muscle activity recorded during opposition was significantly reduced by 29% compared with fifth digit flexion ($P = 0.004$, $r = 0.61$). The opposition task produced 34% less PB muscle activity compared with fifth digit abduction, but did not reach statistical significance ($P = 0.016$, $r = 0.51$). Similarly, the power grip task produced 39% less PB muscle activity compared with the spherical grip, but did not reach statistical significance ($P = 0.011$, $r = 0.54$). The PB muscle activity recorded during the power grip was significantly reduced by 59% and 54% compared with abduction ($P = 0.003$, $r = 0.63$) and flexion of the fifth digit ($P = 0.003$, $r = 0.62$), respectively (Figure 4.3). The PB muscle activity during the spherical grip was 20% and 15% less than abduction ($P = 0.13$, $r = 0.32$) and flexion of the fifth digit ($P = 0.17$, $r = 0.29$), respectively; however, these comparisons were not statistically significant ($P > 0.005$). Similarly, the PB muscle activity recorded during the

opposition task was 14% lower compared with the spherical grip, but did not reach statistical significance ($P = 0.25$, $r = 0.25$).
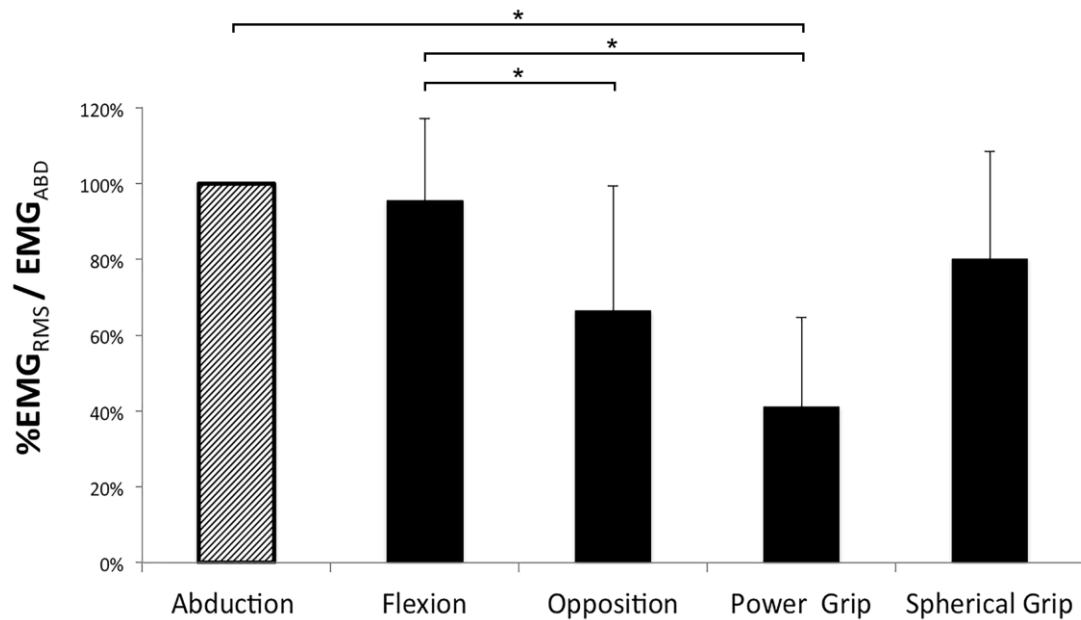
Figure 4.3 Palmaris Brevis (PB) Muscle Activity During Maximal Effort Movements of the Fifth Digit and Functional Grasping Tasks.

The PB muscle activity recorded from each task is displayed as a percentage of PB EMG_{RMS} normalized to the PB muscle activity recorded during maximal abduction of the fifth digit (EMG_{ABD}). Non-prehensile tasks (fifth digit): abduction, flexion, opposition; prehensile tasks: power grip (carpenter's hammer), spherical grip (tennis ball). EMG_{RMS}, root mean square electromyography; all data presented as means $\pm$ SD; * denotes $P < 0.005$. Statistical trends were observed in the comparisons between both fifth digit abduction and opposition ($P = 0.016$), and the spherical and power grips ($P = 0.011$).

4.3.2   Ultrasound Imaging

Pairwise comparisons using Wilcoxon signed-rank tests were conducted with a Bonferroni correction applied, resulting in a significance level set at $P = 0.006$. During abduction of the fifth digit, the mean length of the PB decreased by $28 \pm 11\%$ (range: 8–40%, $P = 0.002$, $r = 0.62$) and $32 \pm 5\%$ (range: 18–59%, $P = 0.002$, $r = 0.62$) in the left and right hands, respectively (Table 4.1). PB muscle thickness increased by $68 \pm 30\%$ (range: 23–130%, $P = 0.002$, $r = 0.62$) and $85 \pm 44\%$ (range: 39–162%, $P = 0.002$, $r = 0.63$) in the left and right hands, respectively (Table 4.1). There were no significant differences between resting and contracted states between the left and right hands ($P > 0.006$). The ulnar artery and nerve were located deep to the PB in all ultrasound images, and these structures were identifiable in both images acquired at rest (Figure 4.4)

Table 4.1 Ultrasound-derived Measures of Palmaris Brevis Muscle Architecture

(n = 12)	Left Hand		Right Hand	
	Rest	Contraction	Rest	Contraction
Length (cm)	2.0 ± 0.3 (1.5 – 2.5)	1.4 ± 0.2* (1.2 – 1.8)	2.0 ± 0.3 (1.1 – 2.5)	1.3 ± 0.3* (0.9 – 1.7)
Thickness (mm)	1.9 ± 0.6 (1.3 – 2.9)	3.1 ± 1.0* (1.9 – 4.7)	1.6 ± 0.5 (1.1 – 3.0)	3.0 ± 1.7* (1.7 – 7.7)

Contraction: maximal abduction of the fifth digit. Values are means $\pm$ SD
* Denotes significant from resting condition using Bonferroni correction factor
($P<0.006$)
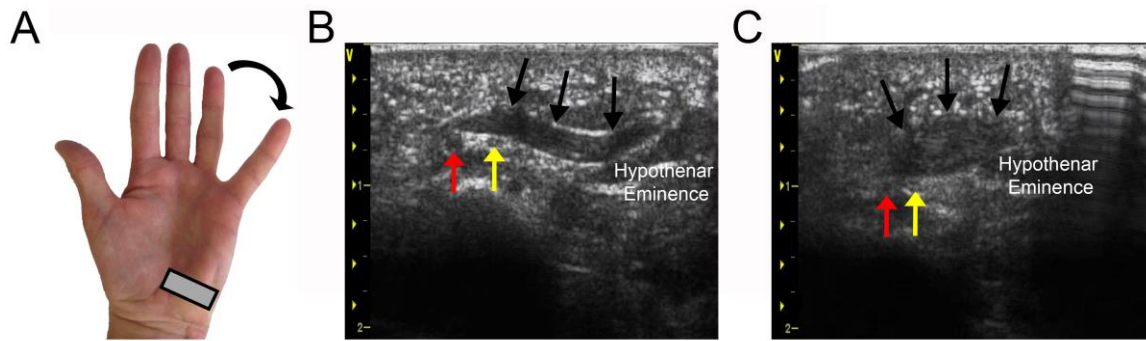
Figure 4.4 Visualizing Dynamic Changes in Palmaris Brevis (PB) Muscle Architecture during Abduction of the Fifth Digit using Ultrasound Imaging.

(A) Ultrasound probe (gray rectangle) aligned longitudinally with the PB muscle. (B) PB appearance at rest. (C) PB appearance during contraction. Ulnar artery (red arrow), ulnar nerve (yellow arrow), superficial border of the PB (black arrow).

4.3.3   Histology

Histological investigation of the cadaveric PB tissue revealed typical features of skeletal muscle tissue, striations and peripherally located nuclei, when viewed in longitudinal and cross-sectional orientations, respectively (Figure 4.5).
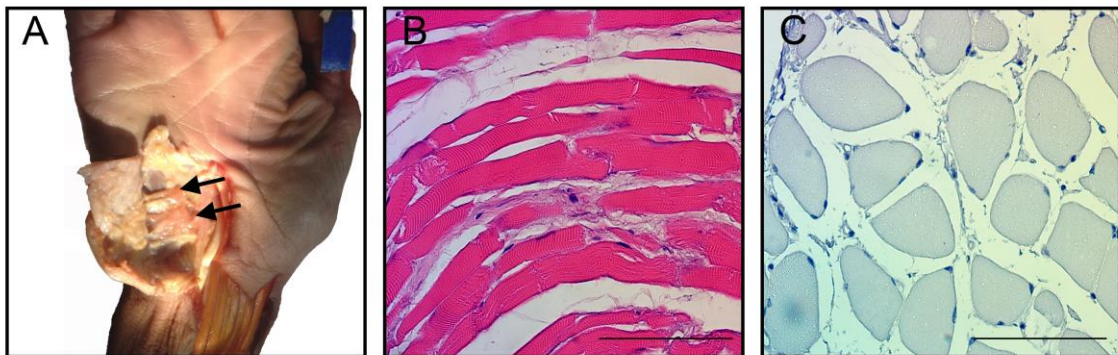
Figure 4.5 Histological Appearance of the Palmaris Brevis (PB).

(A) PB harvested from a fresh frozen cadaveric specimen (black arrows). (B) PB muscle fibers oriented longitudinally (hematoxylin–eosin stain). (C) PB muscle fibers oriented in cross-section (hematoxylin stain). Note the presence of muscle fiber striations, and peripherally located nuclei typical of skeletal muscle. Scale bar: 100 μm

4.4   Discussion

The current study examined the PB EMG and muscle architecture during specific movements of the fifth digit and during functional grasping tasks. A few studies have examined single motor unit PB EMG *in vivo* in healthy participants (Chiou-Tan et al. 1998), during clinical examination (Serratrice et al. 1995; Liguori et al. 2003; Tarsy et al. 2004; Eswaradass et al. 2014), and PB muscle architecture from cadavers (Shrewsbury et al. 1972; Przystasz, 1977; Chiou-Tan et al. 1998). We investigated PB global EMG from a functional perspective and imaged the PB muscle during dynamic contractions using ultrasound. The results indicated that PB EMG activity is under voluntary control and is highly dependent on movements of the fifth digit. The PB muscle is capable of significant changes in muscle architecture during voluntary muscle contraction. In addition, histological analyses indicated that the PB is composed of striated skeletal muscle fibers and should be in under the control of the somatic nervous system.

For resting PB M_T and M_L, the ultrasound-determined values (Table 4.1) are in agreement with measurements from embalmed (M_T: 1–3 mm; Przystasz, 1977) and fresh (mean M_L: 2.1 cm; Kim et al. 2017) cadaveric specimens. Although a reliability study assessing the inter- and intra-rater reliability of the ultrasound-derived PB measurements was not performed, the results were comparable to those data obtained from cadavers (Przystasz, 1977; Kim et al. 2017). An inter- and intra-rater reliability study of the PB validated against magnetic resonance images from the same participants might be useful for future studies. From a functional perspective, a resting M_T of 1–3 mm may be insufficient to protect the neurovasculature of the ulnar canal. Passive movements in which the palm is simply resting on a surface will likely not produce PB muscle contraction, thereby providing minimal protection during prolonged palmar compression. The susceptibility of the superficial branch of the ulnar nerve to compression injury may explain the spontaneous intermittent PB contractions in occupations requiring long hours using a computer mouse and keyboard (PB spasm syndrome) (Liguori et al. 2003). The etiology of PB spasm syndrome remains unclear but may involve peripheral nerve stretch injury, or ulnar nerve entrapment at the wrist (Serratrice et al., 1995). In recreational and

elite-level cyclists, the PB may not provide the necessary relief from prolonged overlying pressure during conditions in which the palm is passively resting on a surface such as a classic-style handlebar typical of a road bicycle (Slane et al. 2011). An absence of PB muscle activity and the constant pressure imposed on the hypothenar eminence may require cyclists to wear protective gloves to prevent compression-related nerve injuries.

When the PB contracts, it visibly draws the skin of the hypothenar eminence radially producing a dimpling effect on the ulnar margin of the hand. Ultrasound imaging allows for improved visualization of dynamic PB contraction and the relationship to the ulnar neurovasculature beyond dimpling on the skin surface, or static cadaveric and magnetic resonance imaging investigations. In all subjects, maximal abduction of the fifth digit produced significant changes in PB muscle architecture resulting in a relatively thick muscular barrier between the neurovasculature of the ulnar canal and the palmar hypothenar fat (Figure 4.4). The unique quantification through ultrasound showed significant changes in PB M_T of 68% and 85%, in the left and right hands, respectively, indicating that the muscle is capable of forming a relatively thick muscular barrier to the neurovasculature of the ulnar canal but only during hypothenar muscle contraction. Kirk (1924) proposed that the PB is essential for anchoring the mobile hypothenar fat pad during grasping movements. Considering this potential muscular barrier in conjunction with the hypothenar fat pad found adjacent to the PB suggests a protective function to the ulnar nerve and ulnar artery. Although we imaged the PB during abduction of the fifth digit, we expect similar changes in PB muscle architecture during fifth digit flexion at the MCP joint, and during the spherical grip based on the PB muscle activity evoked during these tasks. Functional movements that sufficiently activate the intrinsic muscles of the hypothenar eminence will likely produce PB muscle contraction.

The power grip produced the least amount of PB muscle activity when grasping the carpenter's hammer. During the power grip, finger flexion is achieved mainly by the forearm flexors (flexor digitorum superficialis, flexor digitorum profundus) while relying on the thenar and hypothenar intrinsic hand muscles for support and stabilization (Napier,

1956). The hypothenar eminence acts as a muscular cushion to the hammer during this functional task (Napier, 1956). The PB EMG activity was reduced significantly during the power grip as grasping the carpenter's hammer does not require the fifth digit to deepen the palm to achieve a 'cupping' action typical of a spherical grip. Thus, the PB may not provide a protective benefit to the ulnar canal neurovasculature during this functional task based on the reduced PB EMG recorded.

The spherical grip is considered a powerful grip with greater precision and reliance on the intrinsic hand muscles for object manipulation compared with grasping the carpenter's hammer (Napier, 1956). During the spherical grip, the hand is positioned by producing a 'cupping' action in which the thumb and the fifth digit are in a position of support. To achieve this position, the fifth digit moves by contracting all hypothenar muscles in a combination of flexion, abduction, and opposition. This coordinated hypothenar muscle contraction would explain the large PB muscle activity (80%) as the fifth digit supports the ball and resists the movement of the thumb. The PB muscle activity recorded during the spherical grip supports the postulate by Shrewsbury et al. (1972) of the protective benefit of the PB during functional tasks associated with repetitive intermittent trauma or contact associated with prehensile maneuvers. Therefore, the PB may provide a protective benefit when the hand repeatedly grasps a spherical-shaped object such as catching a baseball or grasping various-sized and shaped elements during climbing tasks.

4.4.1   Palmaris Brevis Function in Palmar Grip

Textbooks typically describe the function of the PB as deepening the palm to aid in palmar grip (Standring, 2008; Moore et al. 2014); however, the extent that the PB deepens the palm seems insignificant to the depth created by the muscles of thenar and hypothenar eminences. Shrewsbury et al. (1972) disagreed with the interpretation that the PB improves palmar grip as the muscle is found in the forelimbs of quadriped mammals such as the cat, mouse, and opossum species, which are not capable of grasping objects. This idea seems probable considering the PB can be excised for surgical reconstruction of

palmar thumb defects (Ueda & Inoue, 1994) or is divided during standard open carpal tunnel release surgery (Rodner & Katarincic, 2006; Malhotra et al. 2007); however, a systematic description of the functional limitations in grip ability and susceptibility to compression-related deficits due to the absence of a PB has yet to be explored. Despite the relatively unknown functional limitations imposed by PB absence, some clinicians have proposed preserving this muscle during surgical procedures based on its proposed protective functions of ulnar neurovasculature of the palm (Shrewsbury et al. 1972) and use in diagnosing the location of an ulnar neuropathy at the wrist (Pleet & Massey, 1978; Saadeh, 1989). Compared with an open approach to carpal tunnel release surgery, an improved recovery time of grip and pinch strength using the endoscopic approach has been attributed by some to the preservation of both the PB and palmar fascia (Malhotra et al. 2007). The current study results provide support for the preservation of the PB during surgical procedures, especially in individuals whose palms are frequently subjected to repetitive trauma or compression whether through sport or occupational demands.

4.4.2   Involuntary Palmaris Brevis Activation

Although PB EMG and PB contraction could be evoked during specific movements of the hand, the PB contractions were not in isolation but occurred in conjunction with hypothenar muscle contractions. The idea that the PB is not under voluntary control has likely been precipitated by historical reports of automatic reflex contraction of the PB initially referred to as the palm reflex (Boynton-Lee, 1888; Montagu, 1952). Boynton-Lee (1888) reported involuntary reflexive contraction of the PB by pinching of the skin above the pisiform bone or by firm mechanical compression of the same region. Montagu (1952) reported that the PB muscle could be involuntarily activated by compressing the ulnar nerve at the wrist, or by conditioned response producing PB contraction without any tactile stimulation. It is unknown whether the PB response is a physiological reflex by definition, acting in a spinal loop, or whether compression of the pisiform bone produces an involuntary discharge, or spasm, by indirectly compressing the superficial branch of the ulnar nerve. Based on the evidence

provided by histological examination, the PB is under voluntary control as it contains skeletal muscle fibers and thus is capable of voluntary contraction.

4.5 Conclusion

Although the PB is a small rudimentary muscle of variant morphology, it is capable of significant changes in muscle architecture overlying the neurovasculature of the ulnar canal. The PB EMG and ultrasound imaging findings support cadaveric observations that the PB can function as a potential protective muscular barrier, but only when actively engaging the fifth digit either independently or during functional movements. Although involuntary contraction of the PB may be possible through potential reflexive or indirect mechanical compression of the ulnar nerve, the PB muscle is a dynamic structure that can be voluntarily contracted in conjunction with muscles of the hypothenar eminence. This study further supports suggestions that the PB should be spared during surgical interventions based on its proposed protective function to the ulnar artery and nerve in the palm.

4.6   References

Basmajian JV, Stecko G. 1962. A New Bipolar Electrode for Electromyography. Journal of applied physiology 17:849-849.

Boynton-Lee HB. 1888. Palm Relfex (?). The Lancet 2:1267.

Chiou-Tan FY, Reno SB, Magee KN, Krouskop TA. 1998. Electromyographic localization of the palmaris brevis muscle. American journal of physical medicine & rehabilitation / Association of Academic Physiatrists 77:243-246.

Eswaradass PV, Kalidoss R, Ramasamy B, Gnanashanmugham G. 2014. Familial palmaris brevis spasm syndrome. Ann Indian Acad Neurol 17:141-142.

Halaki M, Ginn K. 2012. Normalization of EMG Signals: To Normalize or Not to Normalize and What to Normalize to? In: Naik G, editor. Computational Intelligence in Electromyography Analysis - A Perspective on Current Applications and Future Challenges: InTech.

Iyer VG. 1998. Palmaris brevis sign in ulnar neuropathy 1998. Muscle & nerve 21:675-677.

Kaplan EB. 1984. Kaplan's functional and surgical anatomy of the hand: Lippincott Williams & Wilkins.

Kim DH, Bae JH, Kim HJ. 2017. Anatomical insights of the palmaris brevis muscle for clinical procedures of the hand. Clin Anat 30:397-403.

Kirk T. 1924. Some Points in the Mechanism of the Human Hand. Journal of anatomy 58:228-230.

Liguori R, Donadio V, Di Stasi V, Cianchi C, Montagna P. 2003. Palmaris brevis spasm: an occupational syndrome. Neurology 60:1705-1707.

Malhotra R, Kiran EK, Dua A, Mallinath SG, Bhan S. 2007. Endoscopic versus open carpal tunnel release: A short-term comparative study. Indian J Orthop 41:57-61.

Montagu MF. 1952. Conditioning of the palmaris brevis muscle. Science 115:153.

Moore KL, Dalley AF, Agur AMR. 2014. Clinically Oriented Anatomy, 7th ed. Philadelphia Lippincott Williams & Wilkins.

Napier JR. 1956. The prehensile movements of the human hand. J Bone Joint Surg Br 38-B:902-913.

Nayak SR, Krishnamurthy A. 2007. An unusually large palmaris brevis muscle and its clinical significance. Clin Anat 20:978-979.

Patil S. 2013. Clinico-anatomical Considerations Of Palmaris Brevis Muscle. International Journal of Advanced Research 1:341-344.

Perotto A, Delagi E, Iazzetti J, Morrison D. 2011. Anatomical guide for the electromyographer: the limbs and trunk, 5th ed. Springfield, IL: Charles C Thomas Publisher.

Pillen S. 2010. Skeletal muscle ultrasound. European Journal of Translational Myology 20:145-156.

Pleet AB, Massey EW. 1978. Palmaris brevis sign in neuropathy of the deep palmar branch of the ulnar nerve. Annals of neurology 3:468-469.

Przystasz T. 1977. Morphology of the palmaris brevis muscle in man. Folia Morphol (Warsz) 36:77-82.

Rodner CM, Katarincic J. 2006. Open carpal tunnel release. Techniques in orthopaedics 21:3-11.

Saadeh PB. 1989. Examination of the palmaris brevis. Muscle & nerve 12:425-426.

Serratrice G, Azulay JP, Serratrice J, Pouget J. 1995. Palmaris brevis spasm syndrome. Journal of neurology, neurosurgery, and psychiatry 59:182-184.

Shrewsbury MM, Johnson RK, Ousterhout DK. 1972. The palmaris brevis--a reconsideration of its anatomy and possible function. The Journal of bone and joint surgery American volume 54:344-348.

Slane J, Timmerman M, Ploeg HL, Thelen DG. 2011. The influence of glove and hand position on pressure over the ulnar nerve during cycling. Clin Biomech (Bristol, Avon) 26:642-648.

Standring S. 2008. Gray's Anatomy: The Anatomical Basis of Clinical Practice, 40th ed. Edinbrugh: Churchill Livingstone.

Stecco C, Lancerotto L, Porzionato A, Macchi V, Tiengo C, Parenti A, Sanudo JR, De Caro R. 2009. The palmaris longus muscle and its relations with the antebrachial fascia and the palmar aponeurosis. Clin Anat 22:221-229.

Tarsy D, Apetaurova D, Rutkove SB. 2004. Palmaris brevis spasm: An occupational syndrome. Neurology 62:838.

Tubbs RS, Louis RG, Jr., Loukas M, Gupta AA, Shoja MM, Oakes J. 2007. The first description of the palmaris brevis muscle. J Hand Surg Eur Vol 32:382-383.

Ueda K, Inoue T. 1994. The new palmaris brevis musculocutaneous flap. Ann Plast Surg 32:529-534.

Chapter 5

5 Fiber Type Composition of the Palmaris Brevis: Implications for Palmar Function[4]

5.1 Introduction

The palmaris brevis (PB) is a small muscle located superficial to the hypothenar eminence in the ulnar aspect of the palm. The morphology of the PB is variable and can be classified as either developed or regressive in form based on the course and arrangement of the muscle fibers present (Przystasz, 1977). Despite the variability in morphological appearance, the PB is rarely (~ 3%) absent in humans (Przystasz, 1977). Moreover, the PB is among several subcutaneous muscles considered to be atavistic remnants of the *panniculus carnosus*, an extensive sheet of skeletal muscle found in animal species used to remove noxious stimuli on the skin such as insects and birds (Bergman et al. 1985). In humans, other remnants of this muscle layer include the facial muscles, corrugator cutis ani, and the dartos muscle of the scrotum (Patil, 2013). Several proposed functions of the PB include deepening the palm to aid in palmar grip (Standring, 2008; Moore et al. 2014), preventing displacement of the hypothenar fat pad during compressive grasping tasks (Kirk, 1924) and protecting the ulnar nerve and artery at the wrist when grasping hard objects (Henle, 1855; Shrewsbury et al. 1972; Przystasz, 1977). Shrewsbury et al. (1972) proposed that the PB is protective of the ulnar neurovasculature during prolonged palmar compression or intermittent trauma. This is a reasonable hypothesis based on previous cadaveric studies investigating PB gross morphology; however, no studies have investigated PB tissue architecture to further

---

[4] A version of this chapter has been published. Used with permission from John Wiley and Sons Inc.

characterize its functional capabilities. Thus, it remains unknown whether the PB has the contractile or metabolic capacity to support these functional demands.

Intramuscular electromyography (EMG) is a useful technique to provide insight into the functional specialization of palmar musculature by recording muscle activation patterns during movements. The abductor pollicis longus and brevis are among several palmar muscles that have been investigated using this technique (van Oudenaarde & Oostendorp, 1995); however, EMG investigations of the PB have been limited to clinical investigations characterizing PB spasm syndrome in patients (Serratrice et al. 1995; Iyer, 1998; Liguori et al. 2003; Tarsy et al. 2004; Eswaradass et al. 2014). As an alternative to EMG, functional insight into the contractile and metabolic capabilities of a skeletal muscle can be achieved by characterizing the muscle fiber-type composition by staining for myosin heavy chain (MHC) isoforms of constituent muscle fibers using immunohistochemical methods.

In human muscle, the three major fiber types are classified as type I, type IIa and IIx, and can be further sub-classified into hybrid fibers, in which two MHC isoforms are co-expressed within a single muscle fiber (i.e. MHC type I/IIa and MHC type IIa/IIx) (Scott et al. 2001; Pette & Staron, 2000). The ability of skeletal muscle to adapt to a variety of functional demands is due to its heterogeneous fiber-type composition, and the mechanical and metabolic properties of each muscle fiber (Staron, 1997). Type I muscle fibers have an oxidative metabolism, slow shortening speed, and are fatigue-resistant, whereas type II muscle fibers have a glycolytic metabolism, fast shortening speed, and are susceptible to fatigue. Determining the fiber-type composition of the PB will provide indirect insight into its contractile and metabolic capacity and its proposed protective role during prolonged palmar compression. If the PB is capable of protecting the ulnar neurovasculature at the wrist during prolonged palmar compression, we expect to observe a large proportion of type I muscle fibers, thereby imparting fatigue-resistant properties. Therefore, the purpose of the current study was to quantify the proportion of type I, type

II and hybrid fibers using immunohistochemistry to provide insight into PB in palmar function based on its histological structure.

5.2   Materials and Methods

5.2.1   Cadaveric Specimens

Sixteen PB specimens were harvested from the hands (eight right, eight left) of eight embalmed cadavers (Mean age: 75 ± 14 years; three males, five females). Cadaveric specimens were obtained from the body bequeathal program at the University of Western Ontario, London, ON, Canada, and approved for research use by the Committee for Cadaver Use in Research (REF#: 21092016). The cadavers received through the body bequeathal program are typically embalmed within 24 h postmortem. To ensure muscle fiber type proportions were not influenced by other comorbidities such as disease, the cadaveric specimens were excluded from the investigation based on the following criteria: presence of a neuromuscular disease indicated in the cause of death report, and visible evidence of finger deformation indicating presence of rheumatoid or osteoarthritis.

5.2.2   Palmaris Brevis Morphological Variant Classification

The dissected palms of each cadaveric specimen were photographed and their PB morphology was classified, prior to tissue harvesting, based on the criteria proposed by Przystasz (1977). A single investigator with extensive experience in palmar dissection was responsible for classifying the morphological variants. These morphological forms were categorized based on the following specific features: a single muscular plate with fibers arranged in parallel or in fan-shaped arrangement (*Type A*); intermittent muscle bundles divided into two to four parts (*Type B*); a rudimentary form with one to three fibers embedded in adipose tissue (*Type C*); or a chaotic fiber arrangement interspersed with adipose tissue (*Type D*). As per Przystasz (1977), the specimens were further

grouped based on these morphological variants into developed (*Types A & B*) and regressive forms (*Types C & D*).

5.2.3   Immunohistochemistry

Whole muscle PB tissues were excised from their origin and insertions at the palmar aponeuroses and hypothenar fascial insertions, respectively. The PB specimens were carefully trimmed to remove excess adipose and connective tissues surrounding the muscle fibers. Upon harvesting, the PB tissue samples were immediately immersed in a 10% formalin solution for a minimum of 24 hours prior to processing and paraffin embedding. PB specimens were serially sectioned at a thickness of 5 μm using a microtome (Microm HM-325). All sections were heated to 37 °C for a minimum of 12 hours, and then stained using standard immunohistochemical procedures. Antigen retrieval was performed in citrate buffer (pH 6.0) in a de-cloaking chamber before blocking with 10% horse serum. Slides were incubated with mouse monoclonal antibodies specific to either MHC type I (Sigma-Aldrich NOQ7.5.4D) or MHC type II (Sigma-Aldrich MY-32) at a dilution of 1 : 3200 for one hour at room temperature, as established by preliminary titrations. The antibodies NOQ7.5.4D and MY-32 label type I (slow-twitch) fibers and all type II (i.e. type IIa and IIx) (fast-twitch) fibers, respectively. The application of the secondary antibody was completed using an ImmPRESS Anti-Mouse Ig Peroxidase Polymer Detection Kit (Vector Laboratories, Cat. No. MP-7402) and was then labeled with DAB (DAB Peroxidase Substrate Kit, 3,3′–diaminobenzidine, Vector Laboratories, Cat. No. SK-4100). All sections were counterstained using hematoxylin. Specimen-matched negative control sections underwent identical procedures, save for the application of the primary antibody. Positive controls for the experiments were performed using a section of the soleus muscle (a known MHC-type I dominant muscle), and triceps brachii muscle (a known MHC-type II dominant muscle).

5.2.4   Image Acquisition and Muscle Fiber Quantification

Images of the PB tissue sections were captured with a 14-megapixel digital USB microscope camera (OMAX, model: A35140U3) attached to a Leitz Laborlux S microscope. High-resolution images were saved in a .tiff file format using ToupView computer software (OMAX, Ver. X64, 2.7.5849). Two to three sites from each slide were imaged at $40\times$ magnification such that a minimum of 1500 representative muscle fibers were imaged for analysis per specimen. PB muscle fibers were quantified using the counting tool in Adobe Photoshop CC software (2015.5.0 Release). The PB serial cross-sections were compared side-by-side to classify each muscle fiber into one of three categories: type I, type II and hybrid fibers (Figure 5.1). First, PB muscle fibers co-expressing both MHC type-I and MHC type-II isoforms (hybrid fibers) were identified and quantified using the counting tool. Secondly, muscle fibers that stained positive for only MHC type-II (type II fibers) were quantified. Finally, the remaining fibers staining positive for MHC type-I only (type I fibers) were quantified. Due to gross morphological differences among the PB forms, an inherently smaller whole muscle tissue volume was obtained when harvesting the regressive form. Therefore, in each PB specimen, the proportion of each fiber type was calculated as a percentage by dividing the fiber number of each fiber type (type I, type II, hybrid) by the total number of muscle fibers counted in the histological section to normalize the values for statistical analysis.
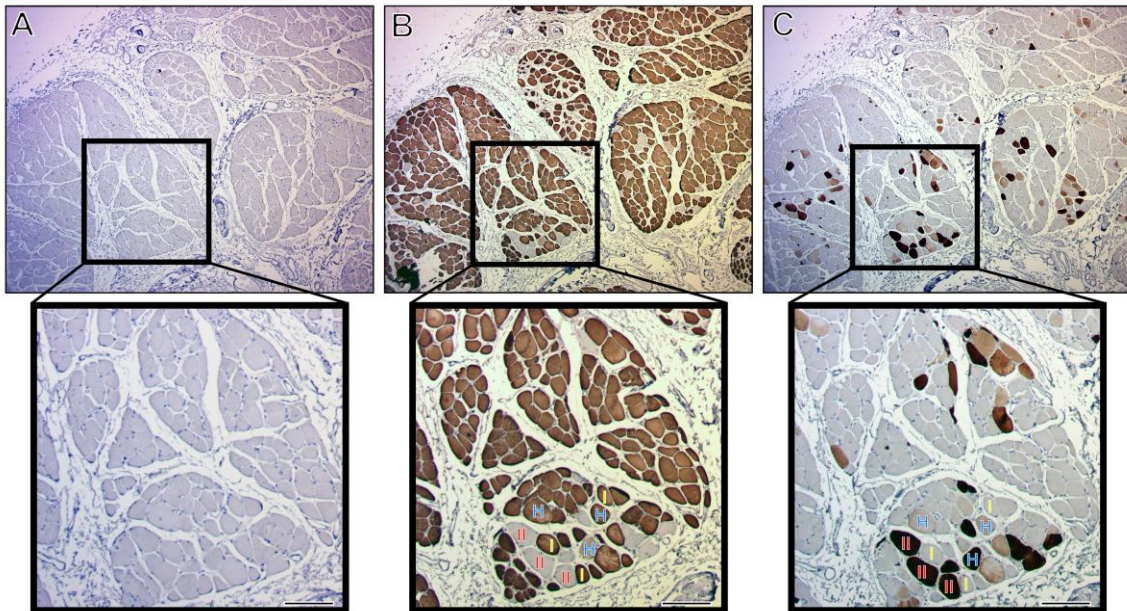
Figure 5.1 Immunohistochemical Labeling of Two Serial Cross-Sections of the Palmaris Brevis from One Specimen.

(A) Control slide. (B) Labeled with NOQ7.5.4D antibody against MHC type I (slow-twitch). (C) Labeled with MY-32 antibody against all MHC type II isoforms (fast-twitch). Representative type II (*red*), type I (*yellow*) and hybrid (*blue*) muscle fibers are identified in both serial cross-sections. Note the predominant proportion of positively stained type I fibers in panel (B). The histological sections depict tissue harvested from a developed (Type B) palmaris brevis morphological form. Scale bar: 200 μm.

5.2.5   Statistical Analysis

All data handling and calculations were performed using excel (Version 2016, Microsoft Corporation). Statistical tests were completed using spss statistical software (Version 24, SPSS Inc., Chicago, IL, USA) and power was determined with G*Power (v 3.1.9.2). To determine whether the percent of muscle fiber types present in the PB specimens differed by fiber type (i.e. type I, type II or hybrid) and/or by hand (left vs. right) a two-way analysis of variance (ANOVA) was used with power $(1 - \beta = 0.8, \alpha = 0.05)$ to detect a large effect size. Similarly, a two-way ANOVA was performed to explore whether the proportion of muscle fibers types differed between Type A and B morphological variants of the PB. A Bonferroni correction was used to account for multiple comparisons. All descriptive statistics are presented as means ± SD

5.3   Results

5.3.1   Morphological Classification

Of the 16 PB muscles harvested, 14 (87.5%) were classified as developed forms (*Type A*: 8; *Type B*: 6). Regressive forms consisting of poorly developed muscles were observed in two (12.5%) PB specimens harvested from the hands of a single cadaver (*Type C*). Of the 16 specimens, there were no PB morphological variants with a chaotic fiber arrangement (*Type D*). Exemplar PB morphological forms can be seen in Figure 5.2.

Regressive Form:

I. Fan-shaped Muscle
(Type A)

II. Solid Muscle Plate
(Type A)

III. Muscle bundles
(Type B)

IV. Undeveloped with few fibers
(Type C)
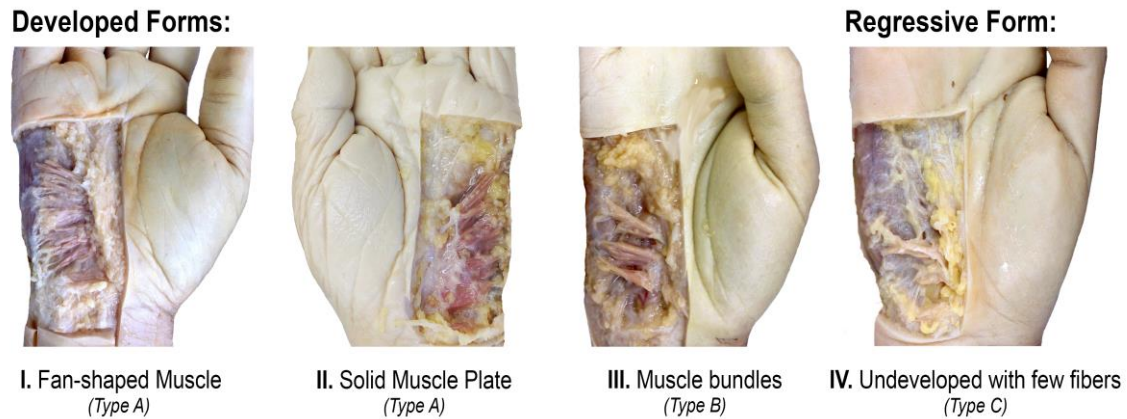
Figure 5.2 Palmaris Brevis Morphological Variants Harvested for Immunohistochemical Analysis.

Type A *(I-II):* Solid muscular plate with fan-shaped or parallel fiber arrangement; Type B *(III)*: Developed muscular bundles separated by adipose tissue; Type C *(IV)*: regressive form consisting of only a few fibers embedded in adipose tissue. PB morphological classifications are based on criteria established by Przystasz (1977).

5.3.2   Muscle Fiber Quantification

A total of 44 624 PB muscle fibers (left hands: 20 473 fibers; right hands: 24 151 fibers) were examined throughout the histological sections. Of these, 32 005 were type I, 5 585 were type II, and 7 034 were hybrid muscle fibers.

Using a two-way ANOVA, the effect of fiber type and hand on the proportion of muscle fibers was examined. An analysis of simple main effects revealed a significant difference in the proportion of each fiber type within the PB ($F_{2,42} = 119.7$, $P < 0.025$), but also showed no difference in the proportion of fiber types between the left and right hands; no interaction effect was observed. A post hoc analysis (Tukey's HSD) indicated the proportion of type I fibers (mean $= 72.2 \pm 13.7\%$, range $= 54.4$–96.7%) was significantly different ($P < 0.025$) than the type II (mean $= 12.0 \pm 11.2\%$, range $= 0.04$–32.0%) and hybrid fibers (mean $= 15.8 \pm 10.7\%$, range $= 2.9$–37.3%). The results of the statistical analysis are shown graphically in Figure 5.3.
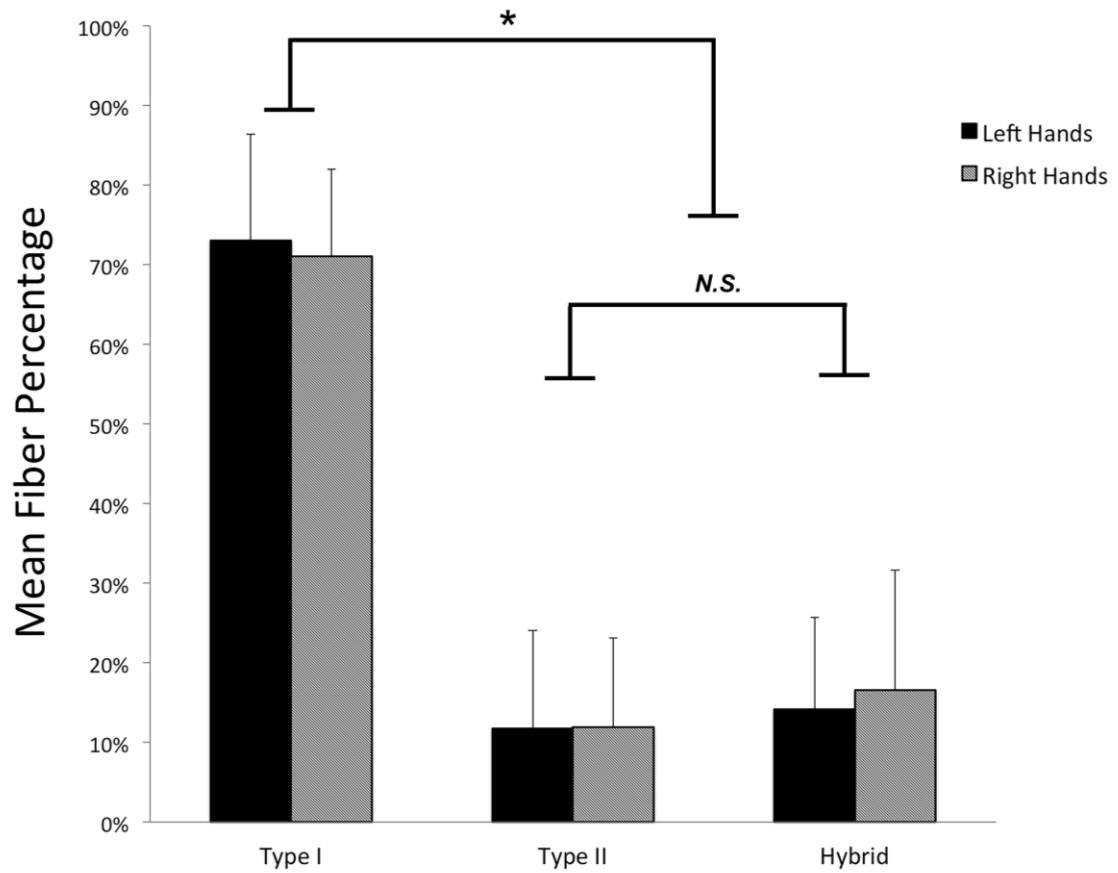
Figure 5.3 Palmaris Brevis Fiber Type Composition Between Left and Right Hands of Aged Cadavers

A predominance of type I fibers was observed and was significantly different ($P < 0.025$) from the type II and hybrid fiber types. No significant difference was detected between left and right hands. Error bars represent one standard deviation. N.S. denotes non-significance.

To examine whether the proportion of the three fiber types differed between morphological variants (i.e. Type A and B morphologies as described by Przystasz, 1977), a two-way ANOVA was performed. No significant interaction was observed and analysis of the simple main effects for morphological variants was not significant ($F1,38 = 0.013$, $P > 0.025$), indicating no difference between the percentages of type I, type II and hybrid fibers among specimens with Type A and B morphology. Because only two Type C variants were identified, they were not included in the present statistical analysis. Still, these specimens exhibited a predominance of type I fibers (78 and 81%) in comparison with type II (19 and 5%) and hybrid (3 and 15%) fibers in the left and right hands, respectively. These findings indicate the PB is predominantly composed of type I fibers, irrespective of hand or variant morphology.

5.4   Discussion

The palmaris brevis in humans is a unique muscle due to its palmar location, variant morphology (Przystasz, 1977) and its proposed functionality for improving palmar grip (Kirk, 1924) in addition to possibly protecting the ulnar neurovasculature at the wrist (Shrewsbury et al. 1972). In the present study, 16 specimens were histologically examined to perform the first quantification of fiber type proportions in the human PB muscle. Importantly, an understanding of the proportion of fiber types constituting the PB provides insight into its potential role protecting the ulnar neurovasculature during prolonged palmar compression. Using immunohistochemistry, it was found that a predominance of type I fibers was present in all PB specimens, irrespective of the hand (side) or morphological variant investigated.

The finding of a predominant type I muscle fiber-type composition in human skeletal muscle is not unique to the PB. Muscles demonstrating a similar predominance (e.g. > 60%) of either type I or type II muscle fibers have been observed in muscles of the face, hand and the lower limb (Table 5.1). Another palmar muscle, the adductor pollicis,

has a relatively homogeneous fiber-type composition (> 80% type I) and shares a similar innervation, albeit by different branches of the ulnar nerve (Round et al. 1984; Moore et al. 2014). Unlike the adductor pollicis and other intrinsic muscles of the hand, the PB does not act upon a joint and thus is not required to generate large forces for gross movements. PB muscle fibers are uniquely orientated and are arranged perpendicular to the hypothenar muscles. When contracted, the PB will produce a visible dimpling of the skin on the ulnar aspect of the palm due to its anatomical insertion into the skin and hypothenar fascia. Thus, the PB must only generate enough force to draw the skin and fascia of the hypothenar eminence radially through its distinct tendinous insertions. Based on the predominant type I muscle fiber composition (> 70%) of the PB observed in the current study, the metabolic properties associated with this fiber type would confer a fatigue-resistant property. This would prevent unwanted displacement of the hypothenar fat pad due to muscular fatigue during repetitive or prolonged palmar contractions. In addition to this function, it has been suggested that by anchoring the large hypothenar fat pad, the PB-hypothenar fat pad complex could protect the ulnar neurovasculature at the wrist when objects are firmly compressed into the palm (Henle, 1855; Kirk, 1924; Shrewsbury et al. 1972) or during prolonged sustained grasping tasks. Importantly, the predominance of type I fibers in the PB observed in the present study supports the fatigue-resistant and protective functions proposed in the previous literature.

Table 5.1 Human Skeletal Muscles of the Face, Hand, and Lower Limb with Predominant Fiber Type Compositions

Muscles	Muscle Fiber Proportions		Reference
	% Type I	% Type II	
Orbicularis oculi	11%	89%	Goodmurphy & Ovalle (1999)
Platysma	19%	81%	Dittert & Bardosi (1989)
Orbicularis oris	29%	71%	Stal et al. (1990)
Frontalis	64%	36%	Johnson et al. (1973)
Adductor pollicis	80%	20%	Round et al. (1984)
Lumbrical (1st digit)[†]	43%	57%	Hwang et al. (2013)
First dorsal interosseous[†]	57%	43%	Johnson et al. (1973)
Soleus	89%	11%	Johnson et al. (1973)
Tibialis anterior	73%	27%	Johnson et al. (1973)
† Hand muscles composed of a relatively heterogeneous fiber type composition included for comparison			

The PB is among several cutaneous skeletal muscles that insert into the skin, such as the platysma, orbicularis oculi and oris (Goodmurphy & Ovalle, 1999; Stal et al. 1990), and corrugator supercilii muscles (Goodmurphy & Ovalle, 1999). Despite sharing a similar classification with the PB as discrete muscular remnants of the *panniculus carnosus* (Bergman et al. 1985; Patil, 2013), the facial muscles have a predominance of type II muscle fibers ($> 70\%$); a property that indicates divergent functions compared with the PB itself (Table 5.1). The facial muscles are generally prone to fatigue (Brach & VanSwearingen, 1995), as experienced when one finds it increasingly challenging to hold a prolonged smile when posing for a photographic portrait. The disparate muscle fiber composition between muscles (Table 5.1) demonstrates how the muscle fiber composition can reflect overall muscle function. Compared with the facial muscles, a postural leg muscle such as the soleus is fatigue-resistant because it is chronically activated in both locomotion and quiet stance (Honeine et al. 2013). This function can be inferred from its predominate proportion of type I muscles fibers (Table 5.1). Therefore, in some skeletal muscles, the muscle fiber composition can yield valuable insight into muscle function based on the fiber-type composition alone.

In the present study, the type II muscle fibers in the PB accounted for only 12% of the total muscle fibers quantified in both the left and right hands. Because the MY-32 antibody stains for all MHC type II isoforms, we could not further distinguish type IIa or IIx fibers in our histological sections. However, because the type I muscle fibers accounted for $> 70\%$ of the total muscle fibers, it was not necessary to further investigate the proportion of MHC type II isoform subtypes.

Fiber type co-expression (hybrid fibers) can occur due to either cycles of collateral reinnervation and denervation associated with human aging (Andersen et al. 1999; Rowan et al. 2012), or alterations in neural stimulation to the muscle fibers (Pette & Staron, 2000). It has been established that the transition of MHC isoforms is ordinal, such that two 'neighboring' MHC isoforms (e.g. MHC I/IIa or MHC IIa/IIx) are usually co-expressed within a single muscle fiber (Scott et al. 2001). We observed mixed fibers

staining positive for both MHC type I and MHC type II on serial cross-sections, which were classified as hybrid fibers likely containing MHC type I and type IIa isoforms (Figure 5.1). The high mean age (75 ± 15 years) of the cadavers used in this study may explain the proportion of hybrid fibers detected in our PB tissue sample. To determine whether the MHC co-expression observed in the PB tissue is age-related or an inherent phenotype of the muscle, further investigation of younger PB tissues are required. Although the presence of hybrid fibers may be indicative of alterations in neural stimulation, aging or other potential factors, only a small number of hybrid fibers were observed and they contributed a relatively small percentage to the total fiber number (14 and 17%) in the left and right hands, respectfully.

The proportion of type I and type II muscle fibers within a skeletal muscle can vary based on depth of sampling (Johnson et al. 1973; Elder et al. 1982), muscle width (Dittert & Bardosi, 1989) or between architecturally distinct regions (Kim et al. 2013). In the histological preparation shown in Figure 5.1, type I fibers were distributed throughout both the peripheral and central regions of the muscle, whereas type II and hybrid fibers were mainly located in the central regions; however, this was not a consistent finding in all the histological preparations. The fiber-type distribution within individual fascicles is dependent upon several physiological and mechanical factors such as vascular supply, muscle activation patterns and differential mechanical stresses experienced by superficial and deeper muscular portions (Sjostrom et al. 1986). Further study is needed to examine whether regional differences (e.g. proximal vs. distal segments; superficial vs. deep regions) in muscle fiber-type proportions exist within the PB tissue volume. Although investigation into functionally distinct regions within the PB would be valuable, the primary focus of this study was to determine the overall fiber-type composition indicative of the whole PB tissue volume.

We further investigated whether the fiber-type composition varied between two groups of developed PB morphological forms identified in our sample. When grouped by morphological variant (*Types A and B*), there were no apparent differences in the

proportions of type I, type II and hybrid fibers between these developed forms. Furthermore, the regressive form observed in the hands of the single cadaveric specimen had a similar mean percentage of type I muscle fibers (78% left hand, 80% right hand) proportional to the developed forms found in the other cadaveric specimens. Therefore, it appeared the PB morphological variant had no bearing on the muscle fiber-type composition. Although we observed no significant differences in fiber-type composition between left and right hands, and PB developed forms, the lack of apparent differences in these measures could be explained by the relatively small sample of PB tissues harvested. It is possible that a larger sample size might help solidify these observations, in both dominant and regressive forms, thus allowing for a more comprehensive analysis and potential comparisons in fiber-type composition between males and females. Nevertheless, the present study results indicate that muscle fibers of the regressive PB forms have the same fatigue-resistance as the developed PB forms but a reduced functional capacity due the relatively few muscle fibers present.

5.5   Implications for Palmar Function

Kirk (1924) postulated that the PB functions to anchor and stabilize the hypothenar fat pad during palmar grasping; however, a sufficiently large muscle tissue mass is likely necessary for supporting the hypothenar fat pad and resisting compressive forces incurred at the hypothenar eminence. In our sample, the developed PB muscles covered a broad area from the pisiform bone to an area approaching the transverse palmar crease, which would provide a large coverage area for support of the hypothenar fat pad located superficially. Although some developed PB morphological forms can appear divided into various discrete muscle fiber bundles (Figure 5.2), the range of muscle separation is only 1–5 mm based on cadaveric observations (Shrewsbury et al. 1972). Therefore, the overall functionality of the PB specimens with divided musculature is likely similar to those found in solid muscular plates.

The regressive form in our sample was limited to the region near the pisiform bone and likely had minimal functionality in anchoring the hypothenar fat pad or providing any meaningful protection to the ulnar neurovasculature when subjected to palmar compressive forces (Figure 5.2). This is consistent with Przystasz (1977), who suggested the PB regressive forms likely provide no functional contribution to stabilizing the hypothenar fat pad or resisting compressive forces when grasping hard objects. We observed the PB developed forms with equal frequency between hands; however, Przystasz (1977) found the PB developed forms occurred more frequently in the right hands (70%) compared with the left hands (38%) using a large sample of 101 upper limbs. Although we observed different proportions of developed to regressive PB forms from the aforementioned study, we cannot discern from cadaveric examinations whether handedness influences the morphological form present. Therefore, further studies are necessary to determine whether PB morphology is related to handedness and whether the presence of a regressive form causes a predisposition to ulnar nerve compression-related injuries.

5.6   Conclusions

Although the PB is a relatively small muscle of variant morphology, its location at the hypothenar eminence conveys potential functionality in both protecting and supporting the ulnar neurovasculature and hypothenar fat pad from overlying compression. The predominant type I muscle fiber composition supports the hypotheses that the PB has a protective capacity during repetitive or prolonged grasping tasks based on the overall fatigue-resistance imparted by the proportionally dominant type I muscle fiber-type composition.

5.7   References

Andersen JL, Terzis G, Kryger A. 1999. Increase in the degree of coexpression of myosin heavy chain isoforms in skeletal muscle fibers of the very old. Muscle Nerve 22:449-454.

Bergman RA, Thompson SA, Afifi AK, Saadeh FA. 1985. Anatomy Atlases: Illustrated encyclopedia of human anatomic variation: Opus I: Muscular system: Alphabetical listing of muscles: P: Panniculus Carnosus. In.

Brach JS, VanSwearingen J. 1995. Measuring fatigue related to facial muscle function. Arch Phys Med Rehabil 76:905-908.

Dittert DD, Bardosi A. 1989. Distribution of different fiber types in whole cross-sections of human platysma. A histological and morphometric study. Acta Anat (Basel) 134:206-211.

Elder GC, Bradbury K, Roberts R. 1982. Variability of fiber type distributions within human muscles. J Appl Physiol Resp Environ Exerc Physiol 53:1473-1480.

Eswaradass PV, Kalidoss R, Ramasamy B, Gnanashanmugham G. 2014. Familial palmaris brevis spasm syndrome. Ann Indian Acad Neurol 17:141-142.

Goodmurphy CW, Ovalle WK. 1999. Morphological study of two human facial muscles: orbicularis oculi and corrugator supercilii. Clin Anat 12:1-11.

Henle J. 1855. Handbuch der Systematischen Anatomie des Menschen, 2 ed. Braunschweig: Friedrich Vieweg & Sohn.

Honeine JL, Schieppati M, Gagey O, Do MC. 2013. The functional role of the triceps surae muscle during human locomotion. PloS one 8:e52943.

Hwang K, Huan F, Kim DJ. 2013. Muscle fibre types of the lumbrical, interossei, flexor, and extensor muscles moving the index finger. J Plast Surg Hand Surg 47:268-272.

Iyer VG. 1998. Palmaris brevis sign in ulnar neuropathy 1998. Muscle Nerve 21:675-677.

Johnson MA, Polgar J, Weightman D, Appleton D. 1973. Data on the distribution of fibre types in thirty-six human muscles. An autopsy study. J Neurol Sci 18:111-129.

Kim SY, Lunn DD, Dyck RJ, Kirkpatrick LJ, Rosser BW. 2013. Fiber type composition of the architecturally distinct regions of human supraspinatus muscle: a cadaveric study. Histol Histopathol 28:1021-1028.

Kirk T. 1924. Some Points in the Mechanism of the Human Hand. J Anat 58:228-230.

Liguori R, Donadio V, Di Stasi V, Cianchi C, Montagna P. 2003. Palmaris brevis spasm: an occupational syndrome. Neurology 60:1705-1707.

Moore KL, Dalley AF, Agur AMR. 2014. Clinically Oriented Anatomy, 7th ed. Philadelphia Lippincott Williams & Wilkins.

Patil S. 2013. Clinico-anatomical Considerations Of Palmaris Brevis Muscle. Int J Adv Res 1:341-344.

Pette D, Staron RS. 2000. Myosin isoforms, muscle fiber types, and transitions. Microsc Res Tech 50:500-509.

Przystasz T. 1977. Morphology of the palmaris brevis muscle in man. Folia Morphol (Warsz) 36:77-82.

Round JM, Jones DA, Chapman SJ, Edwards RH, Ward PS, Fodden DL. 1984. The anatomy and fibre type composition of the human adductor pollicis in relation to its contractile properties. J Neurol Sci 66:263-272.

Rowan SL, Rygiel K, Purves-Smith FM, Solbak NM, Turnbull DM, Hepple RT. 2012. Denervation causes fiber atrophy and myosin heavy chain co-expression in senescent skeletal muscle. PloS one 7:e29082.

Scott W, Stevens J, Binder-Macleod SA. 2001. Human skeletal muscle fiber type classifications. Phys Ther 81:1810-1816.

Serratrice G, Azulay JP, Serratrice J, Pouget J. 1995. Palmaris brevis spasm syndrome. J Neurol Neurosurg Psychiatry 59:182-184.

Shrewsbury MM, Johnson RK, Ousterhout DK. 1972. The palmaris brevis--a reconsideration of its anatomy and possible function. J Bone Joint Surg Am 54:344-348.

Sjostrom M, Downham DY, Lexell J. 1986. Distribution of different fiber types in human skeletal muscles: why is there a difference within a fascicle? Muscle Nerve 9:30-36.

Stal P, Eriksson PO, Eriksson A, Thornell LE. 1990. Enzyme-histochemical and morphological characteristics of muscle fibre types in the human buccinator and orbicularis oris. Arch Oral Biol 35:449-458.

Standring S. 2008. Gray's Anatomy: The Anatomical Basis of Clinical Practice, 40th ed. Edinbrugh: Churchill Livingstone.

Staron RS. 1997. Human skeletal muscle fiber types: delineation, development, and distribution. Can J Appl Physiol 22:307-327.

Tarsy D, Apetaurova D, Rutkove SB. 2004. Palmaris brevis spasm: An occupational syndrome. Neurology 62:838.

van Oudenaarde E, Oostendorp RAB. 1995. Functional-Relationship between the Abductor Pollicis Longus and Abductor Pollicis Brevis Muscles - an Emg Analysis. J Anat 186:509-515.

Chapter 6

6   General Discussion & Summary

6.1   General Discussion

The studies presented in Chapters 2 to 5 explore the role of the palmaris longus (PL) and palmaris brevis (PB) in the hand by investigating *in vivo* their muscle activity and architectural changes during functional movements. These observations were further supported by determining the type I and type II fiber proportions within each muscle *in-situ*, which presumably contribute to whole muscle function through the contractile and metabolic properties of their constituent fibers. The main findings of this dissertation provide evidence that the PL and PB contribute to hand function despite being generally perceived as insignificant musculature in the process of evolutionary recession in humans. These findings build upon the understanding of the PL and PB in the literature, and provide more clarity into their functional role *in vivo*. By providing a more comprehensive understanding of PL and PB anatomy and physiology, the results of this dissertation will be useful in further characterizing the functional loss of each, which may occur through surgical removal or hereditary absence.

In Chapter 2, the PL was shown to provide significant muscle activity and synchronous co-contraction during thenar abduction, flexion, opposition, and circumduction movements. The muscle activity was greatest during thenar abduction, which supports the PL acting as an extrinsic thenar muscle contributing to the thenar abduction strength. The muscle activity recordings were supported by ultrasound imaging, in which significant increases in muscle thickness were observed during thenar abduction movements. The contributions of the PL to thenar function were direction dependent as minimal changes in muscle activity and muscle thickness were observed in response to thenar adduction. Although several studies attribute the success of PL tendon transfer in opponensplasty surgery to an established synergy between the PL and the abductor pollicis brevis (APB), this synergistic relationship has not been investigated

comprehensively in previous literature (Fahrer, 1973). Chapter 2 provides evidence to confirm that the PL contributes to thumb movements, which supports studies proposing thenar abduction be universally accepted as a PL action by anatomists and hand surgeons (Fahrer, 1973, 1977; Fahrer and Tubiana, 1976; Gangata et al., 2010).

In Chapter 3, the APB muscles with contiguous origins with the PL consisted of significantly greater type II fiber proportions than those with non-discrete PL origins. This disparate fiber composition between two anatomical arrangements may represent quality of synergy established between the PL and APB. This indicates that the synergy is dependent not only on the presence of the PL but also on the robustness of its tendon with the APB per se. Furthermore, the contiguous relationship between the PL and APB indicates that these muscles function as a digastric unit. A homogeneity in fiber type composition in APB fascicles arranged in a digastric manner with the PL may reflect a functional inter-relationship similar to the digastric muscle proper (Monemi et al., 1999) and to the medial and lateral heads of the quadratus plantae (Schroeder et al., 2014). The PL and lateral head of the quadratus plantae may still contribute function despite being considered under evolutionary recession (Schroeder et al., 2014). Although surgical literature attributes the success of PL tendon transfer in opponensplasty to an established synergy amongst the PL and APB (Kato et al., 2014), this synergy may not be fully established in all individuals based on differences in tendon morphology and PL evolutionary regression.

In Chapter 4, the PB was investigated during dynamic grasping tasks to determine its muscle activity. Several functions of the PB have been proposed including aiding in palmar grip and ulnar neurovasculature protection (Shrewsbury et al., 1972). However, there is lack of consensus regarding its function as some have even described the PB as incapable of voluntary contraction (Serratrice et al., 1995). The histological composition of the PB was confirmed as striated skeletal muscle, and thus, under voluntary control by the somatic nervous system. Several human skeletal muscles, however, are incapable of voluntary contraction including the middle ear muscles, the tensor tympani and stapedius,

which are primarily driven at the unconscious level (Standring and Gray, 2008). Although the PB could not be contracted independently, the greatest muscle activity was recorded during abduction and flexion movements of the fifth digit. This suggests that the PB is engaged in a functional relationship with the fifth digit, similar to other muscular complexes (ex: triceps brachii, triceps surae) incapable of independent contractions of their constituent muscles. Jones (1920) attributed the lack of PB volitional control to a small cortical representation; however, all participants where capable of producing significant changes in PB architecture (length, thickness) and muscle activity in response to functional grasping tasks and individual fifth digit movements. Based on the comparative anatomy evidence in the literature and the proximity of the PB to the ulnar nerve and artery, the significant muscle activity recorded from the PB suggests a protective function when grasping round elements (tennis ball) as opposed to more cylindrical-shaped objects (Carpenter's hammer). From an evolutionary perspective, the ulnar nerve and artery likely would need protection from repetitive impacts during climbing as opposed to hanging from tree limbs. For arboreal mammals, the ulnar aspect of the palm would experience limited, if any, contact or compression when simply hanging from tree limbs. In Chapter 5, the fiber type composition demonstrated that the PB consisted of a predominant type I muscle fiber population, thereby imparting the PB with a fatigue resistant profile based on type I muscle fiber contractile properties. This further supports functional postulates of the PB in repetitive, or intermittent climbing, or other activities subjecting the palm to repetitive compression, in which, the PB may provide protection for the neurovasculature of the piso-hamate tunnel.

The functional purpose of the "reflexive" involuntary contraction of the palmaris brevis still remains unclear (Chapter 4). Most reports are anecdotal (Boynton-Lee, 1888; Jones, 1920; Montagu, 1952) with some ascribing its involuntary contraction as protective of the ulnar nerve and artery (Przystasz, 1977). Considering other neonatal palmar reflexes, the grasping and palmomental reflexes are considered primitive appearing in infancy prior to their inhibition after several weeks after birth (Karimianpour et al., 2015; Schott and Rossor, 2003, 2016). Interestingly, these reflexes may become

disinhibited in clinical disorders such as frontal lobe damage and dementia, indicating the presence of cortical degeneration (Karimianpour et al., 2015; Schott and Rossor, 2003). In an early anecdotal account of the PB reflex, Boynton-Lee (1888) identified the phenomenon in several hands and proposed that it may serve a potential clinical purpose in the future. Similar to the aforementioned reflexes, the PB reflex may serve a similar clinical purpose indicating the presence of cortical degeneration in the brain; however, this has yet to be evaluated.

6.2   Limitations

Indwelling fine wire electromyography (EMG) is advantageous as it allows for investigation of individual muscles; however, this technique records muscle activity from a relatively small region assumed to be representative of whole muscle function. In other vestigial muscles, such as the anconeus, functional regions have been identified within the muscle volume based on variations in fiber direction and regional differences in muscle EMG recordings (Bergin et al., 2013). In the PB, functional regions may exist based the fiber orientation, direction, and separation between distinct muscle bundles (Przystasz, 1977; Shrewsbury et al., 1972); however, this was not the specific aim of these initial studies.

In Chapter 2, ultrasound imaging was used to record architectural changes in PL muscle thickness in response to thenar abduction contractions. Although significant changes in PL muscle thickness were recorded, the force generating capacity of skeletal muscle is dependent upon several other architectural parameters that were not assessed such as physiological cross-sectional area and fascicle length. These factors, including compliance of the PL tendon, and morphological arrangement of the tendon at the wrist will further influence the relative force contributions to thumb function. Despite these muscle and tendon properties not being assessed in this thesis, they could be addressed in a future study to further characterize the role of the PL in thumb function.

Normalization of EMG signals is necessary to compare muscle activity among individuals (Halaki and Ginn, 2012). A popular normalization method is determining the maximal EMG activity from a given muscle and dividing the EMG of subsequent submaximal movements by the maximal EMG value (Halaki and Ginn, 2012); however, this may be challenging for several muscle groups not acting on specific joints such as the serratus anterior and here, the PB. Determining maximal EMG from muscles that move explicit joints (eg. biceps brachii, PL) are more easily studied compared to muscles not necessarily joint exclusive such as the PB. Due to inter-individual variation in muscle activity, there is lack of consensus among research studies as to which movement produces the greatest activity in some muscles (e.g. serratus anterior) (Halaki and Ginn, 2012). A similar challenge was encountered in determining the maximal muscle activity in the PB as five of the eleven participants were able to achieve maximal EMG activity during fifth digit flexion as opposed to the remaining participants achieving maximal activation during fifth digit abduction. The dermal insertion, variability in individual PB morphology, and challenging method of evoking PB contraction likely contributed to the participants ability to achieve maximal activation; however, the majority of participants (~60%) were consistent in the method of PB maximal activation.

The function of the PB was interpreted to support postulates as protective of the ulnar nerve and ulnar artery during intermittent grasping or compression actions; however, the studies presented in Chapters 2 and 3 did not evaluate the protection of these structures beyond visual affirmation that the PB has the capacity to act as a physical barrier in conjunction with the hypothenar fat pad. Further study of ulnar nerve and ulnar artery physiological properties are required (e.g.: nerve conduction velocity or blood flow measures) in the presence and absence of PB musculature in response to palmar compression. Furthermore, intra- and inter-rater reliability of the ultrasound-derived PB measurements were not assessed; however, these measures could be assessed further as part future PB-related studies (*see future directions below*).

The PL and PB tissues used in this study were harvested from aged formalin embalmed cadavers [mean ages: 75y (Chapter 3); 74y (Chapter 5)] due to their availability through the Schulich School of Medicine & Dentistry body donation program. Although access to these tissues was convenient, applying immunohistochemical techniques on aged tissues limited further analysis of fiber cross-sectional area as the formalin-embalming processes may have affected these properties. Immunohistochemical staining is advantageous as it allows for staining of formalin embalmed archival tissues and has been validated against myosin ATPase staining (Behan et al., 2002). Although analysis of muscle fiber cross-sectional area could be useful, Klein et al. (2003) found no significant differences in overall fiber number in biopsied biceps brachii from young (21y) and old (82y) individuals, despite reductions in mean fiber diameter and overall biceps brachii area. These and other observations indicate age-related fiber loss may be muscle specific. Therefore, the ratio type I to type II fibers may be unaffected by age in some muscles, but this remains to be comprehensively studied in all muscle groups.

6.3   Future Directions

Despite advancing the functional understanding of the PL and PB in the hand, it would be valuable to study these muscles in specific athletic and patient populations. Although the ipsilateral PL is routinely harvested as an autologous tendon graft for ulnar collateral ligament reconstruction in elite college and professional-level baseball pitchers (Cain and Mathis, 2016), the functional consequences of its removal in terms of thenar function remains unknown. For professional level pitchers relying on fine thenar motor control, removing the PL may affect the learned motor control patterns necessary for various pitches depending on its thenar contributions. Beyond grip strength, a longitudinal study during recovery from ulnar collateral ligament reconstruction could be conducted that monitors thenar strength and function over 12 to 14 months; the typical time of surgical recovery. This could provide further insight into PL function if a significant loss of thenar abduction strength persists post-surgical removal of PL.

For surgical harvesting of the PL tendon, the Schaeffer test can be used to identify the presence of the PL tendon at the wrist; however, the Schaeffer test is associated with a 10% false negative ratio, which necessitates the use of imaging in preoperative planning for PL autologous tendon harvesting procedures (Dabrowski et al., 2018). Beyond PL presence, the tendon length and diameter are important parameters to be considered for grafting procedures; however, most PL tendons do not meet the minimal criteria (length: 15cm, diameter: 3mm) due to insufficient PL tendon length (Jakubietz et al., 2011). Ultrasound or magnetic resonance imaging may be useful for PL tendon measurements *in vivo* to determine the length and diameter for sufficient transfer. In addition to tendon morphological measurements, the quality of tendon could be investigated non-invasively using quantitative magnetic resonance imaging techniques.

Magnetization transfer imaging has been used to evaluate normative and pathological changes in muscle tissue quality in healthy individuals and patient populations (Henkelman et al., 2001; Moore et al., 2016; Schwenzer et al., 2009; Sinclair et al., 2012). Similarly, magnetization transfer imaging has been used to detect pathological changes in tendon quality in the Achilles tendon by detecting a reduction in bound collagen in a patient with arthritic psoriasis (Hodgson et al., 2011). This technique may be a useful non-invasive method to evaluate the PL tendon quality prior to its use in surgical procedures. Furthermore, the PL tendon could be studied biomechanically for its tensile strength relative to quantitative magnetization transfer measurements to determine if reductions in bound collagen influence the tensile strength of the PL tendon.

Future PB studies could investigate individuals whose palms are subjected to repetitive compression such as rock climbers, string musicians, and gymnasts. Use of magnetic resonance imaging for 3D volume rendering and quantification could be a useful non-invasive measure in detecting evidence of PB hypertrophy in these individuals. Comparison of muscle fiber diameter in biopsied PB muscle tissue would be ideal, but harvesting PB tissue may require more precision than typical Bergstrom needle biopsy techniques used in large muscle groups (e.g. quadriceps, biceps brachii)

Furthermore, physiological measurements of the ulnar nerve and ulnar artery may also provide evidence of its protective function if individuals with undeveloped or absent PB musculature have reductions in blood flow or conduction velocity or other physiological measures in response to palmar compression.

Kim et al. (2017) investigated the PB from a clinical perspective by delineating PB topography in cadaveric hands to better approximate the ideal injection site for botulism toxin to treat PB spasm syndrome. Although these cadaveric topographical measurements may be useful, there is extensive individual PB variation in the hand that may warrant ultrasound guided injections on an individual basis (Przystasz, 1977). In addition to previous PB cadaveric studies (Chiou-Tan et al., 1998; Kim et al., 2017; Shrewsbury et al., 1972), future investigations should assess PB morphology more comprehensively with respect to its morphological form using ultrasound imaging. A study assessing the reliability of the PB ultrasound measures in reference to a standardized location (e.g. hook of the hamate) may be useful for avoiding neurovasculature during injection procedures.

6.4   Summary

Although considered atavistic muscles, the PL and PB further contribute to the complexity of hand function. This dissertation consists of a series of foundational studies concerning PL and PB function *in vivo*. Firstly, it provides support for the PL as an extrinsic thenar muscle in conjunction with discrete fascicles of the APB muscle (Chapters 2 and 3). Secondly, it provides support for the PB as a protective barrier to the contents of the piso-hamate tunnel neurovasculature, in addition to its potential reflexive mechanisms (Chapters 4 and 5). The implications of these results may be applicable to several surgical procedures, hand injury rehabilitation protocols, sports medicine injury management, and biomechanical simulation studies of the hand. Overall, these foundational studies may provide a basis for further applied studies of the PL and PB in surgical, clinical, or athletic populations, and may further assist in characterizing the functional loss when their absence occurs through either surgical or hereditary means.

6.5   References

Behan WM, Cossar DW, Madden HA, McKay IC. 2002. Validation of a simple, rapid, and economical technique for distinguishing type 1 and 2 fibres in fixed and frozen skeletal muscle. J Clin Pathol 55:375-380.

Bergin MJG, Vicenzino B, Hodges PW. 2013. Functional differences between anatomical regions of the anconeus muscle in humans. J Electromyogr Kinesiol 23:1391-1397.

Boynton-Lee HB. 1888. Palm Relfex (?). The Lancet 2:1267.

Cain EL, Mathis TP. 2016. Ulnar collateral ligament reconstruction: current philosophy in 2016. Am J Orthop (Belle Mead NJ) 45:E534-E540.

Chiou-Tan FY, Reno SB, Magee KN, Krouskop TA. 1998. Electromyographic localization of the palmaris brevis muscle. Am J Phys Med Rehabil 77:243-246.

Dabrowski KP, Stankiewicz-Jozwicka H, Kowalczyk A, Markuszewski M, Ciszek B. 2018. The Sonographic Morphology of Musculus Palmaris Longus in Humans. Folia Morphol (Warsz).

Fahrer M. 1973. Proceedings: the role of the palmaris longus muscle in the abduction of the thumb. J Anat 116:476.

Fahrer M. 1977. On the form and function of the abductor pollicis brevis muscle. Aust N Z J Surg 47:243-247.

Fahrer M, Tubiana R. 1976. Palmaris longus, anteductor of the thumb. Hand 8:287-289.

Gangata H, Ndou R, Louw G. 2010. The contribution of the palmaris longus muscle to the strength of thumb abduction. Clin Anat 23:431-436.

Halaki M, Ginn K. 2012. Normalization of EMG Signals: To Normalize or Not to Normalize and What to Normalize to? In: Naik G, editor. Computational Intelligence in Electromyography Analysis - A Perspective on Current Applications and Future Challenges: InTech.

Henkelman RM, Stanisz GJ, Graham SJ. 2001. Magnetization transfer in MRI: a review. NMR Biomed 14:57-64.

Hodgson RJ, Evans R, Wright P, Grainger AJ, O'Connor PJ, Helliwell P, McGonagle D, Emery P, Robson MD. 2011. Quantitative magnetization transfer ultrashort echo time imaging of the Achilles tendon. Magn Reson Med 65:1372-1376.

Jakubietz MG, Jakubietz DF, Gruenert JG, Zahn R, Meffert RH, Jakubietz RG. 2011. Adequacy of palmaris longus and plantaris tendons for tendon grafting. J Hand Surg Am 36:695-698.

Jones FW. 1920. The Principles of Anatomy as Seen in the Hand. London: J. &. A. Churchill.

Karimianpour A, Nagpal SJ, Parker K. 2015. Palmomental reflex. Am J Med Sci 350:e2.

Kato N, Yoshizawa T, Sakai H. 2014. Simultaneous modified Camitz opponensplasty using a pulley at the radial side of the flexor retinaculum in severe carpal tunnel syndrome. J Hand Surg-Eur Vol 39:632-636.

Kim DH, Bae JH, Kim HJ. 2017. Anatomical insights of the palmaris brevis muscle for clinical procedures of the hand. Clin Anat 30:397-403.

Klein CS, Marsh GD, Petrella RJ, Rice CL. 2003. Muscle fiber number in the biceps brachii muscle of young and old men. Muscle Nerve 28:62-68.

Monemi M, Thornell L, Eriksson P. 1999. Diverse changes in fibre type composition of the human lateral pterygoid and digastric muscles during aging. J Neurol Sci 171:38-48.

Montagu MF. 1952. Conditioning of the palmaris brevis muscle. Science 115:153.

Moore CW, Allen MD, Kimpinski K, Doherty TJ, Rice CL. 2016. Reduced skeletal muscle quantity and quality in patients with diabetic polyneuropathy assessed by magnetic resonance imaging. Muscle Nerve 53:726-732.

Przystasz T. 1977. Morphology of the palmaris brevis muscle in man. Folia Morphol (Warsz) 36:77-82.

Schott JM, Rossor MN. 2003. The grasp and other primitive reflexes. J Neurol Neurosurg Psychiatry 74:558-560.

Schott JM, Rossor MN. 2016. The palmomental reflex: stop scratching around! Pract Neurol 16:500-501.

Schroeder KL, Rosser BW, Kim SY. 2014. Fiber type composition of the human quadratus plantae muscle: a comparison of the lateral and medial heads. J Foot Ankle Res 7:54.

Schwenzer NF, Martirosian P, Machann J, Schraml C, Steidle G, Claussen CD, Schick F. 2009. Aging effects on human calf muscle properties assessed by MRI at 3 Tesla. J Magn Reson Imaging 29:1346-1354.

Serratrice G, Azulay JP, Serratrice J, Pouget J. 1995. Palmaris brevis spasm syndrome. J Neurol Neurosurg Psychiatry 59:182-184.

Shrewsbury MM, Johnson RK, Ousterhout DK. 1972. The palmaris brevis--a reconsideration of its anatomy and possible function. J Bone Joint Surg Am 54:344-348.

Siegel DB, Kuzma G, Eakins D. 1995. Anatomic investigation of the role of the lumbrical muscles in carpal tunnel syndrome. J Hand Surg Am 20:860-863.

Sinclair CD, Morrow JM, Miranda MA, Davagnanam I, Cowley PC, Mehta H, Hanna MG, Koltzenburg M, Yousry TA, Reilly MM, Thornton JS. 2012. Skeletal muscle MRI magnetisation transfer ratio reflects clinical severity in peripheral neuropathies. J Neurol Neurosurg Psychiatry 83:29-32.

Standring S, Gray H. 2008. Gray's anatomy: the anatomical basis of clinical practice, 40th, anniversary ed. Edinburgh: Churchill Livingstone/Elsevier.

Appendices

Appendix A Research Ethics Approval Notice

Western Research

Research Ethics

Western University Health Science Research Ethics Board
HSREB Full Board Initial Approval Notice

Principal Investigator: Dr. Charles Rice
Department & Institution: Schulich School of Medicine and Dentistry\Anatomy & Cell Biology, Western University

Review Type: Full Board
HSREB File Number: 107505
Study Title: Motor neuron and muscle fiber resilience in humans
Sponsor: Natural Sciences and Engineering Research Council

HSREB Initial Approval Date: March 07, 2016
HSREB Expiry Date: March 07, 2017

Documents Approved and/or Received for Information:

Document Name	Comments	Version Date
Other	Biopsy Information Sheet	2015/12/01
Letter of Information & Consent		2016/03/07
Western University Protocol	Received Feb 23, 2016	2016/03/01
Advertisement	poster	2016/01/01
Advertisement	recruitment email script and announcement	2016/01/01
Other	Transcranial Magnetic Stimulation Screening Form	2016/03/01

The Western University Health Science Research Ethics Board (HSREB) has reviewed and approved the above named study, as of the HSREB Initial Approval Date noted above.

HSREB approval for this study remains valid until the HSREB Expiry Date noted above, conditional to timely submission and acceptance of HSREB Continuing Ethics Review.

The Western University HSREB operates in compliance with the Tri-Council Policy Statement Ethical Conduct for Research Involving Humans (TCPS2), the International Conference on Harmonization of Technical Requirements for Registration of Pharmaceuticals for Human Use Guideline for Good Clinical Practice Practices (ICH E6 R1), the Ontario Personal Health Information Protection Act (PHIPA, 2004), Part 4 of the Natural Health Product Regulations, Health Canada Medical Device Regulations and Part C, Division 5, of the Food and Drug Regulations of Health Canada.

Members of the HSREB who are named as Investigators in research studies do not participate in discussions related to, nor vote on such studies when they are presented to the REB.

The HSREB is registered with the U.S. Department of Health & Human Services under the IRB registration number IRB 00000940.

Ethics Officer, on behalf of Dr. Joseph Gilbert, HSREB Chair

Western University, Research, Support Services Bldg., Rm. 5150
London, ON, Canada N6G 1G9 t. 519.661.3036 f. 519.850.2466 www.uwo.ca/research/ethics
Ethics Officer to Contact for Further Information: Erika Basile ___ Katelyn Harris ___ Nicole Kaniki ___ Grace Kelly ___ Vikki Tran ___

This is an official document. Please retain the original in your files

Appendix B Hematoxylin & Eosin Staining Protocol

Hemotoxylin & Eosin Staining Protocol

The slides are completely immersed in the following solutions for the allotted time, and in separate containers. The estimation of 300 mL per slide was assumed throughout the protocol.

- Xylene for 5 minutes
- Xylene for 5 minutes
- Xylene for 3 minutes
- Absolute alcohol for 2 minutes
- Absolute alcohol for 1 minute
- 95% alcohol for 2 minutes
- 95% alcohol for 1 minute
- 70% alcohol for 1 minute $\rightarrow$ 70 mL anhydrous EtOH with 30 mL of dH_2O
- Water for 2 minutes
- Hematoxylin for 3 minutes
- Rinse well in tap water
- 2-3 dips in acid alcohol
- Rinse well in tap water
- 2-3 dips in ammonium alcohol
- Rinse well in tap water
- Eosin for 3 minutes
- Rinse well in tap water
- 10 dips in 70% alcohol
- 10 dips in 95% alcohol
- 10 dips in 95% alcohol
- 10 dips in absolute alcohol
- 10 dips in absolute alcohol
- Xylene for 5 minutes
- Xylene for 5 minutes
- Mount and coverslip using Cytoseal® permount in a fume hood

Acid Alcohol Solution: Using glass pipette, mix 1 mL of hydrochloric acid (HCL) with 250 mL of 70% ethanol (EtOH).

Ammonium Alcohol Solution: Using glass pipette, mix 5 mL of ammonium hydroxide (NH_4OH) with 250 mL of 70% ethanol (EtOH).

Appendix C Immunohistochemistry Staining Protocol

Staining Protocol for Monoclonal Mouse anti-human MHC (Immunohistochemistry)

Slides are completely immersed in the following solutions for the allotted time, and in separate containers. The estimation of 300 mL per slide was assumed throughout the protocol.

1. Xylene for 5 minutes
2. Xylene for 2 minutes
3. Xylene for 3 minutes
4. Xylene for 2 minutes
5. Absolute alcohol for 2 minutes
6. Absolute alcohol for 2 minute
7. 95% alcohol for 2 minutes
8. 95% alcohol for 1 minute
9. 70% alcohol for 1 minute
10. Water for 2 minutes
11. Quenched with fresh 3% Hydrogen Peroxide (H_2O_2) in methanol for 5 minutes (*20 mL 30% H2O2 and 180 mL Methanol*); The solution is prepared from 30% H_2O_2
    - Hydrogen peroxide in fridge, methanol in "flammable cabinet" with blue lid
    - 180 mL methanol + 20 mL of 30% hydrogen peroxide
12. Rinsed in distilled water for 5 minutes then subsequently immersed in phosphate buffered saline (PBS) for 5 minutes on shaker
    - *Shaker:*
        i. Turn on
        ii. Press '050' then enter
        iii. Give it a shove to move it
13. Antigen retrieval is performed in citrate buffer pH 6.0 in a de-cloaking chamber
    - 500 mL distilled water in bottom of pressure cooker
    - *Decloaker:*
        i. Turn on, press start
        ii. Let warm to ~125 degrees until it beeps, press start, and check pressure reading
        iii. Wait till cools and beeps and turn off, unplug
14. Rinsed in running tap water, followed by PBS, for 5 minutes each
15. Blocked in 10% horse serum for 30 minutes at room temperature; the blocking serum is then drained onto a paper towel

- Just fill up horse serum to 15 mL with PBS
16. Slides are *not* rinsed with PBS
17. Incubated with the monoclonal mouse antihuman myosin heavy chain type II or type II at the dilution of 1:3200, which was determined by previous titrations.
    - Using 10% horse serum
    - Do not stain negative slides with primary antibody
18. Rinsed thoroughly with PBS for 5 minutes on shaker
19. Incubated with *ImmPress* kit anti-mouse horse-radish peroxidase micropolymer solution for no longer than 30 minutes at room temperature
20. Rinsed thoroughly with PBS for 5 minutes on shaker
21. Incubated with DAB for no longer than 10 minutes, then drained into a waste container using distilled water in order to halt the reaction
    - DAB oxidizes the tissue, thus giving a brown-ish appearance
22. Stained using filtered Hematoxylin for 1 minute
23. Rinsed with running tap water, until water is clear
24. Dipped 2-3 times in Ammonium Alcohol (2% Ammonium Hydroxide in 70% alcohol)
25. Rinsed with running tap water, until no foam or residue is present and water is clear
26. 70% alcohol for 1 minute
27. 95% alcohol for 1 minute
28. 95% alcohol for 1 minute
29. Absolute alcohol for 2 minutes
30. Absolute alcohol for 1 minute
31. Xylene for 5 minutes
32. Xylene for 3 minutes
33. Mount and coverslip using Cytoseal® permount under a fume hood

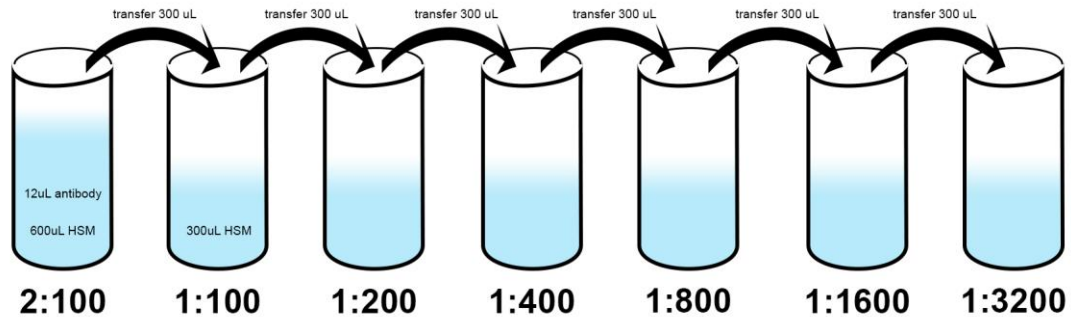*Diaminobenzidine (DAB) Solution:*

To 5 mL distilled H_2O, add 2 drops of buffer, 4 drops of DAB, and 2 drops of H_2O_2, in that particular order, with vortexing after each step

Citrate Buffer Preparation:

- 950 mL of distilled water + 2.1 g of citric acid, anhydrous
    - Citric acid on shelf
- Put on mixer and place both temperature and pH electrode in solution
    - Remove storage bottle from pH electrode
- Slowly add Sodium Hydroxide (NaOH) 10.00N form base cabinet using a pipette until pH reaches 6.0
- Top up to 1000 mL with distilled water

Appendix D Titration Experiments to Establish Working Ratio of MHC Antibody

Antibody Dilutions:

transfer 300 uL   transfer 300 uL   transfer 300 uL   transfer 300 uL   transfer 300 uL   transfer 300 uL

12uL antibody
600uL HSM   300uL HSM

2:100   **1:100**   **1:200**   **1:400**   **1:800**   **1:1600**   **1:3200**

Myosin Heavy Chain Type I and II - Titration Experiments

MHC Type I	Slide #1	Slide #2	Slide #3	Slide #4	Slide #5	Slide #6	Slide#7	Slide #8
	Control	1:50	1:100	1:200	1:400	1: 800	1:1600	1:3200

MHC Type II	Slide #1	Slide #2	Slide #3	Slide #4	Slide #5	Slide #6	Slide#7	Slide #8
	Control	1:50	1:100	1:200	1:400	1: 800	1:1600	1:3200

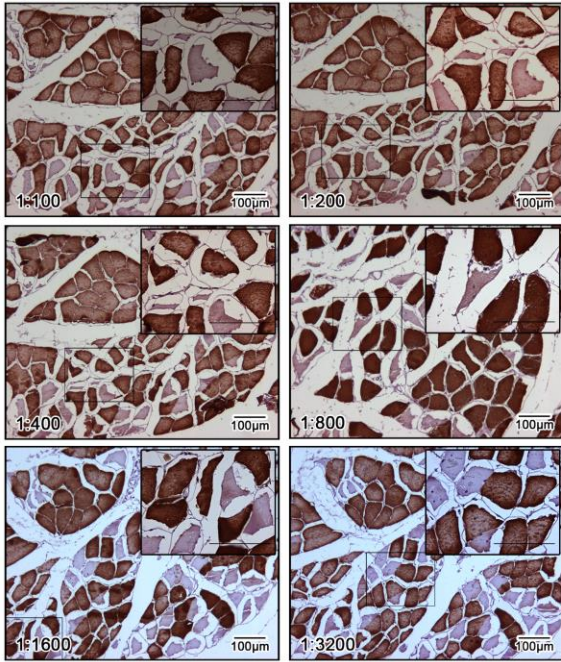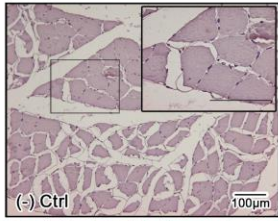Example: 1 slide requires 300 uL of diluted antibody:

ex: 1:50 Ratio = 1uL antibody: 50 uL of horse serum (HSR)
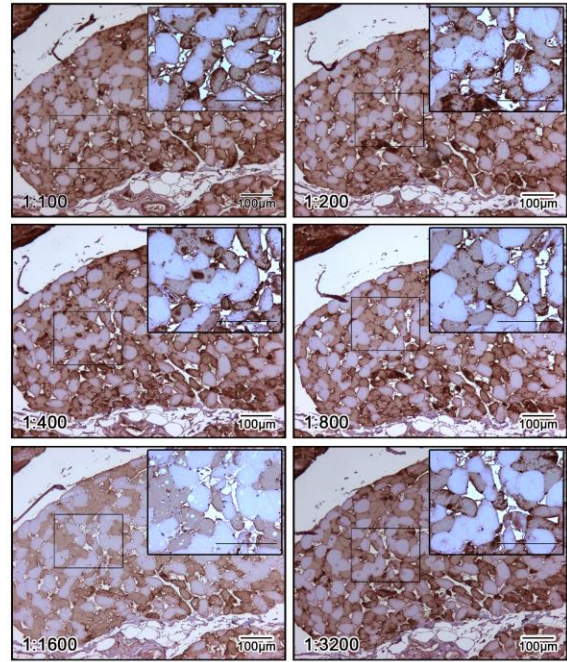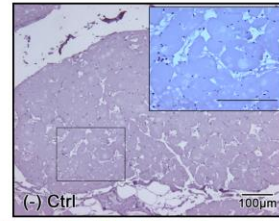
$$\frac{1}{50} = \frac{X}{300uL\ HSR}$$

$$X = \frac{300 \times 1}{50} = 6uL\ antibody$$

$$\therefore {}^{6\ uL\ antibody}/_{300uL\ Horse\ serum}$$

Soleus (MHC I)

Lateral Head of the Triceps Brachii (MHC II)

Appendix E Copyright Permissions for Published Materials

JOHN WILEY AND SONS LICENSE
TERMS AND CONDITIONS

Feb 12, 2018

This Agreement between Mr. Colin Moore ("You") and John Wiley and Sons ("John Wiley and Sons") consists of your license details and the terms and conditions provided by John Wiley and Sons and Copyright Clearance Center.

License Number	4285980802743
License date	Feb 11, 2018
Licensed Content Publisher	John Wiley and Sons
Licensed Content Publication	Journal of Anatomy
Licensed Content Title	Structural and functional anatomy of the palmaris brevis: grasping for answers
Licensed Content Author	Colin W. Moore,Charles L. Rice
Licensed Content Date	Aug 8, 2017
Licensed Content Pages	8
Type of use	Dissertation/Thesis
Requestor type	Author of this Wiley article
Format	Print and electronic
Portion	Full article
Will you be translating?	No
Title of your thesis / dissertation	Functional Anatomy of Palmar Musculature
Expected completion date	Apr 2018
Expected size (number of pages)	150
Requestor Location	Mr. Colin Moore
Publisher Tax ID	EU826007151
Total	0.00 CAD

This Agreement between Mr. Colin Moore ("You") and John Wiley and Sons ("John Wiley and Sons") consists of your license details and the terms and conditions provided by John Wiley and Sons and Copyright Clearance Center.

License Number	4285980698577
License date	Feb 11, 2018
Licensed Content Publisher	John Wiley and Sons
Licensed Content Publication	Journal of Anatomy
Licensed Content Title	Fiber type composition of the palmaris brevis muscle: implications for palmar function
Licensed Content Author	Colin W. Moore,Tyler S. Beveridge,Charles L. Rice
Licensed Content Date	Jun 16, 2017
Licensed Content Pages	8
Type of use	Dissertation/Thesis
Requestor type	Author of this Wiley article
Format	Print and electronic
Portion	Full article
Will you be translating?	No
Title of your thesis / dissertation	Functional Anatomy of Palmar Musculature
Expected completion date	Apr 2018
Expected size (number of pages)	150
Requestor Location	Mr. Colin Moore
Publisher Tax ID	EU826007151
Total	0.00 CAD

Curriculum Vitae

Colin W. Moore

Education

2014 – present	**PhD Candidate,** Kinesiology, University of Western Ontario

Dissertation: *Functional Anatomy of Palmar Musculature*
Supervisor: Dr. Charles L. Rice
Anticipated completion: April 2018

2009 – 2010   **Master of Science**, Anatomical Sciences, Queen's University
Thesis: *A Comparison of Soft Embalming Methods for Colonoscopy Model Development*
Supervisor: Dr. Ronald A. Easteal

2004 – 2008   **Honors Bachelor of Arts,** Kinesiology, York University

Academic Employment

I. Anatomy Demonstrator

2011 – 2013   *Anatomy Demonstrator*, Ross University School of Medicine, Dominica, West Indies (Caribbean)
- Taught cadaveric gross anatomy to medical students in the anatomy laboratory (full body dissection), ~350 students
- Facilitated problem-based learning (PBL) groups, 8-10 students
- Provided anatomical expertise during airway management simulation sessions, 8-10 students/group

II. Anatomy Prosector

2014 – 2016   *Anatomy Prosector* (Summer work-study), Department of Anatomy & Cell Biology, Schulich School of Medicine & Dentistry, University of Western Ontario. *Supervisor*: Dr. Marjorie Johnson
- Prepared and dissected cadaveric specimens for the undergraduate medical curriculum and laboratory exams

Teaching Assistantships

I. University of Western Ontario

Functional Human Gross Anatomy for Kinesiology, 2014-2015, Fall/Winter 2017
- Delivered several lectures: joints of the upper limb, lower limb anatomy
- Taught undergraduate kinesiology (BSc.) students cadaveric anatomy (full-body dissection)
- Guided students through 3D projected models of pelvic anatomy
- Conducted verbal anatomy laboratory examinations (VIVA)

II. Queen's University

Human Visceral System, Winter 2010
Human Musculoskeletal System, Fall 2010
Introductory Human Anatomy (Online), Fall 2010
- Taught undergraduate life science students gross anatomy using prosected and bell jar specimens in anatomy museum
- Managed online discussion forums and queries using Moodle software
- Proctored and graded assignments, exams

Research Contributions:

I. Peer Reviewed Publications

Groh, AM., **Moore, CW**., Beveridge, TS et al. Electroejaculation functions primarily by direct activation of pelvic musculature: perspectives from a porcine model. *Translational Research in Anatomy* (Accepted: Jan 26, 2018)

Moore, CW., Fanous, J. and Rice, CL. (2017), Revisiting the functional anatomy of the palmaris longus as a thenar synergist. *Clin. Anat.*, DOI: 10.1002/ca.23023 (IN PRESS)

Moore, CW., Rice CL. (2017) Rare muscular variations identified in a single cadaveric upper limb: a four-headed biceps brachii and muscular elevator of the latissimus dorsi tendon. *Anat Sci Int.,* 93 (2), 311-316 DOI: 10.1007/s12565-017-0408-8

Moore, CW., Rice, CL. (2017), Structural and functional anatomy of the palmaris brevis: grasping for answers. *J. Anat.,* 231: 939–946. DOI: 10.1111/joa.12675

Moore, CW., Beveridge, TS and Rice, CL. (2017), Fiber type composition of the palmaris brevis muscle: implications for palmar function. *J. Anat*., 231: 626–633. DOI: 10.1111/joa.12652

Moore, CW., Wilson, TD., Rice CL. (2017) Digital preservation of anatomical variation: 3D-modeling of embalmed and plastinated cadaveric specimens using uCT and MRI. *Ann Anat.,* 209, 69-75. DOI: 10.1016/j.aanat.2016.09.010

Moore, CW., Allen, MD, Kimpinski, K, Doherty, TJ, Rice, CL. (2016) Reduced skeletal muscle quantity and quality in patients with diabetic polyneuropathy assessed by magnetic resonance imaging. *Muscle & Nerve* 53(5):726-32. DOI: 10.1002/mus.24779

Kirk, EA., **Moore, CW**., Chater-Diehl, EJ., Singh, SM. and Rice, CL. (2016) Human COL5A1 polymorphisms and quadriceps muscle-tendon mechanical stiffness in vivo. *Exp Physiol*. 101 (12), 1581-1592. DOI: 10.1113/EP085974

II. Peer Reviewed Publications (*Submitted*)

Moore, CW., Rice, CL. Fiber type composition of the palmaris longus and "lumbrical"-like fascicles of the abductor pollicis brevis: implications for thenar function. Journal of Anatomy (*Submitted: Feb 6, 2018)*

III. Published & Presented Conference Abstracts

Moore, CW., Wilson, TD., Rice, CL. Evaluating three-dimensional (3D) digital models of anatomical variations as assessment tools for undergraduate and graduate anatomy education. *Abstract Submitted to Experimental Biology Meeting, San Diego, CA 2018*

Moore, CW., Beveridge TS., Rice, CL (2017) Does palmaris previs structure allow for protection against prolonged overlying compression? an ultrasound and immunohistochemical investigation. *The FASEB Journal,* **31,** 902.15. [Poster]

Moore, CW., Rice, CL (2017) Rare muscular variations identified in a single cadaveric upper limb: a four-headed biceps brachii and coracobrachialis brevis muscle variant. *The FASEB Journal,* **31,** 896.19. [Poster]

Beveridge, TS., Groh, AM.**, Moore, CW.,** et al. (2017) Development of a Porcine Model to Study the Aortic Plexus and Innervation to the Internal Urethral Sphincter: Implications for Preventing Retrograde Ejaculation. *The FASEB Journal,* **31,** 899.3. [Poster]

Moore, CW., Rice, CL (2016). Functional anatomy of the palmaris brevis: grasping for Answers. *The FASEB Journal*, *30* (1 Supplement), 231-3. [Platform Presentation]

Moore, CW., Allen, MD., Kimpinsky, K., Doherty, TJ., Rice, CL. (2016). Intermuscular differences in leg muscle protein quality in human diabetic neuropathy. *Medicine & Science in Sports & Exercise*. 47(5S):756 [Poster]

Moore, CW., Allen, MD., Kimpinsky, K., Doherty, TJ., Rice, CL (2014). A new spin on muscle quality: magnetization transfer imaging of the tibialis anterior in human diabetic polyneuropathy. *Applied Physiology, Nutrition, and Metabolism*. (39) S1 (2014): S33 [Poster]

Presentations

Moore, CW., Rice, CL. Revisiting the function of the palmaris longus in the human hand: thumbs up or thumbs down? Exercise Neuroscience Group Meeting, University of Guelph, June 15-16, 2017

Moore, CW., Rice, CL. Anconeus architectural changes in response to voluntary contraction: an ultrasound investigation. Exercise Neuroscience Group Meeting. Brock University. June 23-24, 2015

Moore, CW., Allen, MD, Kimpinski, K., Doherty TJ., Rice, CL. A new spin on muscle quality: magnetization transfer imaging of the tibialis anterior in human diabetic neuropathy. Clinical Neurological Sciences Research Day, Western University. Mar 10, 2015

Moore, CW. A comparison of soft embalming methods for colonoscopy model development. Departmental Seminar, Department of Anatomy & Cell Biology, Queen's University, Dec 1, 2010

Postgraduate Imaging Course

Postgraduate Course in Ultrasound Anatomy & Medical Education.
> *American Association of Clinical Anatomists* Conference hosted by St. Georges University, Grenada, West Indies. July 2012

Scholarships

2016 – 2017 Anatomy Education Research Scholarship, $6700
      American Association of Anatomists

2016 – 2017 Ontario Graduate Scholarship, $15,000

University of Western Ontario

2015 – 2016　　　　Ontario Graduate Scholarship, $15,000
University of Western Ontario

2004 – 2005　　　　Provost Entrance Scholarship, $1000
York University

Awards

I. Presentations:

Non-invasive Interest Group Graduate Student Poster Award (PhD)
American College of sports Medicine Conference, San Diego, California. May 28, 2015, $250

Graduate Student Platform Presentation Award (PhD)
Clinical Neurological Sciences Research Day, University of Western Ontario. Mar. 10, 2015, $200

Graduate Student Poster Award (PhD)
Canadian Society for Exercise Physiology Conference, St. Johns, Newfoundland, Oct. 23, 2014, $250

II. Travel & Other Awards:

FHS Travel Award, University of Western Ontario, (PhD), Apr 25, 2017, $260

FHS Travel Award, University of Western Ontario, (PhD), Apr 22, 2016, $300

FHS Travel Award, University of Western Ontario, (PhD), Nov. 13, 2015, $500

Kinesiology Travel Award, University of Western Ontario (PhD), May 29, 2015, $500

Queen's Graduate Award, Queen's University (MSc) Sept. 2009, $3000

Elected Positions

2015 – 2017　　　　Society of Graduate Students (SOGS) Councilor (*Kinesiology Representative*)

Professional Memberships

2015 – Present   **Member**, American Association of Anatomists

2014 – Present   **Member**, American College of Sports Medicine

2012 – 2013   **Member**, American Association of Clinical Anatomists